Department of Information Science and Technology

Research on Port AGV Composite Positioning Based on UWB/RFID

Dongchen Ni

A Dissertation presented in partial fulfillment of the Requirements for the Degree of

Master in Telecommunications and Computer Engineering

Supervisor:

Dr. Octavian Adrian Postolache, Associate Professor

ISCTE-IUL

Co-supervisor:

Dr. Chao Mi, Associate Professor

Shanghai Maritime University

September 2019

Resumo

Nos últimos anos, portos de vários países realizaram sucessivamente pesquisas e aplicações de terminais totalmente automatizados. O terminal adota o processo de automação "Double car shore bridge + AGV + ARMG", que é a solução totalmente automatizada mais amplamente utilizada e relativamente madura. Atualmente, a navegação AGV do terminal é baseada no posicionamento da etiqueta RFID e a precisão é boa. No entanto, hoje em dia, a tecnologia UWB tornou-se na tecnologia mais popular relativamente ao alcance e posicionamento. A pesquisa neste trabalho é baseada no posicionamento composto por UWB / RFID, usado principalmente para tarefas de localização específicas nos portos, podendo desta forma localizar-se com precisão a posição do AGV.

Este projeto de mestrado estuda em primeiro lugar o sistema de posicionamento UWB, e depois um algoritmo tradicional de posicionamento 3D. A contribuição da importância expressa pelo algoritmo de posicionamento “time of arrival” (TOA) 3D foi proposta. Para o sistema de posicionamento RFID, a conexão entre o leitor e a transportadora é projetada e a etiqueta de referência é ocultada. Por fim, o algoritmo de “k-nearest neighbor” baseado numa base de dados e no método de análise de cena é adotado para realizar o posicionamento. Em segundo lugar, a base do sistema de posicionamento composto é a tecnologia de fusão de dados. O algoritmo de fusão mais amplamente utilizado e maduro é o algoritmo de filtro Kalman e o filtro de partículas. Finalmente, é realizada a análise experimental do sistema de posicionamento composto UWB e RFID. Os resultados experimentais mostram que o sistema de posicionamento composto UWB e RFID pode reduzir o custo do sistema de posicionamento. O sistema desenvolvido é caracterizado por uma maior precisão de posicionamento e robustez .

Palavras-chave: Porto; UWB; RFID; Localização composta

Abstract

In recent years, ports in various countries have successively carried out research and application of fully automated terminal. The terminal adopts the "Double car shore bridge + AGV + ARMG" automation process, which is the most widely used and relatively mature fully automated solution. At present, the AGV navigation of the terminal is based on RFID magnetic nail positioning and the accuracy is good. However, nowadays UWB technology has become the most popular technology in ranging and positioning. The research in this work is based on UWB/RFID composite positioning, which is mainly used for the specific localization tasks in the port and it can accurately locate the position of the AGV.

This MSc work studies the UWB positioning system first and then researches the traditional 3D positioning algorithm. Importance contribution expressed by 3D TOA localization algorithm. For RFID system, this connection between the reader and the carrier is designed, and the reference tag is buried. At last, data-based on RFID localization algorithm in scene analysis method is adopted for positioning. Secondly, the basis of the composite positioning system is data fusion technology. The most widely used and mature fusion algorithm is the Kalman filter algorithm and Particle filter. Finally, the experimental analysis of UWB and RFID composite positioning system is implemented. The results indicate that UWB and RFID composite positioning system can reduce the cost of the positioning system. Higher positioning accuracy and robustness are characterizing the developed system.

Keywords: Port; UWB; RFID; Composite localization

Acknowledgments

Firstly, I would like to express my sincere thanks to my supervisor, Professor Octavian Postolache and co-supervisor Chao Mi, for all the availability and supporting during the realization of this work.

Special acknowledgments go to the Telecommunications Institute IT-IUL and ISCTE-IUL, for providing all the material and resources needed for this dissertation.

My biggest thanks goes to my family for the unconditional support, especially to my parents, Yong Ni and Jing Shi.

A big thanks to my good friends of Portugal, Mr.João Monge, and Ms Mariana Jacob Rodrigues, for all the help, support and for having patience the size of the world.

Finally, a huge thanks to all my friends and colleagues of China who accompanied me on this journey.

Contents

List of Figures

List of Tables

List of Acronyms

3D	3-Dimensional
ADC	Analog-to-Digital Converter
AGV	Automated Ground Vehicle
AOA	Angle of Arrival
BPSK	Binary Phase Shift Keying
DAC	Digital to analog converter
DCM	Database Correlation Method
DMA	Direct Memory Access
DS-CDMA	Direct Sequence —Code Division Multiple Access
EAN	European Article Number
EKF	Extended Kalman filter
EPC	Electronic Product Code
FCC	Federal Communications Commission
GNSS	Global Navigation Satellite System
GPIO	General-purpose input/output
GPS	Global Positioning System
GSM	Global System for Mobile Communications
IBM	International Business Machines Corporation
IEC	International Electrotechnical Commission
IOT	Internet of Things
ISO	International Organization for Standardization
KF	Kalman Filter
KNN	K-Nearest Neighbors
LDO	Low dropout regulator
LOS	Line-of-Sight
MAP	Maximum aposterior estimation
MB-OFDM	Multi-band Orthogonal Frequency-Division Multiplexing
MEMS-AHRS	Mechanical System - Attitude Heading Reference System

MSE	Mean Square Error
NLOS	Non-Line-of-Sight
PAM	Pulse Amplitude Modulation
PAL	Precision Asset Location
PDR	Pedestrian Tracking Algorithm
PF	Particle Filter
PPM	PulsePosition Modulation
RAM	Random Access Memory
RF	Radio Frequency
RFID	Radio Frequency Identification
RMSE	Root Mean Squared Error
RSSI	Received Signal Strength Indication
SIS	Sequential Importance Sampling
SPI	Serial Peripheral Interface
SRAM	Static Random Access Memory
SWD	Serial single-line debugging
TDOA	Time Difference of Arrival
TOA	Time of Arrival
UMTS	Universal Mobile Telecommunications System
USART	Universal Synchronous/Asynchronous Receiver/Transmitter
UWB	Ultra-wideband
WLAN	Wireless Local Area Network
WLS	Weighted least squares
WPAN	Wireless domain network
WSN	Wireless Sensor Network

Chapter 1 Introduction

1.1 Motivation

With the mature use of Internet of Things (IoT) and cloud computing technologies, the industrial digitalization and automation levels have significantly improved. Additionally the automated logistics transportation system and flexible manufacturing systems have changed dramatically [1]. Previously, although some advantages of the demographic dividend have disappeared, it is still a major trend to upgrade traditional industries with modernization and automation equipment. In the pace of such an era, the world ports are also developing in an intelligent and unmanned direction. With the continuous increase of the world's shipping volume and the increasing size of container ships, stable and efficient container handling, energy saving, environmental protection and low cost have become the focus of port operators. Automated terminals are increasingly demonstrating their superiority in terms of reducing labor costs, improving port capacity, reducing energy consumption in loading and unloading operations, and enhancing port brand image. This is an inevitable trend in future port development [2]. Among them, Automated Ground Vehicle (AGV) are widely used in port container transportation. It is the most used equipment of fully automated terminal with intelligent functions, such as path optimization, automatic navigation and localization[3].

Figure1.1 - Automated terminals and AGV[4]

With continuous development of navigation and positioning technology, people have higher pursuits and expectations for navigation and positioning accuracy. Single navigation and positioning systems have their own merits and shortcomings (See Table 1.1 for details). The special needs of some areas have not been met, and the combined navigation has emerged [5]. The positioning system with different positioning principles and methods is integrated organically by computer and filter to achieve complementary advantages and information redundancy. It can not only enhance the positional accuracy of entire positioning system, but also improve reliability of system. Especially recently, the integrated navigation positioning has been rapidly developed under the help of high technology and powerful theory. It has also become one of the research hotspots in this field [6].

Table 1.1 Comparison of navigation and positioning methods

Navigation method	Advantages	Disadvantages
Electromagnetic navigation	Easy to control and communicate, low cost	Low flexibility, the troublesome expansion path
Tape navigation	Precise positioning and simple tape placement	Poor anti-interference, regular maintenance
Optical navigation	Easy route setting and flexibility	Poor reliability and low positioning accuracy
Laser navigation	Precise positioning and high flexibility	High cost and high environmental requirements
Image recognition navigation	Higher accuracy and reliability	Low flexibility
Inertial navigation	Advanced technology, strong autonomy, wide application fields	High cost and low positioning accuracy for a long time
RFID	Accurate positioning and a wide range of technology transmission	Short acting distance

The accuracy requirements of AGV operation for localization are very high. The accuracy of AGV operation on localization reaches the centimeter level. The main modes are optical guiding, magnetic strip guiding, magnetic nail guiding, laser navigation guiding, Visual navigation, and inertial navigation. At present, the port engineering develops the AGV navigation system based on the magnetic nail guiding type. According to the system design, magnetic nail (RFID tags) are distributed every 2m in the AGV operation area to form a matrix distribution, and the AGV performs its own position positioning by reading the preset magnetic nail information. However, to achieve higher accuracy of positioning, the density of the RFID tags needs to be higher which makes this solution costly [7]. Another problem is that it is very difficult to maintain RFID tags (Figure1.2). Therefore, considering UWB technology in the open space of the ports, localization can be used to ensure accurate positioning and reduce the cost of the positioning system. UWB technology has become the most popular technology in ranging and positioning due to its strong penetrating ability, high multipath resolution capability, and wide bandwidth. UWB technology is generally used for indoor small-scale positioning. This work has new applications for outdoor localization (port case study). In addition, the cost of UWB wireless positioning is relatively cheap, therefore, the developed MSc work carries out research on the composite positioning that combines UWB positioning technology and RFID positioning technology.

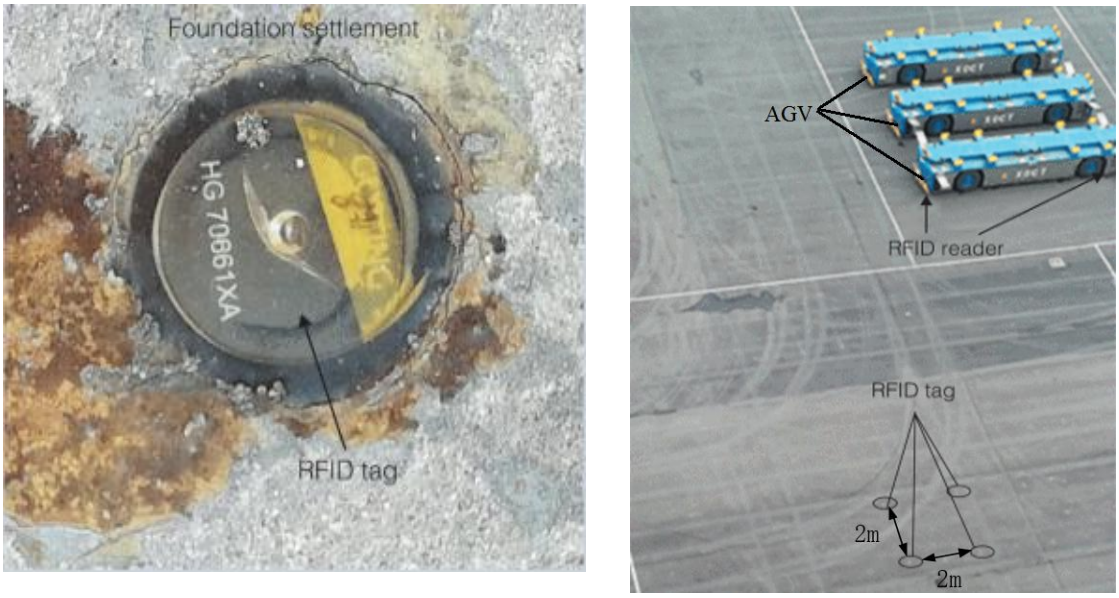

Figure 1.2 - RFID application for AGV navigation in a smart port[8]

1.2 Objectives

Recently, with continuous progress of mobile communication and wireless sensor network (WSN), more and more attention has been paid to the application of location-based services in the environment. Positioning technology is one of the key points to provide location services. With the popularity of intelligent terminals and mobile devices, people need to apply location-based navigation and positioning services in their activities. The requirements for positioning technology and the accuracy of positioning also need to be increased. The required positioning technology has also evolved from a single positioning system to composite positioning in multiple ways. However, a single RFID or UWB technology can hardly meet the positioning requirements in complex environments. Wireless signals can cause larger errors in these environments, such as multipath effects, clock synchronization errors, and NLOS path propagation. Therefore, combining these two technologies can improve the ability of accurate positioning in this type of environment.

Considering the background of current port, this work carries out composite positioning research based on the fusion of UWB and RFID technology. And it proposes a method and research on composite positioning based on UWB and RFID. At present, the location of AGV in the port is based on RFID technology. However, under the port environment, to obtain high-precision positioning, the density of magnetic nails to be laid is large, and the laying cost and maintenance cost are high, which is not conducive to port remodeling and upgrading. UWB technology has the advantages of high positioning accuracy and low cost. Therefore, with an emerging algorithm such as data fusion, these two technologies (UWB and RFID) could work together. When the AGV is driven to the open area of the port and there is no RFID tag on the ground of port, the position information can be obtained by receiving the UWB signal, and the positioning result can be corrected to ensure the accuracy of the positioning. In this work, the accurate positioning performance of UWB is completed with the tag information obtained from RFID reader. Thus a spatial continuity, reliable and accurate positioning are obtained.

1.3 Structure of dissertation

Chapter 2 includes start of art and the literature review on UWB and RFID technologies. The advantages, implementation techniques and application scenarios of these technologies are discussed. Chapter 3 describes think and design of the composite positioning system. In Chapter 4 describes the hardware and the software of RFID system. In Chapter 5, the hardware and the software of UWB system are introduced. In Chapter 6 are presented, experimental results as part of system validation. In Chapter 7 presents the conclusions and future work.

Chapter 2 State of the Art

This chapter introduces these research areas of the proposed work, such as RFID technology, UWB technology, and composite positioning technology. The advantages, implementation techniques and application scenarios of these technologies are introduced.

2.1 RFID technology status

RFID was first used in the military in the 1940s. The combination of RFID technology and radar technology can easily identify friendly military aircraft. As many researchers continued their research, in 1948, Harry Stockman published the paper 《communication technology using reflected power》 in the association of radio engineers [9]. In the 1950s and 70s, researchers applied the development of modular passive reactors in radio transmission, which provided the development direction of RFID technology and related applications. In the 1980s, due to the development of electronic integration technology, RF was integrated into with Shawnecki diode. With the advent of electronic tags, RFID technology can gradually be used to civil[10]. In the 1990s, RFID technology was used in many areas of civil, such as the access to RFID technology in the US highway toll system. The RFID technologies of U.S applied in the highway system greatly improved the efficiency and also made a good promotion for RFID technology. In order to serve more industries in RFID technology, the Auto-ID Center and the EPC global system have been established by organization that the Massachusetts Institute of Technology. And EPC coding standards have been proposed to serve more than 100 companies and government organizations around the world[11].

The research of positioning technology based on RFID started earlier. As early as 2000, the RFID technology proposed SpotON system which records the signal strength of tags read by three or more readers. Then it determines the location of tags by triangulation to achieve positioning [12]. In 2004, a Michigan state university researcher

proposed a system called LANDMARC, which consists of a reader and an active RFID tag. The technology of positioning is realized by receiving signal strength value [13]. In 2005, IBM has a Blue Bot system was put forward. It uses the robot to carry RFID reader continuously monitor and to record after the analysis of data [14]. In 2008, two Indian scholars applied the improvement of LANDMARC algorithm mentioned above to three-dimensional space, so as to realize the spatial positioning of three-dimensional space [15]. In 2009, to reduce location costs, two researchers proposed an algorithm for reading data from a mobile reader [16]. In 2014, researchers began to consider the influence of the antenna directly on the reception of signal intensity value, so they took the direction into account when establishing the database to build the fingerprint database [17]. In 2015, scholars use the normalized idea to normalize the signal strength values to reduce the positioning error caused by equipment fiversity[18]. In 2016, to solve the problem that the RSS values of two adjacent locations are inconsistent. A multidimensional kernel function density estimation method is proposed[19]. In 2017, researchers have proposed a way to combine RSSI and phase information for localization [20].

2.2 UWB technology status

The basis of UWB wireless communication technology is pulse radio technology. The fundamental difference from other wireless communication technologies is that it uses a very narrow RF pulse to communicate between transmitters and receivers. In fact, UWB was adopted by Marconi one hundred years ago. And UWB was invented the transoceanic wireless telegraph[21]. Regarding UWB wireless communication technology, the design technology of its transmitter and receiver has appeared in foreign countries as early as the 1960s, and UWB was also used in communication and radar. By the 1970s, the system concepts of UWB used in communications and radars had been fully established. The study of UWB technology began in the United States. Since (?) Its first application in military, the federal communications commission (FCC) in

2002 formally adopted the civil legislation of UWB technology. New opportunities have been brought for the development of UWB technology, greatly inspired in the related academic research and industrialization process [22].

Table 2.1 UWB technology application field and working frequency

Application Field	Working Frequencies
Landmine Penetrating Imaging System	Below 960MHz,(3.1~10.6GHz)
In-wall Imaging System	Below 960MHz,(3.1~10.6GHz)
Through Wall Imaging System	Below 960MHz,(3.1~10.6GHz)
Medical System	(3.1~10.6GHz)
Monitoring System	(1.99~10.6GHz)
Automotive Radar System	Below 24.1GHz
Communication and Measurement	(3.1~10.6GHz)

UWB technology has many advantages: high speed; high performance; low intercept and detection probability; anti-multipath and low system complexity [23][24]. There are some big advantages in wireless positioning[25]. The frequency band of FCC UWB work from 3.1 GHz to 10.6 GHz, and the signal transmitted power is limited under 41.3 dBm[26][27]. The UWB authorized application fields and its corresponding frequency bands are shown in the table 2.1[28]. UWB wireless communication mainly has three implementation schemes: Carrier less Pulse Scheme, Single-carrier DS-CDMA Scheme, and MB-OFDM Scheme [29][30].

So far, the development of UWB chips and equipment in China has not started, and the major wireless communication companies and consumer electronics companies have not formally carried out the research and development of UWB technology. In the UWB system based on carrier modulation, many advanced technologies in mobile communication are used, such as CDMA, OFDM, etc, so many enterprises are not completely without foundation in the development of UWB system [31].

In recent years, China government departments have increasingly attached importance to UWB technology, and the 863 programs of China project have also given

key support to UWB. A large number of scholars and research institutions have also started tracking research on UWB communication technology, it will mark a new breakthrough in MB-OFDM in China [32].

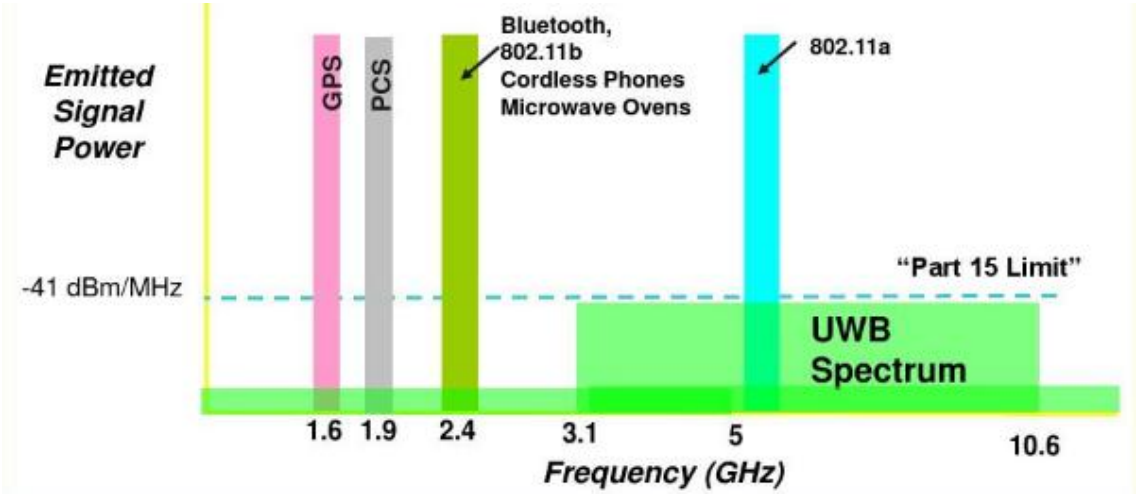

Figure 2.1 - UWB frequency distribution[33]

Studies on the co-existence of the UWB system and existing wireless communication system have also been carried out. For example, for UWB and GPS system, when the parameters of the UWB system are not appropriate, it will cause interference to the conventional GPS system [34]. There are WLAN, GSM, UMTS and so on (See Figure 2.1 for details above).

2.3 Composite positioning technology

The above two positioning methods can meet the requirements of most environments. However, with the increasing demand for positioning accuracy, the composite positioning technology has become a reality (Figure2.2). Therefore, many experts and scholars focus their research on the composite and fusion of various methods.

Figure 2.2 - Application of positioning technology[35]

For the outdoor environment, NakYongKo used theGNSS and MEMS-AHRS to perform UAV navigation attitude estimation. The GNSS measurement is used to correct the magnetic field measurement, reducing the deviation of the magnetic field measurement. The Kalman filtering method is used to integrate the measurement data of GNSS and MEMS inertial measurement components to improve the accuracy of attitude estimation[36]. Shunsuke and Yoshiyuki first established a local positioning system under the bridge through the wireless sensor network. Then they used UWB technology to measure the time of wireless communication, calculated the position of the robot, and obtained the motion attitude of the robot by the IMU measuring component. The data between the various sensors is fused using the EKF algorithm. Finally, precise control of the robot's autonomous flight is achieved. Pittet S et al. used EKF to fuse UWB/PDR data, but EKF filtering did not achieve good results and even caused filter divergence in nonlinear systems. At the same time, the KF cannot correct the heading angle error, which causes the heading angle error to increase with time[37].

Figure 2.3 - Application of positioning in industrial field[37]

During industry 4.0 era, the application field of positioning has also been expanded to the industrial field. Positioning techniques allow the production process to be visualized and tracked, as it is shown in the Figure 2.3.

Chapter 3 System Description

3.1 Overview

RFID has the advantages of non-contact, strong anti-interference and large amount of data. With continuous improvement of science and technology level, the reliability has been continuously improved. However, to achieve higher positional accuracy, RFID tags density needs to be higher which makes this solution costly. UWB technology has widely many applications in industry[38]-[43]. Compared with GPS, RFID and other traditional technologies, this technology has the advantages of high time resolution, strong anti-interference ability, and the ability to have higher localization in range [44]-[47]. So, UWB positioning is considered as a hopeful solution to get higher accuracy localization. Therefore, in practical applications, the effect of composite positioning is better. And UWB and RFID positioning systems form the composite positioning system in a certain way to correct positioning accuracy.

This chapter makes further systematic research on UWB and RFID composite positioning methods and correction methods.

3.2 Composite system

Composite positioning is a method of comprehensively utilizing multiple positioning techniques to determine position. With the popularity of intelligent terminals and mobile devices, people need to apply location-based navigation and positioning services in their activities. The requirements for positioning technology and the accuracy of positioning are important requirements. However, a single positioning technology can hardly meet the positioning requirements in various environments. Therefore, combining these two technologies can improve the ability of accurate

positioning in this type of environments. Figure3.1 presents the architecture of the considered localization system:

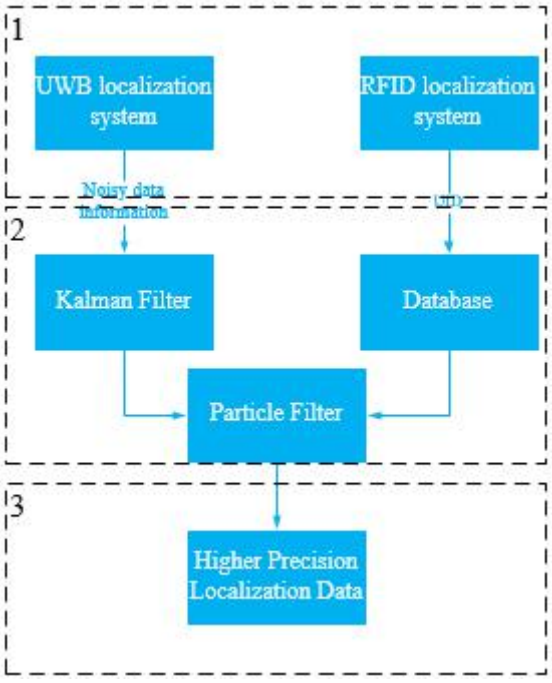

Figure 3.1 - Localization System Architecture

In the composite system, each measuring component in UWB and RFID operates independently. UWB data will be transmitted to the PC through the serial port, and the RFID data will be transmitted by WIFI. Then, the filter is used to process the position data. The filters used in the system are: Kalman filter and Particle filter. Each filter has its own inherent filtering characteristics. The NLOS error caused by NLOS propagation is the main source of UWB positioning deviation. Therefore, the KF will process time information and eliminate effect of the NLOS to enhance the positioning accuracy. The system uses a particle filter to process the position data of the PC. The particle filter is used for any distributed noise and can well fuse the data of different sensors. Figure 3.2 indicates the data fusion process about the composite positioning system.

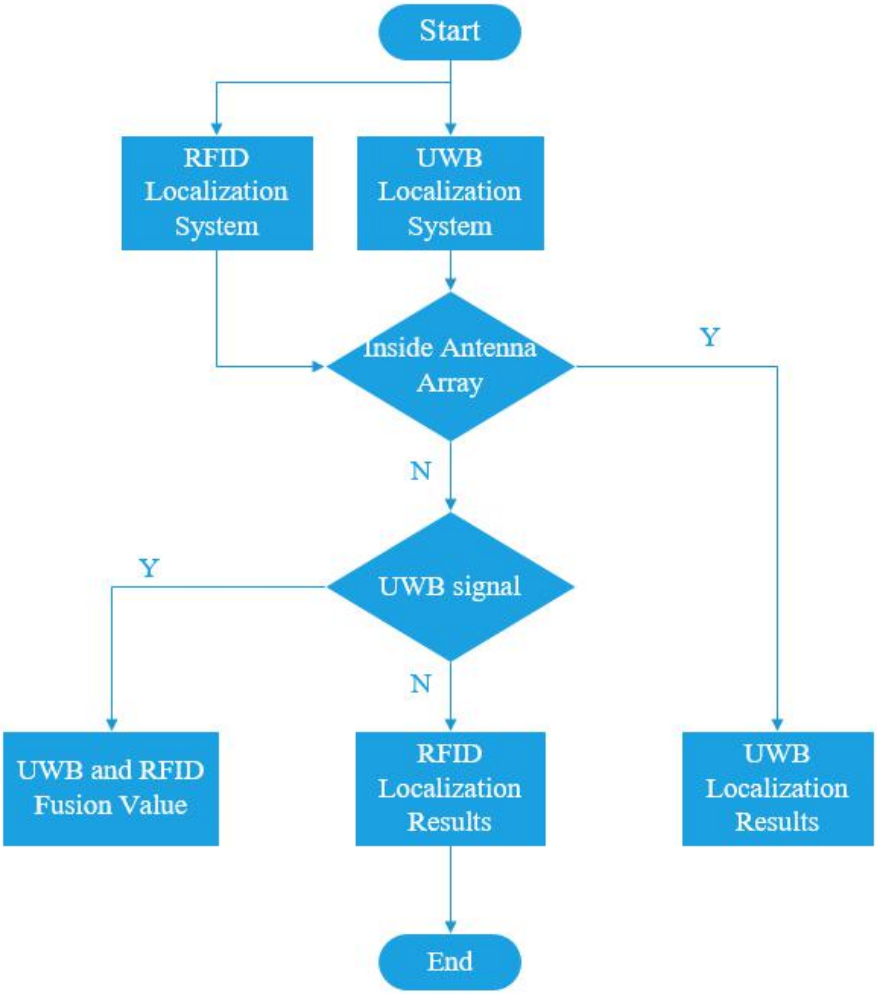

Figure 3.2 - Particle Filtering Workflow

In this data fusion process, since the refresh rates of UWB and RFID are different, three kinds of location data under three different conditions may be acquired: only UWB data; only RFID data; both UWB data and RFID data. When the target node is in the antenna array, since the RFID positioning system cannot perform continuous positioning and the UWB positioning accuracy is good, the composite positioning is switched to the UWB positioning system. When the target node is outside the antenna array and the distance is far, UWB lacks the signal, which causes the composite system to switch to RFID positioning system. When the target node is outside the antenna array and the distance is near, the system can accept both UWB data and RFID data. Therefore, the composite system is switched to UWB and RFID positioning system to

perform positioning together. The positioning data obtained by both UWB and RFID is fused to obtain the positioning coordinates.

3.3 Kalman filter algorithm

When UWB is used to positioned, it will be affected by factors such as the NLOS environment and the noise of the system itself. KF is particularly effective for models. So, to enhance the positioning performance, KF will be used to optimize the UWB positioning data.

KF is a recursive filter which can remove the state of system from measurements that contain noise [48]. The basic KF can be applied under linear conditions, and in practical applications, most of them are nonlinear. For nonlinear systems, we use EKF to improve the system state.

In measurement process, there are two main factors that affecting the positioning accuracy: the first is the error caused by the bad channel environment, which is called the measurement error; The second is the nonlinear problem when solving the nonlinear positioning equations. In the measurement error, NLOS error is caused by obstacle blocking or multipath interference in the actual environment, and NLOS error is the main reason that affects the positioning accuracy. If there is an error in the positioning process, a positive error component will be generated in the measured value from tag to anchor. When measured value of such a large error is used for the position estimation of the tag, the performance of the algorithm is bound to be significantly degraded.

3.3.1 Kalman Filter Model

Due to the good tracking performance of the KF, it is widely used in radar ranging and navigation. KF has two parts: prediction and update. In the prediction section, the filter uses the previous time to estimate the current state. In the update section, the filter optimizes the predicted value from the observations of the current state to gets more the

accurate new estimate. In this way, KF becomes a method for solving unknown state equations and measuring equations. The equations of KF state and measurement are:

$$s(N+1) = H \bullet s(N) + \Gamma \bullet hw \tag{3.1}$$

$$O(N) = G(N) \bullet s(N) + gw \tag{3.2}$$

Among of them: $s(N)$ is state vector at time N; $O(N)$ is the measurement vector at time N; H is state transition matrix of the sampling interval Δ; Γ is noise coupling; The measurement matrix is $G(N)$; hw and gw are noise components.

From (3.1) and (3.2), we can conclude that the state of the moment and the state of the moment are connected by the equation of state. The measurement equation establishes the relationship between time vector and state vector. *Hw* and gw reflect the change error of state and measurement. Therefore, the state of the moment is related to the historical measurement. The state vector can be estimated in real time by iteration.

The iteration of the KF has two steps. The first step is the prediction of state vector:

$$\hat{s}(N/N-1) = H \cdot s(N-1) + hw \tag{3.3}$$

$$P(N/N-1) = HP(N-1)H^T + \Gamma Q(N)\Gamma^T \tag{3.4}$$

$$A(N) = P(N/N-1)\left[R + G(N)P(N/N-1)G(N)^T\right]^{-1} G(N)^T \tag{3.5}$$

The second step is the correction of measured vector:

$$\hat{s}(N) = A(N)\left[O(N) - G(N)s(N/N-1)\right] + \hat{s}(N/N-1) \tag{3.6}$$

$$P(N) = P(N/N-1)\left[I - A(N)G(N)\right] \tag{3.7}$$

Of which, $\hat{s}(N/N)$ and $\hat{s}(N+1/N)$ are state estimation vectors and state prediction vectors, $P(N/N)$ and $P(N+1/N)$ are respectively covariance matrix of the estimation error and the prediction error, respectively, and $A(N)$ represents the Kalman gain.

3.3.2 NLOS error suppression

When the Gaussian variable with gw and hw is zero mean, the unbiased KF can satisfy the requirement. However, in the case of NLOS, the error is a positive random variable. The observation model between tag and anchor now is represented by the equation (3.8):

$$r_m(N) = d_m(N) + n(N) + NLOS_m(N) \tag{3.8}$$

Of which, $d_m(N)$ is the true distance, $n(N)$ represents Gaussian variable, $NLOS_m(N)$ indicates the influence of NLOS error on the ranging. Under different channel environments, it may obey the uniform distribution, the delta distribution or the exponential distribution [49]. In the environment of UWB, the NLOS error obeys the exponential distribution. Therefore, the biased KF is used to process the data measured in the case of NLOS.

Assuming that the mean value of the measured noise is $E[V(N)] = c$, the KF equation (3.3)~(3.7) needs to take into account the existence of the non-zero mean of the measured noise, and its equation (3.6) can be re-introduced as follows:

The measured value vector $O(N)$ is estimated by:

$$\hat{O}(N/N-1) = G(N)\hat{s}(N/N-1) + C \tag{3.9}$$

The difference between measured value vector $m(T)$ and its estimated value is:

$$e(N/N-1) == O(N) - \hat{s}(N/N-1)G(N) - C \tag{3.10}$$

The error $e(N/N-1)$ can be used to correct the $\hat{s}(N/N-1)$ acquisition state matrix:

$$\hat{s}(N) = s(N/N-1) + A(N)[O(N) - \hat{s}(N/N-1)G(N) - C] \tag{3.11}$$

The deduced equation (3.11) and (3.6) have the effect of non-zero mean C, combined with equations (3.3), (3.4), (3.5), (3.7) and (3.11)[50].

According to the literature [51], where the state vector is $s(N)=[r(N) \quad \dot{r}(N)]^T$, $H=\begin{bmatrix}1 & \Delta \\ 0 & 1\end{bmatrix}$, $\Gamma=\begin{bmatrix}0 \\ \Delta\end{bmatrix}$, $G(N)=[1 \quad 0]$, $r(N)$ is the distance from tag to anchor, $\dot{r}(N)$ is the moving speed of the tag relative to the anchor and covariance matrix hw, $Q=\sigma_m^2 I$, covariance matrix gw, $R=\sigma_x^2 I$ [52]. The implemented Kalman Filter code in Matlab is shown in Figure 3.3:

```
%%%%%%%%%%%%%%%%%%%%%%%%%%%%%%%%%%%%%%%%%%%
N=312;                            %Samplings
x=[1,5,5,1];                      %real route
y=[0.5,0.5,1.5,1.5];
Xkf=zeros(1,N);                   %Kalman filter estimated value
P=zeros(1,N);                     %covariance
%-------------Initialization-----------------
P(1)=0.01;                        %The covariance of the initial value
Xkf(1)=Z(1);                      %The initial estimated state of the filter
%-------------noise error--------------------
Q=0.01;                           %process variance
R=0.25;                           %mearsuremnt variance
W=sqrt(Q)*randn(1,N);             %state-transition matrix
V=sqrt(R)*randn(1,N);             %Measurement noise matrix
%-------------system matrix-------------------
F=1;
G=1;
H=1;
I=eye(2);
%%%%%%%%%%%%%%%%%%%%%%%%%%%%%%%%%%%%%%%%%%%%%%%%%
%-------------Kalman filter-------------------
for k=2:N
    X_pre=F*Xkf(k-1);             %state prediction
    P_pre=F*P(k-1)*F'+Q;          %Covariance prediction
    Kg=P_pre*inv(H*P_pre*H'+R);   %Calculate the Kalman gain
    e=x(k)-H*X_pre;
    Xkf(k)=X_pre+Kg*e;            %update the state
    P(k)=(I-Kg*H)*P_pre;          %Covariance update
end
%-------------calculation error---------------
Err_Messure=zeros(1,N);           %The deviation between the measured value and the true value
Err_Kalman=zeros(1,N);            %The deviation between the kalman filter estimate and the measured value
for k=1:N
    Err_Messure(k)=abs(x(k)-Xexpect);
    Err_Kalman(k)=abs(Xkf(k)-x(k));
end
```

Figure 3.3 - Kalman Filter code in Matlab

3.4 Particle filter algorithm

On PC, due to the different refresh rates of UWB and RFID, it is possible to receive location data in three cases. That is, only UWB data, only RFID data, both UWB data and RFID data.

The origin of the particle filter algorithm dates back to the 1940s, and Metropolis et al. proposed the Monte Carlo method [53]. Then in the late 1950s, Hammersley et al. proposed a Sequential Importance Sampling (SIS). The method acquires samples by proposing distribution and approximates the target state distribution by sample approximation. The sequential importance sampling method is introduced into the Monte Carlo algorithm. During the iterative process, the particles will degenerate. The problem of particle degradation has plagued the scholars at that time. In 1993, Gordan et al. proposed Resampling algorithm, which solved the problem of particle degradation in the sequential importance sampling process. Finally, it evolved into the well-known Particle Filter algorithm (PF).

The idea of PF algorithm is to express its distribution by extracting random state particles from the posterior probability. The PF algorithm has high adaptability to nonlinear and non-Gaussian problems and is widely used in various fields, including image processing, chemical engineering and finance, and also applied to target tracking, positioning and navigation.

3.4.1 Bayesian estimation theory

The PF algorithm is an algorithm which consist of Bayesian estimation and Monte Carlo method. Bayesian estimation is an estimation method of recursive calculation. The system state transition equation is used to predict the prior probaility and then combined with observed values of the system, the posterior probability is calculated. Finally, the maximum posterior probability is obtained to obtain the optimal value [54].

First, the Bayesian estimation is built on the first-order Markov chain. When describing the state of the target, two equations are established to represent it: state and observation. The equation of state is shown in equation (3.22), and the equation of observation is as shown in equation (3.23):

$$k_T = f_T(k_{T-1}) + u_T \tag{3.22}$$

$$m_T = h_T(k_T) + v_T \tag{3.23}$$

In equation (3.23), k_T indicates state value at time T. m_T indicates observed value at time T. f_T indicates state transfer function, and h_T indicates observation function. u_T and v_T indicates noise interference during system processes and observations.

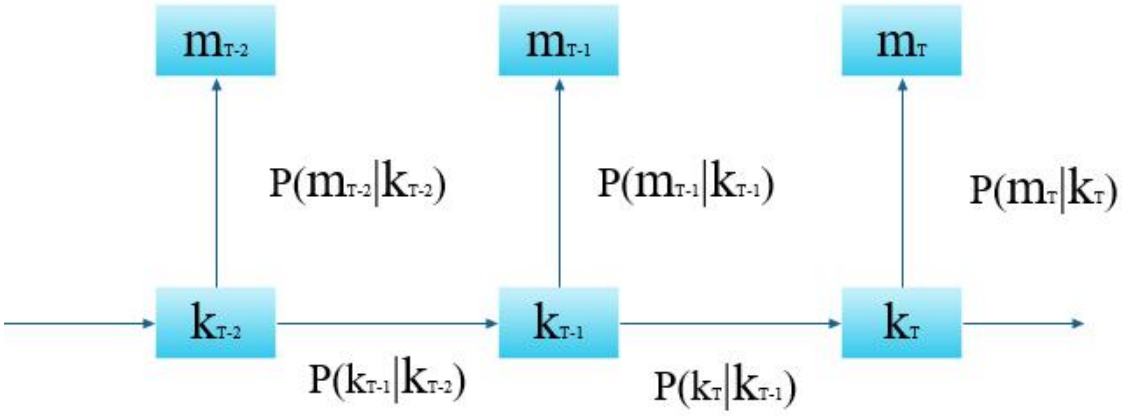

Figure 3.4 - Bayesian estimation method model diagram

The Bayesian estimate consists of two parts: forecast and update. The prior probability $p(k_T \mid m_{1:T-1})$ of the state predicted by the state transition equation in the prediction phase. In the update phase, the prior probability density is corrected by the new observations to get the posterior probability $p(k_{0:T} \mid m_{1:T})$. In practice, only $p(k_T \mid m_{1:T})$ is solved to simplify computational complexity. The model of Bayesian estimation is shown in Figure 3.4.

In the implementation process, it is assumed that the known posterior probability $p(k_{T-1} \mid m_{1:T-1})$ at time T-1. The Bayesian estimation process is as follows:

(1) **forecast phase:** It is known that the posterior probability $p(k_{T-1} \mid m_{1:T-1})$ at time T−1 obtains prior probability density $p(k_T \mid m_{1:T-1})$ of the current moment of the system, as shown in equation (3.24):

$$p(k_T \mid m_{T-1}) = \int p(k_{T-1} \mid m_{1:T-1}) p(k_T \mid k_{T-1}) dx_{T-1} \tag{3.24}$$

Where, $p(k_T \mid k_{T-1})$ indicates state transition probability. The current time position information is only related to the previous time position information.

(2) **update phase:** The posterior probability is obtained by the equation (3.25) by the prior probability $p(k_T \mid m_{1:T-1})$ obtained in the prediction part.

$$p(k_T \mid m_{1:T}) = \frac{p(m_T \mid k_T) p(k_T \mid m_{1:T-1})}{p(m_T \mid m_{1:T-1})} \tag{3.25}$$

When it can get the observed value k_T , the posterior probability is obtained according to equation (3.25). The calculation equation is as shown in equation (3.26):

$$p(m_T \mid m_{1:T-1}) = \int p(k_T \mid m_{1:T-1}) p(m_T \mid k_T) dx_T \tag{3.26}$$

After obtaining the posterior probability of each particle, the maximum posterior probability is obtained according to the Maximum aposterior estimation (MAP), and the particle position of the maximum posterior probability is used as the optimal position estimation of the system. Among them, the maximum posterior probability criterion is as shown in equation (3.27):

$$k_T = \arg\max p(k_T \mid m_{1:T}) \tag{3.27}$$

3.4.2 Important steps in the Particle filter algorithm

3.4.2.1 Monte Carlo approximation

By introducing the Bayesian estimation method, complex integral operations are used in calculating the prior probability and the posterior probability, and the integral

operation increases the complexity of the calculation. The Monte Carlo approximation can transform complex integral operations into summation operations and convert non-random problems into random problems. The idea is to convert the solution problem into the probability of a random event by transforming solution direction. By model sampling statistics, the frequency of event occurrence is approximated as the probability of event occurrence. Finally, the estimation of the probability completion parameter is calculated[55].

The Monte Carlo approximation method randomly collects N samples $\{k_{0:T}^{i}\}_{i=1}^{N}$ in posterior probability density $p(k_T \mid m_{1:T})$. Each sample point is independent of each other. The posterior probability is calculated as shown in equation (3.28):

$$p(k_T \mid m_{1:T}) \approx \frac{1}{N}\sum_{i=1}^{N}\delta(k_{0:T} - k_{0:T}^{i}) \tag{3.28}$$

Of which, $\delta(\cdot)$ is Dirac function.

Monte Carlo approximation step in solving the parameter estimation is divided into three steps:

(1) Establish a probability model describing the event

The deterministic problem without randomness is transformed into a randomness problem.

(2) Sampling from known probability distributions

Sampling is performed in a known probability distribution to obtain a sequence of random variables having known probability distributions and independent of each other. A common sampling method is uniform sampling from (0, 1).

(3) Calculated estimate

After sampling, the value of the random variable needs to be solved and used as the Monte Carlo estimate, which is called unbiased estimation. A plurality of estimated values is established for the random variable, and the estimated values are selected to finally determine an estimated value as a solution to the problem.

3.4.2.2 Sequential importance sampling (SIS)

In the practical application of PF algorithm, the posterior probability is difficult to achieve, and sampling from the posterior probability distribution is more difficult. To deal with this problem, the SIS method is introduced. The core idea is to introduce a known function $q(k_{0:T} \mid m_{1:T})$. In this known distribution function, the acquisition sample is replaced by sampling in the original distribution function, and the sampling result is used to approximate the target state density function. Sampling in a known function yields a group of sample points, particle: $\{k_T^{(i)}, \omega_T^{(i)}\}_{i=1}^N$, where k_T indicates the state of the i-th particle at time T, and w_T indicates the weight of corresponding particle. The posterior probability obtained by importance sampling is as shown in equation (3.29):

$$p(k_T \mid m_{1:T}) \approx \sum_{i=1}^{N} \omega_T^{(i)} \delta(k_{0:T} - k_{0:T}^i) \tag{3.29}$$

Of which, the expression of $\omega_k^{(i)}$ is as shown in equation (3.30):

$$\omega_k^{(i)} = \frac{p(k_{0:T}^{(i)} \mid m_{1:T})}{q(k_{0:T}^{(i)} \mid m_{1:T})} \tag{3.30}$$

From equations (3.29) and (3.30), it is known that when calculating the posterior probability, observations at various times are required. The important sampling method adopted by the PF algorithm is the Sequential Important Sampling (SIS) method, which introduces the sequential idea, and decomposes the importance density function to obtain a recursive calculation method. It is shown in equation (3.31):

$$q(k_{0:T}^{(i)} \mid m_{1:T}) = q(k_{0:T-1}^{(i)} \mid m_{1:T-1}) q(k_T \mid k_{0:T}^{(i)}, m_{1:T}) \tag{3.31}$$

The posterior probability is calculated as shown in equation (3.32):

$$\begin{aligned} p(k_T \mid m_{1:T}) &= \frac{p(m_T \mid k_{0:T}, m_{1:T-1}) p(k_{0:T} \mid m_{1:T-1})}{p(m_T \mid m_{1:T-1})} \\ &\propto p(k_T \mid k_{T-1}) p(m_T \mid k_T) p(k_{0:T-1} \mid m_{1:T-1}) \end{aligned} \tag{3.32}$$

The particle weight can be calculated by recursion, as shown in equation (3.33):

$$\omega_T^{(i)} \propto \frac{p(m_T \mid k_T)p(k_T \mid k_{T-1})p(k_{0:T-1} \mid m_{1:T-1})}{q(k_{0:T-1}^{(i)} \mid k_{1:T-1})q(k_T^{(i)} \mid k_{0:T-1}^{(i)}, m_{1:T})} \tag{3.33}$$

$$= \omega_{T-1}^{(i)} \frac{p(m_T \mid k_T^{(i)})p(k_T^{(i)} \mid k_{T-1}^{(i)})}{q(k_T^{(i)} \mid k_{0:T-1}^{(i)}, m_{1:T})}$$

Finally, the weight w needs to be normalized, as shown in equation (3.34):

$$\tilde{\omega}_T^{(i)} = \frac{\omega_T^{(i)}}{\sum_{i=1}^{N} \omega_T^{(i)}} \tag{3.34}$$

3.4.2.3 Re-sampling

In the process of recursive particle filter algorithm, the particle set will degenerate. The weight of most particles will become very small. The most direct and effective way to solve the problem of particle degradation is to increase particle number but increasing the number of particles will increase the amount of calculation. Another effective method is to re-sample the particles and decompose the particles with larger weights into multiple equal weight particles. The number of particles is always N [56]. The re-sampling schematic is shown in Figure 3.5.

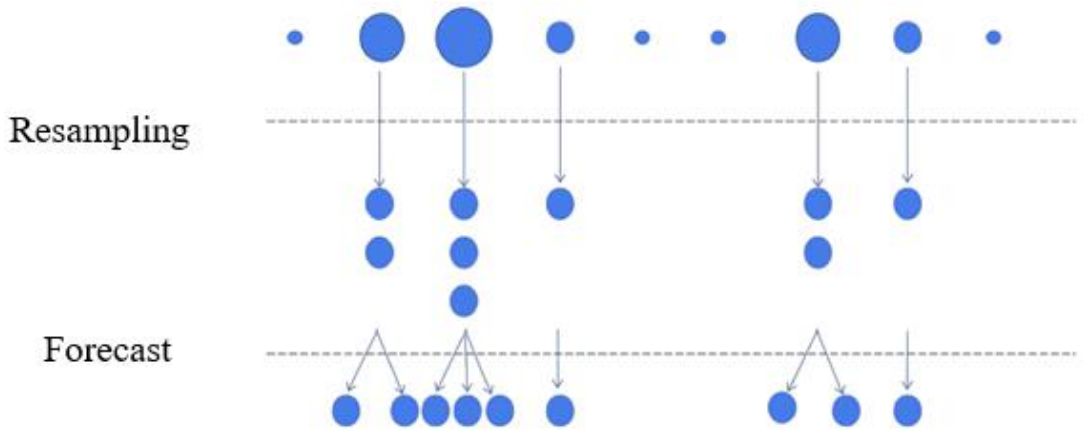

Figure 3.5 - Particle resampling schematic

The implemented Particle Filter code in Matlab is shown in Figure 3.6:

```
%--------------initialize the variables-----------------
x = 0;                                  % initial actual state
x_N = 1;                                % The covariance of system process noise
x_R = 1;                                % Measure the covariance of noise in the process
T = 75;
N = 100;                                % The particle number. The larger the effect, the better
                                           %and the larger the computation
%--------------initilize our initial, prior particle distribution as a gaussian around
%--------------the true initial value-------------------
V = 2;                                  %The variance of the initial distribution
z_out = [x^2 / 20 + sqrt(x_R) * randn]; %Observation of the particle
x_out = [x];                            %the actual output vector for measurement values.
x_est = [x];                            % time by time output of the particle filters estimate
x_est_out = [x_est];                    % the vector of particle filter estimates.
for t = 1:T
    x = 0.5*x + 25*x/(1 + x^2) + 8*cos(1.2*(t-1)) +  sqrt(x_N)*randn;
    z = x^2/20 + sqrt(x_R)*randn;
    for i = 1:N
%--------------Sampling from prior probabilities--------------
        x_P_update(i) = 0.5*x_P(i) + 25*x_P(i)/(1 + x_P(i)^2) + 8*cos(1.2*(t-1)) + sqrt(x_N)*randn;
%--------------Calculate the value of the sample particle-----
        z_update(i) = x_P_update(i)^2/20;
%--------------Calculate the weight for each particle---------
        P_w(i) = (1/sqrt(2*pi*x_R)) * exp(-(z - z_update(i))^2/(2*x_R));
    end
%--------------The normalized.--------------------------------
    P_w = P_w./sum(P_w);
%--------------Resampling-------------------------------------
    for i = 1 : N
        x_P(i) = x_P_update(find(rand <= cumsum(P_w),1));% Particle weight will be more important to get offspring
    end
%--------------state estimation-------------------------------
    x_est = mean(x_P);
%--------------Save data in arrays for later plotting---------
    x_out = [x_out x];
    z_out = [z_out z];
    x_est_out = [x_est_out x_est];
end
```

Figure 3.6 - Particle filter code in Matlab

Chapter 4 RFID Localization System

4.1 RFID characteristics

RFID is an identification technology. It was launched in the 1990s. It automatically identifies target objects and obtains information through RF signals. The processing of whole work doesn't need to use manual intervention. Therefore, the technology greatly improves the work efficiency in a harsh environment [57].

Although RFID technology is already mature, its research and development has not stopped. The current research on this technology is mainly carried out from the following aspects. The first is the development of RFID standards. RFID has not yet formed a unified technical standard in the world, many international standardization organizations have actively developed their own standards, and they hope to promote their own standards as international standards through different channels. The second is communication technology research. The third is the specific application research of the technology. At present, individual national institutions have already taken the lead in the world. The most influential standard is ISO18000, and RFID technology and applications are relatively complete under the standards of this series. In addition, the United States, as a technology power, is not willing to join, EPC Global jointly sponsored by UCC and EAN. There is also a place in the global market, where there are many large companies like retail giants such as Wal-Mart and Tesco in the UK, and technology research has won the support of Microsoft and IBM [58].

4.2 System Structure

The composition of RFID system is made up of roughly three basic parts: terminal control system, reader and tag [59], as shown in Figure 4.1. The label is attached to the object to be identified and each label has EPC. This code is unique, and it is the uniqueness of this code that successfully realizes the recognition or positioning of the

object. Reader (also known as reader/writer): mainly reads the tag information and realizes automatic recognition of the object to be tested. In addition, in order to be able to reuse resources, the label can also be wiped and written. Finally, the tag sometimes has an antenna to increase the transmit power. Central Information System: This system is more complex, not only has two parts of information processing system and database, but also includes middleware.

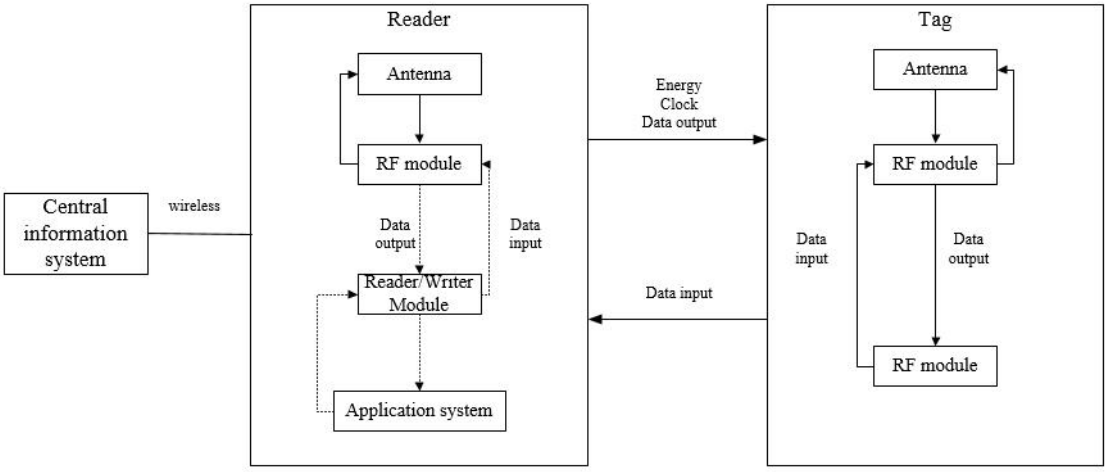

Figure 4.1 - RFID system structure

4.2.1 Hardware System

The hardware of localization system designed in this work mainly includes passive high-frequency tag, Raspberry Pi 3, feeder and RC522(Figure 4.2). Among them, the PC terminal and the reader are set in the same local area network through the router, and the feeder and the antenna are used to connect and communicate with each other. The following is a brief introduction to the operating characteristics of these RFID devices.

(1) RFID reader

RFID reader is indispensable as one of the core components of the positioning system. The reader consists of two basic functional blocks: the read/write module and the RF module. Figure 4.3 presents the structure diagram. The read/write module not

only needs to perform similar modulation and demodulation processing on the collected signals, but also needs to encode and modulate the signals of the transmitted data .

The reader of this article is an RFID reader made by connecting Raspberry Pi3, feeder and RC522, as shown below. The RFID reader is based on MFRC522. The MFRC522 gets data by the SPI protocol. The interface correspondence is shown in Table 4.1 below.

Figure 4.2 - Definition of RC522 RFID Module[60]

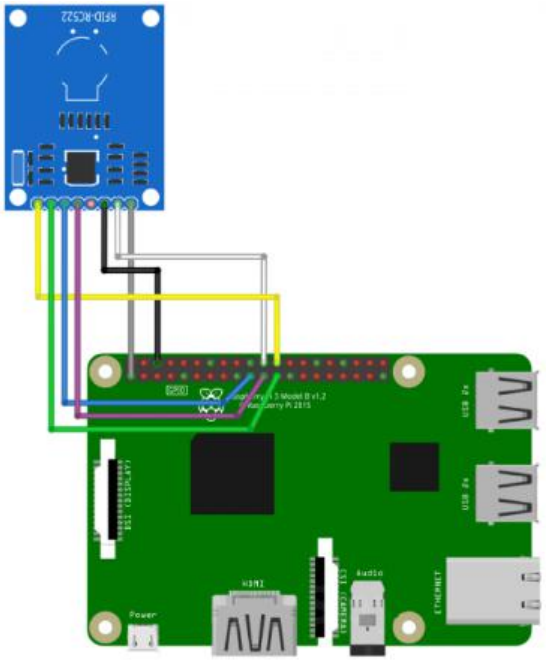

Figure 4.3 - RC522 RFID Module and Raspberry Pi Circuit Connection[60]

Table 4.1 Interface Correspondence

RC522 Header	Diagram Colour	Pi Header	Notes
3.3V	Grey	1	3.3V
RST	White	22	GPIO25
GND	Black	6	Ground

IRQ	-	-	
MISO	Purple	21	GPIO9
MOSI	Blue	19	GPIO10
SCK	Green	23	GPIO11
SDA	Yellow	24	GPIO8

(2) RFID Tag

In the RFID system, an electronic device that stores data and information of an object to be identified is called an electronic tag. The basic structure is a coupling circuit, a chip and a radio frequency interface, and individual electronic tags have micro antennas for increasing the acceptance and transmission power.

The classification of labels is varied [61]. Table 4.2 shows the comparison of tags.

Table 4.2 Tags comparison

Project	**Active tag**	**Passive tag**	**Semi-active tag**
Power supply mode	Power supply	Antenna coupling	Power supply and Antenna coupling
Work frequency	455MHZ、2.45GHZ	13.56MHZ 860-960MHZ	
Comminication distance	20-100m	Within 10m	Less than 30m
Working mode	Beacons	Responder	Responder
Applied range	Large cargo	Small cargo	Large or small cargo
Advantage	Long work distance	Less cost	Fast recognition speed
Disadvantage	Supply	Short distance	Supply

The above describes the selection of the label. This work chooses passive high-frequency tags (13.56MHz), and the physical object of the tag is shown in Figure

4.4. The advantages of this tag are small size and can be applied to different environments.

Figure 4.4 - RFID Passive High-frequency Tags(13.56MHz)[60]

4.2.2 Software System

The system of positioning platform based on passive RFID is composed of embedded platform software system and PC application software system, as shown in the Figure 4.5. The embedded platform software mainly includes embedded real-time operating system, device driver, communication protocol and application software. The main task is to complete the data communication, signal measurement, positioning calculation between the devices, and then send the positioning results to the PC application software. The work of PC application software is to complete real-time display of the positioning results according to the positioning coordinates transmitted from the embedded system.

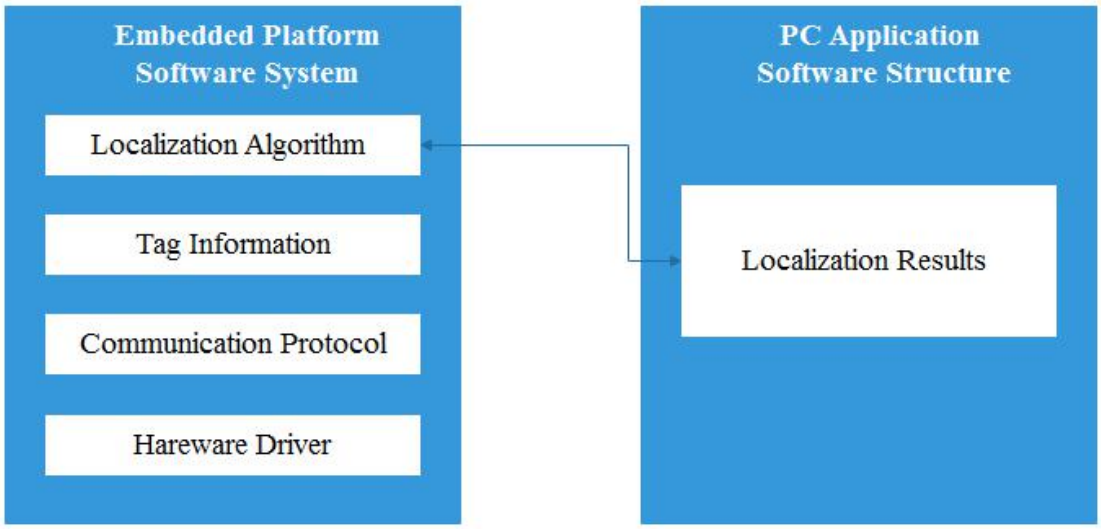

Figure 4.5 - Passive RFID location platform software architecture

The overall workflow of the passive RFID positioning system in this work:

(1) First, lay the high-frequency reference tag, record the code and location of the reference tag, and then create a fingerprint library.

(2) Next, when the RFID reader passes through the various reference tags, the electronic tag will be activated, and the reader will receive the tag information as shown in Figure 4.6.

```
pi@rpispy:~/MFRC522-python $ python Read.py
Welcome to the MFRC522 data read example
Press Ctrl-C to stop.
Card detected
Card read UID: 233,156,85,229
Size: 8
Sector 8 [0, 0, 0, 0, 0, 0, 0, 0, 0, 0, 0, 0, 0, 0, 0, 0]
Card detected
Card read UID: 148,35,65,119
Size: 8
Sector 8 [0, 0, 0, 0, 0, 0, 0, 0, 0, 0, 0, 0, 0, 0, 0, 0]
```

Figure 4.6 - The terminal of RFID localization system

(3) The tag information is transmitted to the Firebase database through the gateway, and then the fingerprint database is matched to obtain a specific positioning result.

4.3 RFID Classic localization algorithm

RFID positioning algorithms are classified into many different types. According to whether the positioning result is absolute coordinate, or the result expression form, it can be split into two categories: absolute positioning and relative positioning. Absolute positioning means that the final output information is absolute position coordinate, and has specific coordinate value or latitude and longitude. Relative positioning means that the final output information is relative position information and is a reference information [62]. According to different positioning targets, it can be split into reader positioning and tag positioning. If a reader is installed on the mobile carrier, the reference label is deployed in the area where the positioning needs to be completed, and the value measured after the carrier enters the positioning area is matched with the reference label value whose position is known, which is the positioning principle of the reader positioning method. However, the label positioning method is the opposite. The fixed reader and the label move with the target cargo to be tested. According to the information collected by the reader, different algorithms are used for positioning. The label positioning method is more commonly used[63]. As shown in Figure 4.7.

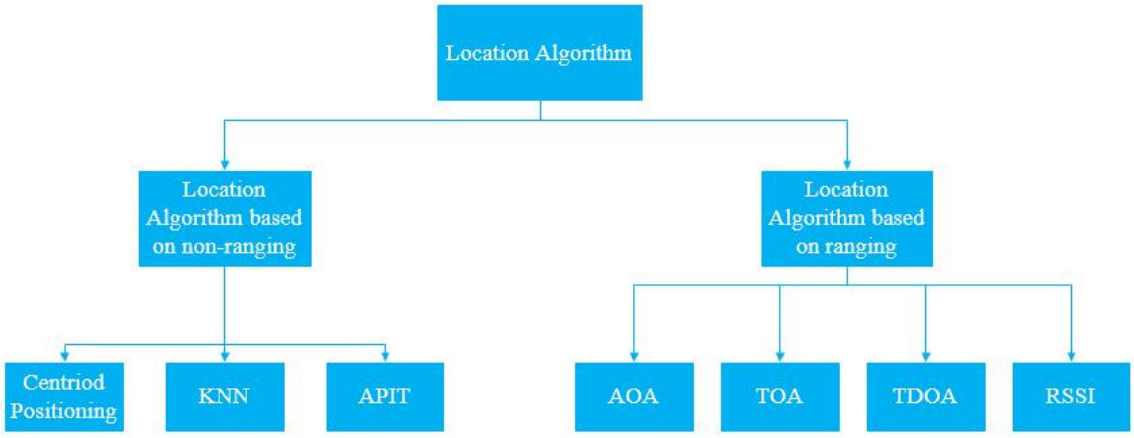

Figure 4.7 - RFID Localization algorithm

4.3.1 Triangulation localization

The triangulation method is to locate position coordinates of the object to be measured by the geometric principle of the triangle based on the measured data [64]. The two positioning methods are similar in positioning principle.

In Figure 4.8, A, B, and C represent three readers, and the positions of the three readers are known. When the target P to be tested enters the scanning range of the reader, the reader will automatically recognize the electronic tag carried on the target P. When measured and calculated, the distance from the reader to the tag r1, r2, r3 can be obtained. In practical applications, there are many ways to obtain the distance between r1, r2 and r3. The current mature is measured by methods, such as AOA、TOA、TDOA and RSSI.

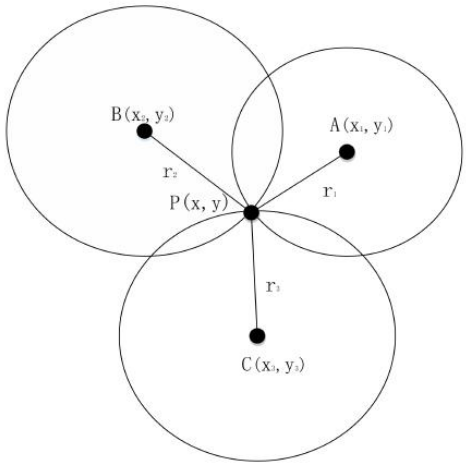

Figure 4.8 - Triangulation localization method

4.3.2 Approximation localization

The approximation positioning method generally provides the relative position information of the target and is the easiest way to implement many positioning methods. Its specific measurement theory: many antennas are arranged in the area where the object is running, and the positions of these antennas are known. When the target to be

positioned carrying the electronic tag enters the range of an antenna, the antenna acquires the signal of the electronic tag, thereby obtaining the location of the electronic tag. However, if the number of detected electronic tags is large, it is processed by RSSI. Compared with the triangulation method, this method has lower hardware requirements for the device and is simpler to implement. However, the method has limited positioning accuracy and usually obtains higher positioning accuracy in combination with other positioning methods [65].

4.3.3 Scene analysis localization

The scene analysis method is also generally called position fingerprint location method, and because its measurement process is based on the database, it is also called database related positioning. The system method firstly collects the buried tag signal of the known position at different positions during the walking of the carrier and establishes a mapping relationship database according to the measurement signal and the measurement position for use. The biggest drawback of this method is that the positioning accuracy is directly linked to the database. To obtain the high precision of the positioning, the amount of information in the database needs to be sufficient. This requires that the electronic label arrangement density be as large as possible. To obtain higher positioning accuracy, the workload in the early stage is larger[66].

4.4 Database-based RFID localization algorithm

RFID tags are divided into active tag and passive tag. RFID active tag generally has the characteristics of large volume and high cost, and its signal strength has a great relationship with the tag battery. RFID passive tag has the advantages of low cost, small size, suitable placement, and relatively short action distance. Therefore, this work adopts the RFID passive tag for positioning.

Passive RFID positioning system is mainly used to arrange reference tags with known location information in the environment. By detecting reference tags, positioning calculation is carried out according to the location information of reference tags. Therefore, it has strong environmental adaptability. By establishing two-dimensional coordinate system, the reference labels are arranged in a regular way, and the reader is placed on the carrier of the moving target. When the reader is carried by the moving target, the reference tag nearby can be read, and the position of the car can be calculated according to the position information of the reference tag.

The average value of all tag positions read by the reader is taken as the position of the moving target, and the positioning calculation equation (4.1) is as follows:

$$\left(x', y'\right)_j = \left(\frac{\sum_{i=1}^{n} x_i}{n} \quad \frac{\sum_{i=1}^{n} y_i}{n} \right)_j \tag{4.1}$$

Of which, $\left(x_i, y_i\right)$ represents the position of $i-th$ reference tag. n represents the total number of reference tags that was read at time j. $\left(x', y'\right)_j$ represents the calculated positioning of the moving vector at time j. Location theory based on reference tags is shown Figure 4.9:

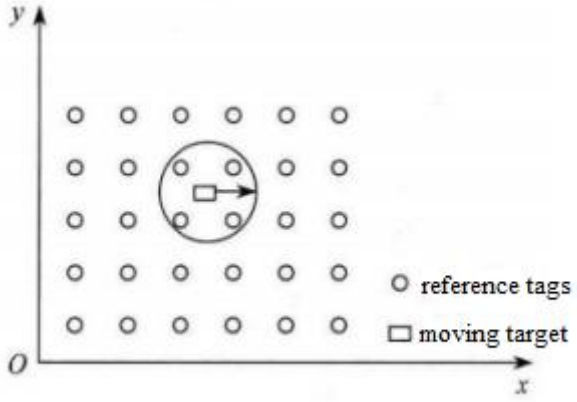

Figure 4.9 - Location theory based on reference tags

Chapter 5 UWB Localization System

5.1 UWB signal characteristics

UWB is a commonly used technique in radio communication, high-precision positioning, and signal tracking applications. As an emerging wireless technology [67], UWB signals have significant features compared to other wireless signals. According to the US FCC [68], UWB must have an absolute bandwidth of more than 500M when applied in the civilian field. The relative bandwidth is defined as:

$$B_f = 2\frac{f_H - f_L}{f_H + f_L} \tag{5.1}$$

Of which, f_H and f_L are the up and down cutoff frequencies of 10 dB bandwidth, respectively. According to the relevant regulations, the UWB signal bandwidth in the civilian field is from 3.1 to 10.6 GHz, and UWB signal system can be divided into two types[69], namely, MB-OFDM and pulse radio. The former divides the entire frequency band into multiple sub-bands, which can improve the frequency band utilization, and each sub-carrier is processed separately, making the UWB system more flexible. The latter communicates by using sub-nanosecond pulse, which has the advantages of high time resolution, anti-interference, and anti-multipath. The UWB module used in this paper uses the latter communication method, namely pulse radio. According to the literature [70], the characteristics of UWB in actual use are as follows:

(1) Low cost and low power consumption

(2) Good concealment

(3) Anti-multipath effect

(4) High positioning accuracy

(5) High transmission rate

In view of the unique characteristics of the above UWB technology, UWB technology has become a hot research direction in high-precision positioning.

5.2 System Structure

This work uses UWB localization system based on DWM1000. It uses the radio frequency transceiver chip DWM1000 produced by Decawave company as the core, and on this basis, it carries out the research of hardware design and development and software algorithm of UWB anchor and the tag. Finally, UWB can achieve that the ranging accuracy is about 10cm in line-of-sight condition and the positioning accuracy is about 30cm in NLOS condition. Figure 5.1 presents structure of UWB localization system.

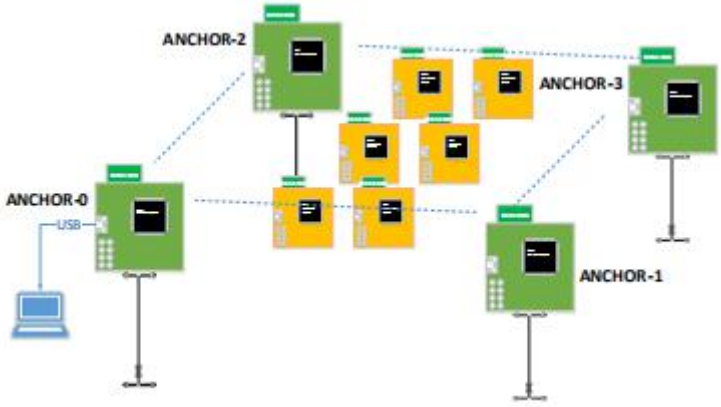

Figure 5.1 - UWB Localization System

The composition of the UWB system is made of roughly three basic parts: anchor, tag, and the location server platform(PC). The anchor is a module for ranging, and the tag receives a ranging request of the anchor. If the final positioning solution is to be completed, the positioning system of UWB needs the anchor, tag and positioning solution platform. In the environment where positioning is required, the anchor is installed and placed in the known position coordinates, and it will be placed together with the target to be located at the tag of the ranging and positioning equipment. In the environment, the anchors need to be placed in the known coordinate positions, and the tags that need to be measured can move freely in the space. The anchor transmits UWB signal, and the measured tag under test after receiving the corresponding UWB signal calculates the distance between them through the signal flight time and sends the distance information to the positioning solution platform. The positioning solution

platform receives the measured distance information and runs the corresponding positioning solution algorithm to obtain the spatial coordinate position of the tag. Finally, the results are sent to the host computer for display through the anchor.

5.2.1 System Hardware

The anchor and tag modules adopt STM32F105 microcontroller as the main control chip. The peripheral circuits include: DWM1000 module, power module, LED indicator module, dial switch and reset circuit,etc. The structure diagram is shown in Figure 5.2 below.

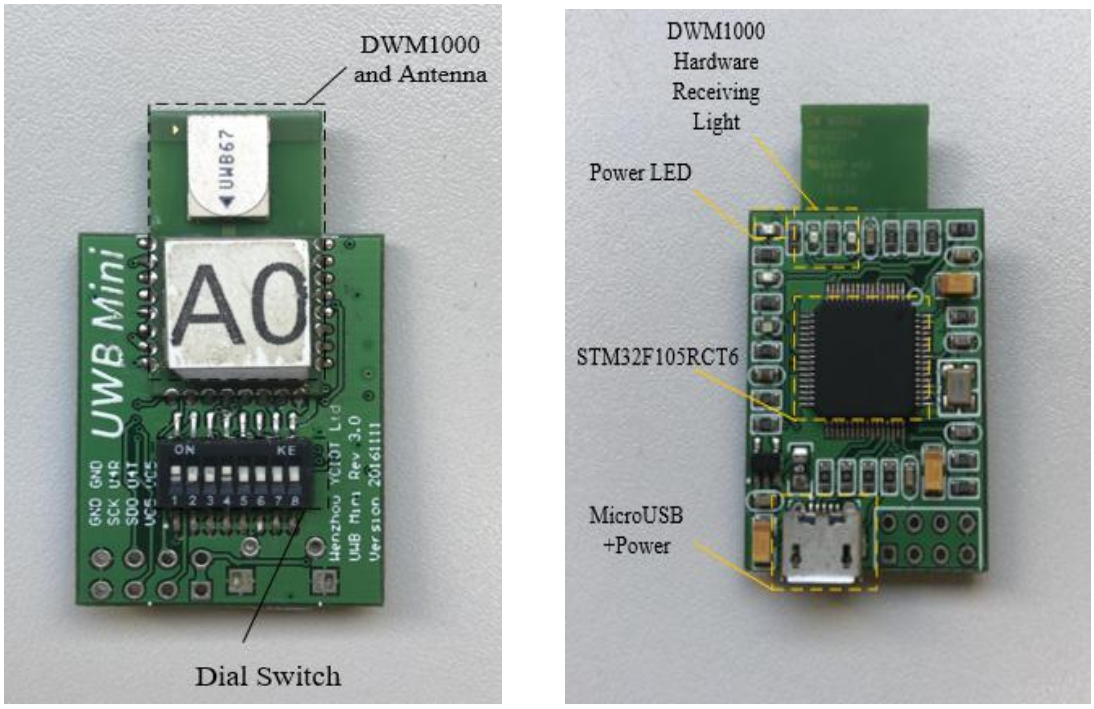

Figure 5.2 - UWB Mini Front View and UWB Mini Rear View

5.2.1.1 Microprocessor Module

STM32 refers to a series of chips based on 32-bit flash microcontroller, which is specially developed for embedded application development. STM32 microcontroller can meet the requirements of high performance, low cost and low power consumption. This has abundant on-chip and off-chip resources, large storage capacity, good user

development environment, low power consumption, simple and convenient peripheral circuit expansion.

The STM32F105 has the following functions:

(1) Core: cortex-m3 controller(ARM32).

(2) Memorizer: The chip is integrated with 128KB Flash memory and can embed up to 20KB of SRAM.

(3) Three low power modes: Stop, sleep, standby; VBAT to power the RTC and backup registers.

(4) 80 I/O ports.

(5) DMA: Seven channel DMA controller.

(6) Nine communication interfaces: two I2C ports; three USART ports; two SPI ports; CAN ports; USB2.0 port.

STM32F105 microcontroller is the controller of the anchor and tag, which can provide corresponding timing sequence for DWM1000 circuit and realize data interaction. It can also complete data interaction with PC through serial port conversion circuit and complete reset of the whole system. The used unit of STM32F105 includes external crystal oscillator, reset and program download JTAG interface. The main clock of STM32F105 system is provided in the way of the 8MHz passive crystal oscillator. The main clock frequency of the system can be changed up to 72MHz by software configuration of the clock frequency multiplier or frequency divider.

5.2.1.2 RF Transceiver Module

UWB radio frequency (RF) transceiver circuit is the main part of this positioning system. The data interaction between the anchor and tag is carried out through UWB and the distance measurement is completed by SDS-TWR ranging algorithm, which provides accurate distance information for the following positioning work.

The UWB RF transceiver module is designed using DWM1000 produced by DecaWave company. DWM1000 module is a low-power, single-chip CMOS RF transceiver high-precision integrated circuit chip that conforms to IEEE 802154-2011

UWB standard. UWB technology has excellent anti-multipath fading ability and can still carry out reliable communication in the high-fading environment, and the positioning accuracy can reach centimeter level. DWM1000 module sends the UWB signal to another DWM1000 module. The latter will calculate the time of received UWB signal by flight time to locate the distance. It is easy to know that the distance can be located, and the ranging error is about 10cm. The block diagram of DWM1000 is shown in the Figure 5.4.

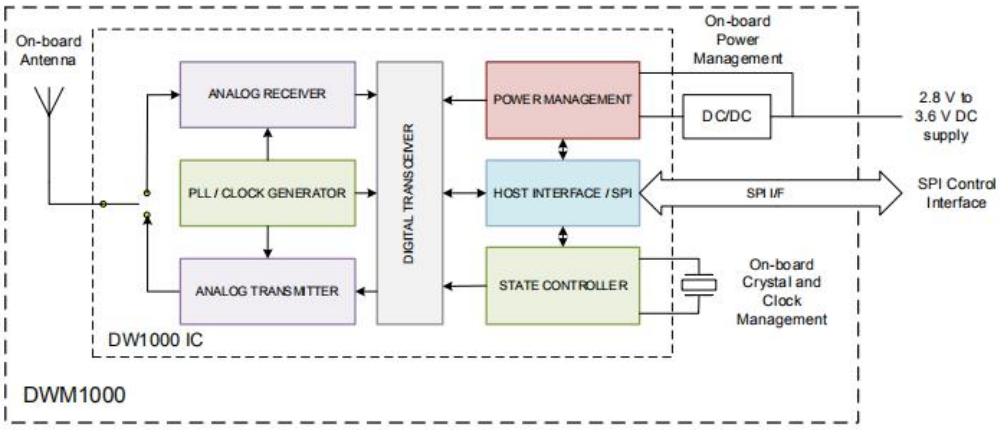

Figure 5.3 - DWM1000 Block Diagram[71]

The arrow directions in the figure represent the interactions between the parts. The digital transceiver mainly receives data from the host processor and provides data received by the host processor.

DWM1000 normally operates at a voltage of + 3.3v. Some resources on the chip can be externally powered by + 3.3v, and the rest can be powered by on-chip LDO step-down to + 1.8v. These LDOs are grounded by an external decoupling capacitor connected to the relevant pins and by a decoupling capacitor of 0.1 F. DWM1000 has 8 GPIO，all of which can be configured as the second function. In this system, the GPIO0, GPIO1, GPIO2, and GPIO3 are connected to the LED light, and the LED indicator is used to display the running state of the system. SPICS, SPICLK, and SPI MISO are connected to the pins corresponding to the SPI module in the master control chip STM32F105 as the communication interface between DWM1000 and STM32F105. The peripheral connecting circuit of the chip DWM1000 is shown in the Figure 5.5.

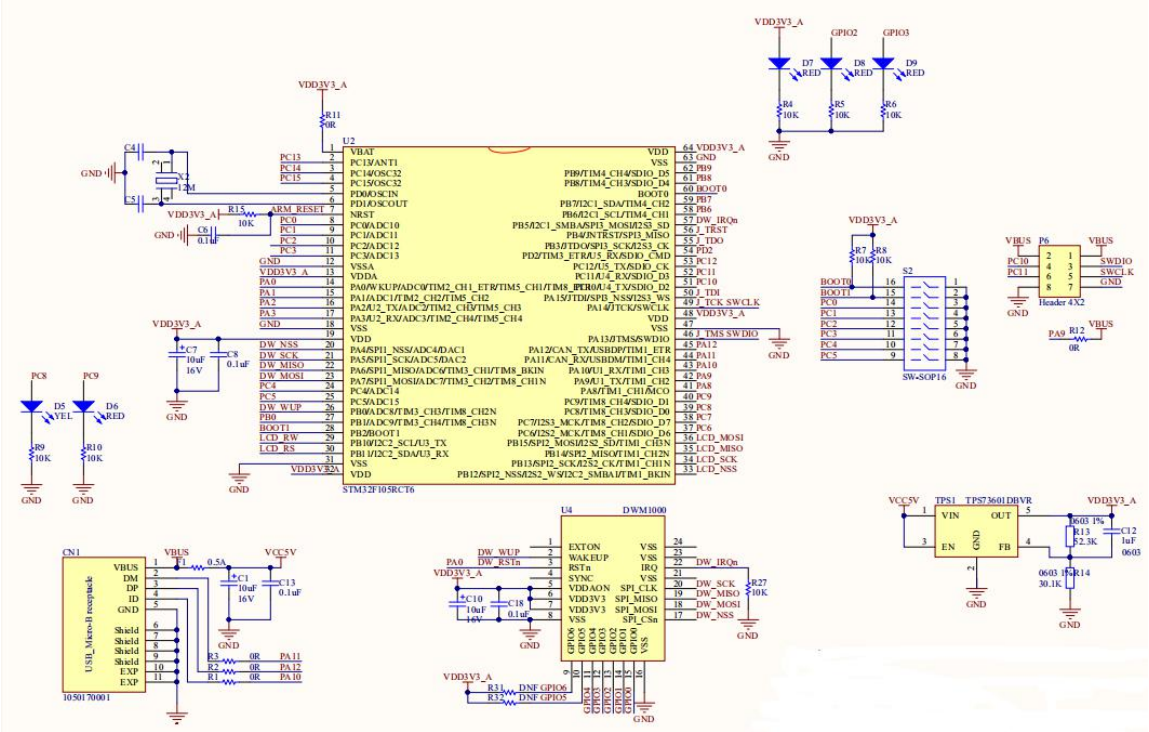

Figure 5.4 - DWM1000 peripheral connecting circuit[72]

UWB has less power than WIFI and should be harmless to people. The viable frequency range of DMW1000 supported UWB channels [65] is shown in the Figure 5.6 and Table 5.1 below.

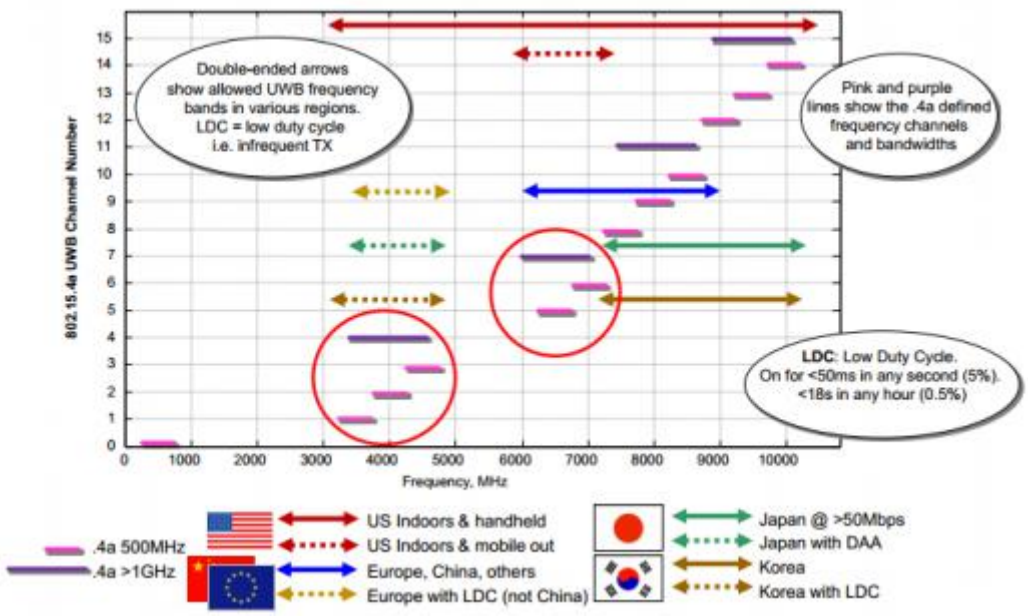

Figure 5.5 - DWM1000 viable frequency range [73]

Table 4.1 UWB IEEE802.15.4-2011 UWB channels supported by DWM

UWB Channel Number	Centre Frequency (MHz)	Band (MHz)	Bandwidth (MHz)
1	3494.4	3244.8-3744	499.2
2	3993.6	3744-4243.2	499.2
3	4492.8	4243.2-4742.4	499.2
4	3993.6	3328-4659.2	1331.2
5	6489.6	6240-6739.2	499.2
7	6489.6	5980.3-6998.9	1081.6

As shown in the Figure 5.6 and Table 4.1, the frequency band used in Europe is 6.0 to 10.6GHZ. In the channel division, there are two types of channels, one is a 500MHz channel and the other is a 1GHz channel. In the UWB product development, a 500MHz channel is currently mainly used. Therefore, this work will choose channel 5.

5.2.2 System Software

The high-level computer software was developed in QT5.7.0MinGM, that supports C++. QT is a graphical user interface application developed by Trolltech. It can be not only used to develop GUI programs, but also develop non-GUI programs. QT is an object-oriented framework.

The implemented main functions for the host computer are:

(1) establishing a connection with the virtual serial port Virtual COM Port of the UWB module.

(2) reading the TOF report message from the UWB module.

(3) Anchor list. In this list, actual placement position of the anchor can be set.

(4) Tag list. This list shows the distance of the tag from the anchor and position of the tag (xyz coordinates)

(5) Map display.

The developed host computer interface is shown in Figure 5.7 below:

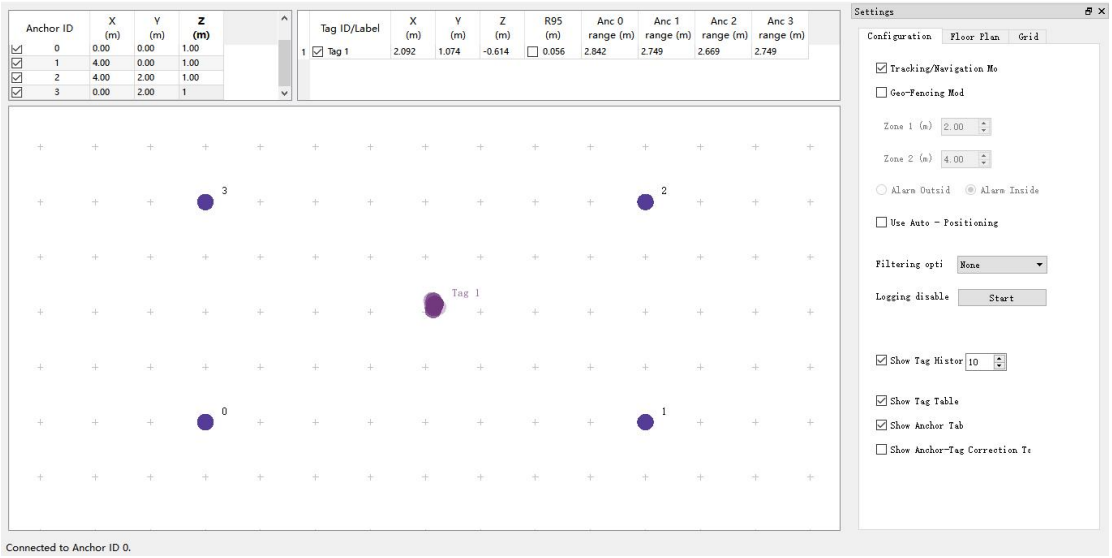

Figure 5.6 - UWB Localization System Interface

5.3 Classic localization algorithm

The execution flow of different wireless positioning technologies is basically the same: the receiver first extracts some eigenvalues from the received signals, and then uses the correlation algorithm to calculate and process the eigenvalues to complete the ranging and positioning. According to the different types of positioning algorithms, they are mainly divided into the positioning algorithm that requires ranging and direction measurement, and the positioning algorithm that does not require ranging and direction measurement. UWB ranging method mainly has four kinds of more mature algorithms, respectively: TOA, TDOA, AOA, RSSI. The type of localization algorithm is generally split into two steps, the first step: measuring time, Angle, Angle of the signal; The second step: according to the geometrical position of the various nodes or fingerprint signal strength, calculate the relative position or matching tag. As shown in Figure 5.8.

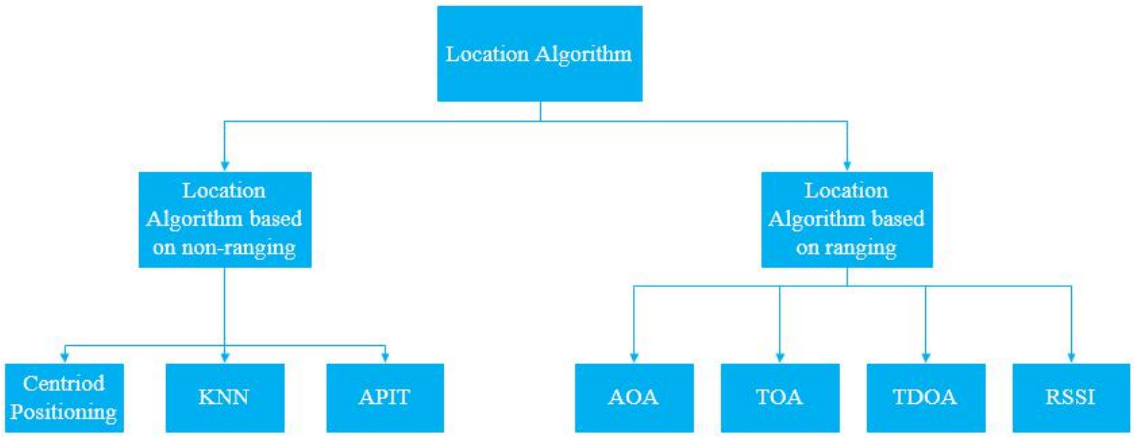

Figure 5.7 - Location Algorithm Classification

5.3.1 Angle of arrival (AOA)

AOA is a wireless positioning technology based on arrival of angle. The premise of the AOA positioning algorithm is that an additional hardware device array antenna is required, and the algorithm complexity is also high. AOA mainly collects the direction information of the signal through the directivity of the antenna. The positioning principle of AOA location estimation technology: the antenna array of the anchor observes the arrival direction of the signal in all directions [74]. The relative orientation or Angle between tag and anchor is obtained by the relative Angle between UWB signal and anchor. And then it can get the location of tag.

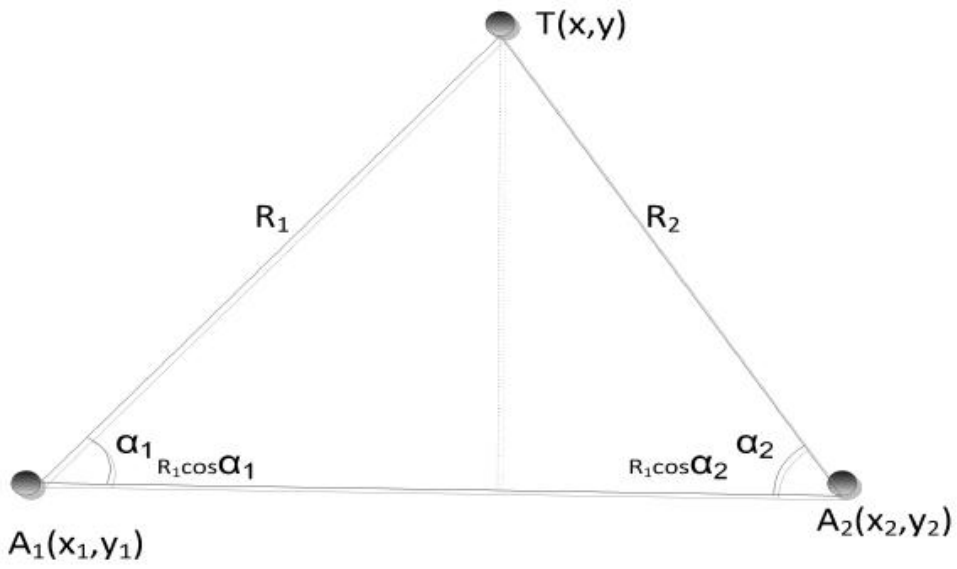

Figure 5.8 - AOA Algorithm Principle

As shown in the Figure 5.9 above, A1 and A2 are anchor nodes, and their position coordinates are known, (x1, y1) and (x2, y2). T is the tag node, and its position coordinates set to (x, y). R1, R2 are the distance between anchor node 1, the anchor node 2 and the label node, respectively. The connection between A1 and A2 is used as the baseline. $\alpha 1$、$\alpha 2$ are the angles measured by the directional antenna, respectively. Therefore, the positional relationship between the tag node T and the anchor nodes A1 and A2 can be expressed by the expression:

$$\begin{bmatrix} x \\ y \end{bmatrix} = \begin{bmatrix} x1 \\ y1 \end{bmatrix} - \begin{bmatrix} R1 \cdot \cos \alpha 1 \\ R1 \cdot \sin \alpha 1 \end{bmatrix} \tag{5.2}$$

$$\begin{bmatrix} x \\ y \end{bmatrix} = \begin{bmatrix} x2 \\ y2 \end{bmatrix} - \begin{bmatrix} R2 \cdot \cos \alpha 2 \\ R2 \cdot \sin \alpha 2 \end{bmatrix} \tag{5.3}$$

Combine the two expressions in the equation to solve for the coordinate position of T (x, y).

The main purpose of Wireless positioning algorithm based on AOA is to get the angle value of anchor to the tag arrival signal by antenna. The final positioning error is determined by the measurement angle error, but due to the serious multipath in the environment. The effect has a relatively large influence on this measurement angle. The

measurement error of this positioning algorithm is larger than that of TDOA and TOA, so the AOA algorithm is not the focus of this thesis research.

5.3.2 Time of arrival (TOA)

The TOA positioning algorithm refers to the measurement of the distance by communication between two anchors. Using two ways-time of flight (TW-TOF) technique can be achieving good accuracy on estimating the point-to-point distance between two wireless transceivers. Figure 5.10 presents the principle of TW-TOF.

$$S = c * \left[\left(T_{a2} - T_{a1} \right) - \left(T_{b2} - T_{b1} \right) \right] \tag{5.4}$$

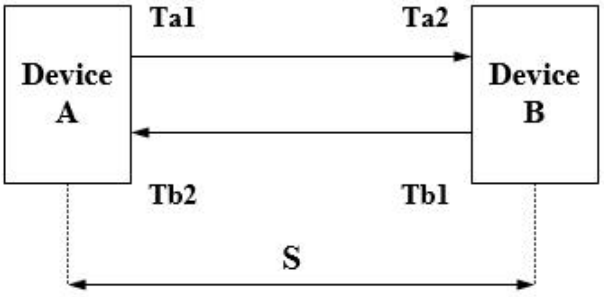

Figure 5.9 - Two-way ranging principle

As long as the distance S is obtained, according to the mathematical geometry principle, the label node is located on the circumference centered on the anchor node (known node) and radius R, and we record it as one measurement data. In the case of an ideal two-dimensional space, as long as three sets of measurement data are calculated, three circles can be obtained, and these three circles get one point, which is the location of a tag[62].

In Figure 5.11 is (shown below), T1, T2, and T3 are anchor nodes of known coordinates, respectively. Their coordinates are $(x_1, y_1), (x_2, y_2)(x_3, y_3)$, and T presents a label node. The coordinates of T are (x, y) and R_i indicates the distance between the

tag and i-th anchor . If the reaction time of each node is not considered, the value of R_i can be expressed by equation:

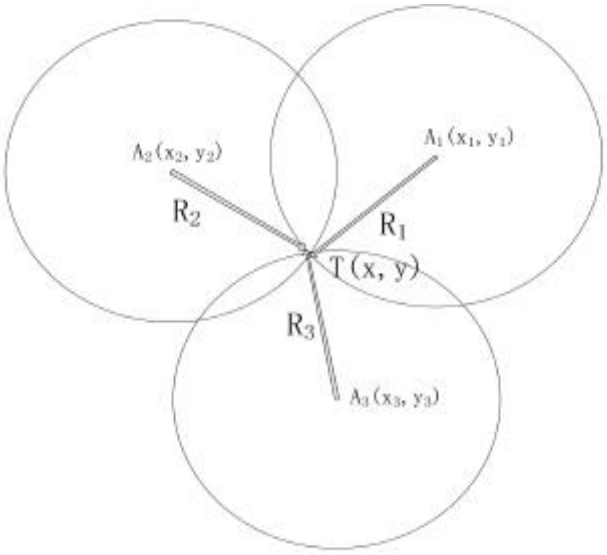

Figure 5.10 - TOA Algorithm Principle

In the equation, t_i represents the timestamp of the tag node receiving the wireless pulse signal of the anchor node, and t_0 represents the timestamp of the anchor node transmitting the wireless pulse signal to the tag node, and c is the light speed. It can be calculated from the equation among three points that R1, R2, R3 can be expressed by the following expressions:

$$\begin{cases} R_1^2 = (x_1 - x)^2 + (y_1 - y)^2 \\ R_2^2 = (x_2 - x)^2 + (y_2 - y)^2 \\ R_3^2 = (x_3 - x)^2 + (y_3 - y)^2 \end{cases} \tag{5.5}$$

As result of the calculation we get:

$$X = (A^T A)^{-1} A^T Y \tag{5.6}$$

Where: $A = \begin{bmatrix} -2x_1 & -2y_1 & 1 \\ -2x_2 & -2y_2 & 1 \\ -2x_3 & -2y_3 & 1 \end{bmatrix}$ $Y = \begin{bmatrix} R_1^2 - K_1 \\ R_2^2 - K_2 \\ R_3^2 - K_3 \end{bmatrix}$ $X = \begin{bmatrix} x \\ y \\ R \end{bmatrix}$

It can be seen from the equation that the TOA positioning algorithm strictly requires anchor and tag to have strict clock synchronization when calculating the time difference of arrival. The hardware requirements are very high, generally for clock

synchronization, or this effect can be achieved by changing the algorithm. At the same time, since the crystal oscillator of the MCU of each node is offset, it is impossible to achieve true clock synchronization. For positioning where accuracy is very sensitive, a little time stamp error is multiplied by light velocity, thus the error will be infinitely magnified.

5.3.3 Time difference of arrival (TDOA)

Base on TDOA positioning algorithm is established and solved by a mathematical model. It is essentially taking advantage of the hyperbolic properties of mathematics. When there are two fixed points, the other moving point will be on the hyperbola with the two fixed points as the focus. When there are such two or more sets of these data structures, the intersection of hyperbola is to get the position of target object[75]. The TDOA algorithm does not require a large correlation between anchor and tag. Unlike TOA, all nodes are required to be clock synchronized. In the field of positioning, the TDOA is generally referred to as an improved TOA. However, the general TDOA also needs to meet the clock synchronization between anchor nodes.

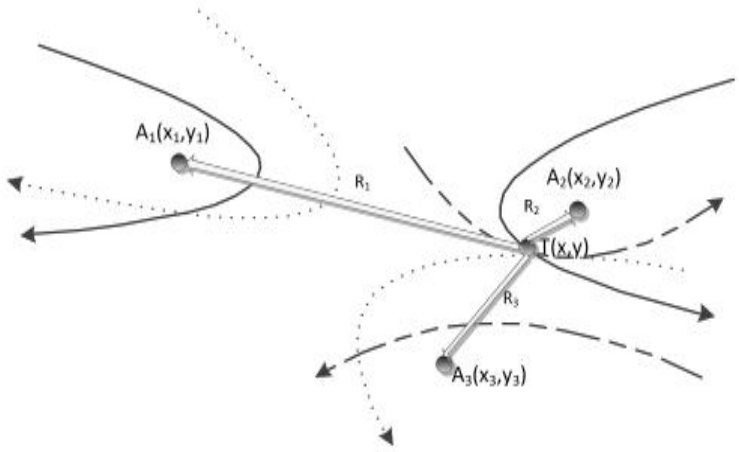

Figure 5.11 - TDOA Algorithm Principle

As shown in the above Figure 5.12, A1, A2, and A3 are anchor nodes, respectively, and the positions can be manually measured as known and are respectively

$(x_1, y_1), (x_2, y_2)(x_3, y_3)$. The location of tag is (x, y), R_i indicates the distance between tag and i-th anchor. It can be expressed as a mathematical expression:

$$R_i = \sqrt{(x_i - x)^2 + (y_i - y)^2} \tag{5.7}$$

$$R_{ij} = c\tau_{ij} = R_i - R_j \tag{5.8}$$

Where : R_{ij} is the distance difference between tag and any two anchors i, j in the positioning environment, c represents light velocity, and $\tau_{i,j}$ represents the measured value of TDOA.

As shown in the Figure 5.12 above, from the characteristics of the hyperbola, the following equation (5.9) and (5.10) is also true:

$$R_{21} = R_2 - R_1 = \sqrt{(x_2 - x)^2 + (y_2 - y)^2} - \sqrt{(x_1 - x)^2 + (y_1 - y)^2} \tag{5.9}$$

$$R_{31} = R_3 - R_1 = \sqrt{(x_3 - x)^2 + (y_3 - y)^2} - \sqrt{(x_1 - x)^2 + (y_1 - y)^2} \tag{5.10}$$

Where: $(R_{21} + R_1)^2 = R_2^2$, then the equation (5.9) and (5.10) can be converted into a quation (5.11).

$$R_{21}^2 + 2R_1R_{21} = R_2^2 - R_1^2 = (x_2 - x)^2 + (y_2 - y)^2 - (x_1 - x)^2 - (y_1 - y)^2 \tag{5.11}$$

$$= x_2^2 + y_2^2 - x_1^2 - y_1^2 - 2(x_2 - x_1)x - 2(y_2 - y_1)y$$

Set: $z_i^2 = x_i^2 + y_i^2$, then the equation (5.11) can be converted tothe equation (5.12) .

$$(x_2 - x_1)x + (y_2 - y_1)y = -R_1R_{21} + \frac{1}{2}(z_2^2 - z_1^2 - R_{21}^2) \tag{5.12}$$

Similarly, the equation (5.12) can be reduced to equation (5.13).

$$(x_3 - x_1)x + (y_3 - y_1)y = -R_1R_{31} + \frac{1}{2}(z_3^2 - z_1^2 - R_{31}^2) \tag{5.13}$$

Put the above equation (5.12) and equation (5.13) together, and use the form of matrix to express it as shown in equation (5.14). .

$$Ax_m = BR_1 + C \tag{5.14}$$

Of which, $A = \begin{bmatrix} x_2 - x_1 & y_2 - y_1 \\ x_3 - x_1 & y_3 - y_1 \end{bmatrix}$ $B = \begin{bmatrix} -R_{21} \\ -R_{31} \end{bmatrix}$

$$C = \frac{1}{2}\begin{bmatrix} z_2^2 - z_1^2 - R_{21}^2 \\ z_3^2 - z_1^2 - R_{31}^2 \end{bmatrix} \qquad X_m = \begin{bmatrix} x \\ y \end{bmatrix}$$

So the position x_m of the tag node can be expressed by the equation (5.15). .

$$x_m = A^{-1}BR_1 + A^{-1}C \tag{5.15}$$

Therefore, TDOA solves the problem that TOA needs clock synchronization between tag and anchor, but it needs clock between anchor nodes, and the crystal oscillator of each module will also drift.

5.3.4 Received Signal Strength Indication (RSSI)

Ranging is defined as calculating distance from reference point to target. The reference point can obtain distance information about the target node by establishing a link to the target node in the network. This communication link is used to calculate the parameter values of the reference point. The parameters are mostly defined on the basis of channel fading or propagation delay [76]. Figure 5.13 shows an example of ranging. In the figure, it is assumed that C is the reference node, and A and B are the target nodes respectively. The ranging information from the reference node to the target node are: r1 and r2 respectively.

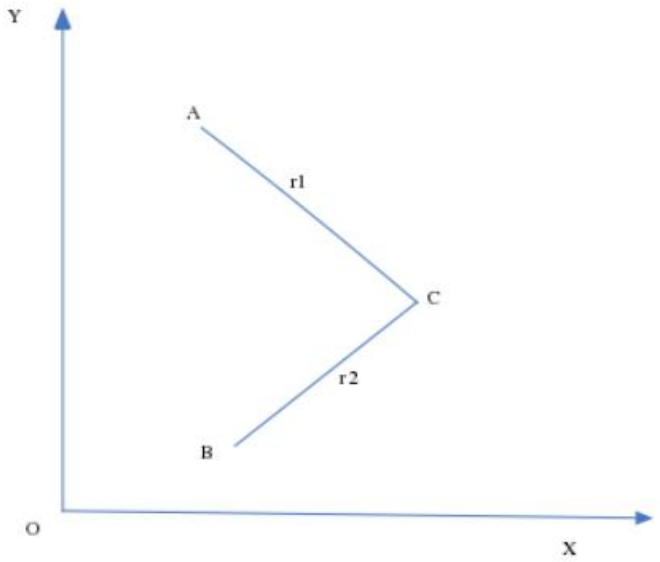

Figure 5.12 - RSSI Ranging Example

Ranging is the estimation of the distance between transmitting node and receiving node. Assuming a given transmission signal $s(t)$, the corresponding received signal is:

$$r(t) = h(t) * s(t) + n(t) \tag{5.16}$$

If the signal propagates on an ideal channel, the ideal channel is assumed to be an UWB radio multipath channel. The channel impulse response expression is:

$$h(t) = A(D)\delta(t - \tau(D)) \tag{5.17}$$

The equation that received signal is:

$$r(t) = A(D)s(t - \tau(D)) + n(t) \tag{5.18}$$

According to the path loss model, it can get the distance between nodes by the received signal energy of a node. Its essence is a distance-based positioning technique. Two-dimensional positioning of a given node requires at least three reference nodes to be obtained by triangulation.

5.4 Improved TOA localization algorithm

This work mainly makes research on 3D positioning algorithms and proposes a 3D-TOA positioning algorithm. The algorithm has a simple structure and a small amount of calculation, which ultimately makes the positioning result more accurate[77].

5.4.1 Localization algorithm

In 3D coordinates, it is assumed that tag is (x, y, z) and anchors that known locations are (X_i, Y_i, Z_i), and it assumes that the distances between tag and anchors are R_i:

$$R_i^2 = (X_i - x)^2 + (Y_i - y)^2 + (Z_i - z)^2 \tag{5.19}$$

$$= K_i - 2X_i x - 2Y_i y - 2Z_i z + R = (c\tau)^2$$

Of which, $K_i = X_i^2 + Y_i^2 + Z_i^2, i = 1,2,3\cdots, R = x^2 + y^2 + z^2$,

Assuming $z_a = [z_p^T, R]^T$ and $z_p = [x, y, z]^T$ as vector. From equation(5.19), an equation with z_a as variable is established:

$$h = G_a z_a \tag{5.20}$$

And the error of tag that the estimated localization is:

$$\psi = h - G_a z_a^0 \tag{5.21}$$

Where: z_a^0 is the z_a value of tag that the actual position.

$$h = \begin{bmatrix} R_1^2 - K_1 \\ R_2^2 - K_2 \\ \vdots \\ R_M^2 - K_M \end{bmatrix}, G_a = \begin{bmatrix} -2X_1 & -2Y_1 & -2Z_1 & 1 \\ -2X_2 & -2Y_2 & -2Z_2 & 1 \\ \vdots & \vdots & \vdots & \vdots \\ -2X_M & -2Y_M & -2Y_M & 1 \end{bmatrix} \tag{5.22}$$

Using the weighted least squares (WLS) method, it will get the covariance matrix of the error ψ:

$$z_a = \left(G_a^T Q^{-1} G_a\right)^{-1}\left(G_a^T Q^{-1} h\right) \tag{5.23}$$

In z_a , (x,y,z) is the approximate estimated location of tag, and the covariance matrix of Q-TOA. Because the Q matrix is a pair of angular matrices .

$$Q = diag\left\{\sigma_1^2, \sigma_2^2, \cdots, \sigma_M^2\right\} \tag{5.24}$$

In equation (5.21), using the Q matrix approximation to replace the covariance matrix of the error vector ψ also introduces some error. Therefore, for the equation, the error of M-TOA measurements is:

$$\psi = 2Bn + n \odot n \approx 2Bn \tag{5.25}$$

$$B = diag\left\{R_1^0, R_2^0, \cdots, R_M^0\right\} \tag{5.26}$$

Set: R_i^0 is distance between i-th anchor and tag.

The error ψ that covariance matrix is constructed by TOA measurements in equation(5.21):

$$\Psi = E\left[\psi\psi^T\right] = 4BQB \tag{5.27}$$

To obtain the B matrix, R_i , obtained by measurement can be replaced for R_i^0 , so the first WLS z_a value is:

$$z_a = \left(G_a^T \Psi^{-1} G_a\right)^{-1}\left(G_a^T \Psi^{-1} h\right) \tag{5.28}$$

Using the value of z_a we get a new B matrix. Next, we calculate the estimated location that covariance matrix:

$$R_i = R_i^0 + cn_i, G_a = G_a^0 + \Delta G_a, h = h^0 + \Delta h \tag{5.29}$$

Where $G_a^0 z_a^0 = h^0$, equation (5.20) indicates:

$$\psi = \Delta h - \Delta G_a z_a^0 \tag{5.30}$$

We set $z_a = z_a^0 + \Delta z_a$,reusing equation (5.25) and (5.30), Δz_a and its covariance matrix are:

$$\Delta z_a = c\left(G_a^T \Psi^{-1} G_a\right)^{-1} G_a^T \Psi^{-1} Bn \tag{5.31}$$

$$\operatorname{cov}(z_a) = E\left[\Delta z_a \Delta z_z^T\right] = \left(G_a^T \Psi^{-1} G_a\right)^{-1} \tag{5.32}$$

The vector z_a is actual value. Equation (5.32) confirms covariance matrix. Therefore, the value of z_a is:

$$z_{a,1} = x^0 + e_1, z_{a,2} = x^0 + e_2$$

$$z_{a,3} = x^0 + e_3, z_{a,4} = x^0 + e_4 \tag{5.33}$$

Of which: e_1, e_2, e_3, e_4 is estimation error of z_a. It can construct new error ψ' that is:

$$\psi' = h' - G_a' z_a' \tag{5.34}$$

Of which: $h' = \begin{bmatrix} z_{a,1}^2 \\ z_{a,2}^2 \\ z_{a,3}^2 \\ z_{a,4}^2 \end{bmatrix}, G_a' = \begin{bmatrix} 1 & 0 & 0 \\ 0 & 1 & 0 \\ 0 & 0 & 1 \\ 1 & 1 & 1 \end{bmatrix}, z_a' = \begin{bmatrix} x^2 \\ y^2 \\ z^2 \end{bmatrix}$

It should substitute the equation(5.33) into equation(5.20) that is:

$$\psi_1' = 2x^0 e_1 + e_1^2 \approx 2x^0 e_1; \psi_2' = 2y^0 e_2 + e_2 \approx 2y^0 e_2 \tag{5.35}$$

$$\psi_1' = 2x^0 e_1 + e_1^2 \approx 2x^0 e_1; \psi_2' = 2y^0 e_2 + e_2 \approx 2y^0 e_2 \tag{5.36}$$

Therefore, it can obtain the error that covariance matrix is:

$$\Psi' = E[\psi'\psi'] = 4B' \operatorname{cov}(z_a) B' \tag{5.37}$$

$$B' = diag\left\{x^0, y^0, z^0, \frac{1}{2}\right\}$$

$\left(x^0, y^0, z^0\right)$ can be approximated by the approximate value of the equation z_a in B matrix, and WLS of z_a' is estimated as:

$$z_a' = \left(G_a'^{T} \Psi'^{-1} G_a'\right)^{-1} \left(G_a'^{T} \Psi'^{-1} h\right) \tag{5.38}$$

Finally, the tag localization result is:

$$z_p = \sqrt{z_a'} \tag{5.39}$$

Chapter 6 Results and Discussion

This chapter includes results of the composite system being developed. The stability of the system and the system itself was tested and real data was collected from the implemented positioning system. There are two experiments in this chapter. The first experiment verifies the effect of improved TOA positioning algorithm. The second experiment validates the effect of the UWB/RFID composite positioning system. The data of UWB/RFID composite positioning system and UWB system and RFID system are tested and analyzed. This test uses UWB localization system and RFID localization system. All the data obtained in the test will be uploaded to the database, and finally imported into Matlab for data process and analysis.

6.1 Improved TOA localization algorithm experiments

6.1.1 Experimental environment

This modified algorithm experiment was implemented in outdoor environment. The environment covers an area the size of 4m * 2m. There are four UWB anchors and their position coordinates are $(0,0,2)$、$(4,0,2)$、$(4,2,2)$ 、$(0,2,2.5)$, respectively. Figure 6.1 shows the experiment structure[77].

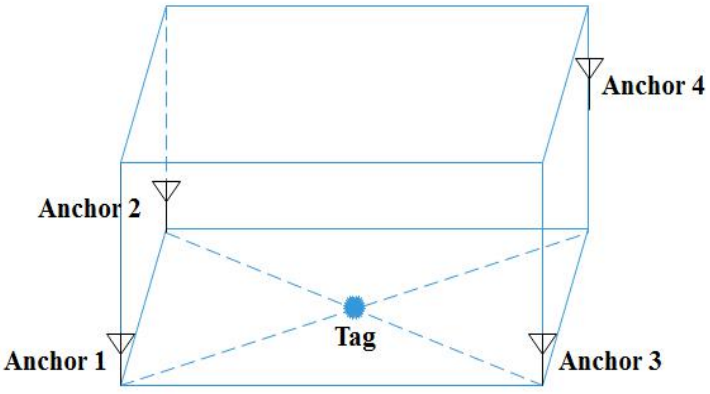

Figure 6.1 - 3D Positioning Arrangement of anchors and tag

6.1.2 Improved Algorithm Analysis

By using Matlab simulation, the performance of these two localization algorithm in X, Y, Z coordinates was compared. The measurement point is represented by X-coordinate. The localization value of X, Y, Z is represented by Y-coordinate. It can be shown from the Figure 6.3, 6.4 and 6.5, the X and Y coordinates are relatively stable, and the Z-coordinate has large fluctuations. This is because the ranging error of X and Y is added to the Z-axis and causes data to float on the Z-axis.

In some conditions, the positioning accuracy of the original algorithm can achieve about 20-30cm. However, as it shown from Figure 6.3, 6.4 and 6.5, the accuracy of the modified algorithm can reach about 7-15cm. This result demonstrates that the modified localization algorithm is very effective.

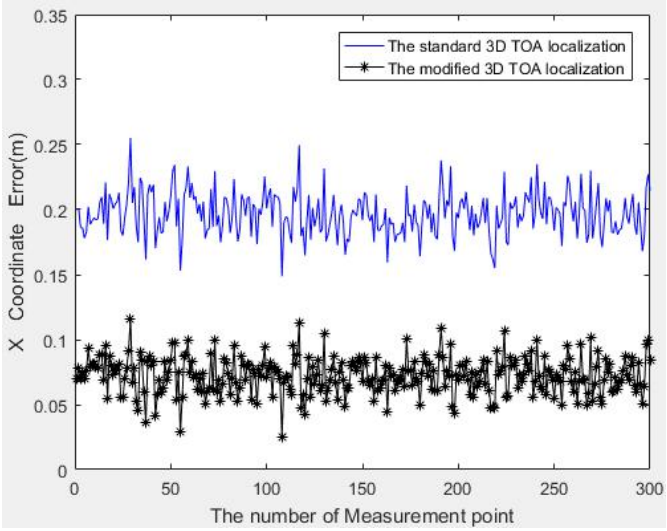

Figure 6.2 - The comparison of X-coordinate

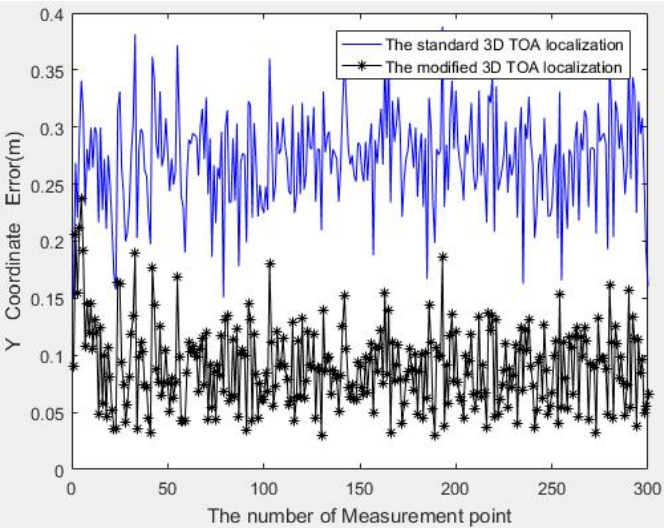

Figure 6.3 - The comparison of Y-coordinate

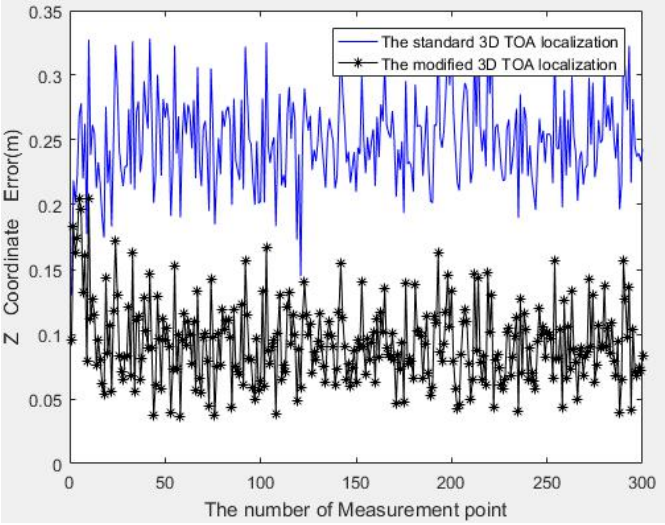

Figure 6.4 - The comparison of Z-coordinate

6.1.3 Experimental Results

The experiment measures positioning information of the tags at nine locations in the filed. The following Table 6.1 is the comparison of the actual coordinates, the original algorithm localization and the improved algorithm localization. As can be shown from Table 6.1, the modified localization algorithm got more accurate results for the localization points.

Table 6.1 Experimental data of tag localization

Actual point(m)	Measured points (standard 3D TOA)	Measured points (modified 3D TOA)
(1,0,2)	(0.8645,0.1517,1.8506)	(0.9785,0.0895,2.0531)
(1,1,1.2)	(0.8486,1.2141,1.4075)	(0.9513,1.1246,1.2845)
(1,2,0.6)	(0.8522,1.7811,0.7523)	(1.0675,2.0494,0.5387)
(2,0,2)	(1.8548,0.1629,1.8711)	(2.1027,0.0786,1.9397)
(2,1,1.2)	(2.1465,0.8611,1.3789)	(2.0682,0.9548,1.1376)
(2,2,0.6)	(2.1850,2.2083,0.8144)	(1.9365,1.9546,0.7114)
(3,0,2)	(3.2047,0.1202,2.1816)	(2.9486,0.0593,2.0872)
(3,1,1.2)	(3.1800,1.2543,1.0475)	(3.1148,1.0763,1.2794)
(3,2,0.6)	(3.1599,2.1848,0.7865)	(3.0596,1.9372,0.5289)

6.2 UWB/RFID composite localization experiments

6.2.1 Experimental environment

This composite localization experiment was implemented in outdoor environment. The environment covers the size of 5 m * 2 m, and RFID tags were placed every 2 cm in this area. The area set by the four anchors of the UWB system is 2m*2m, and the position coordinates are $(0,0)$、$(2,0)$、$(2,2)$、$(0,2)$ respectively, and the unit is m. The experimental layout is shown in the Figure 6.6 below.

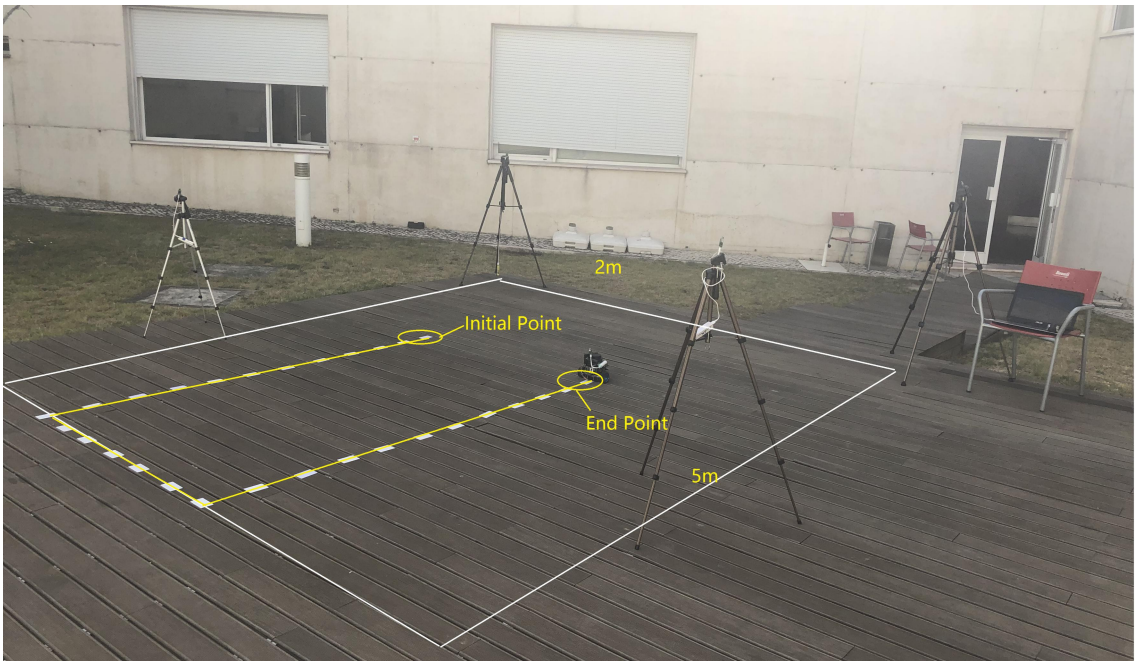

Figure 6.5 - Experimental geometrical setup

6.2.2 Experimental setup

The designed experiment contains the following hardware devices in Figure 6.7:

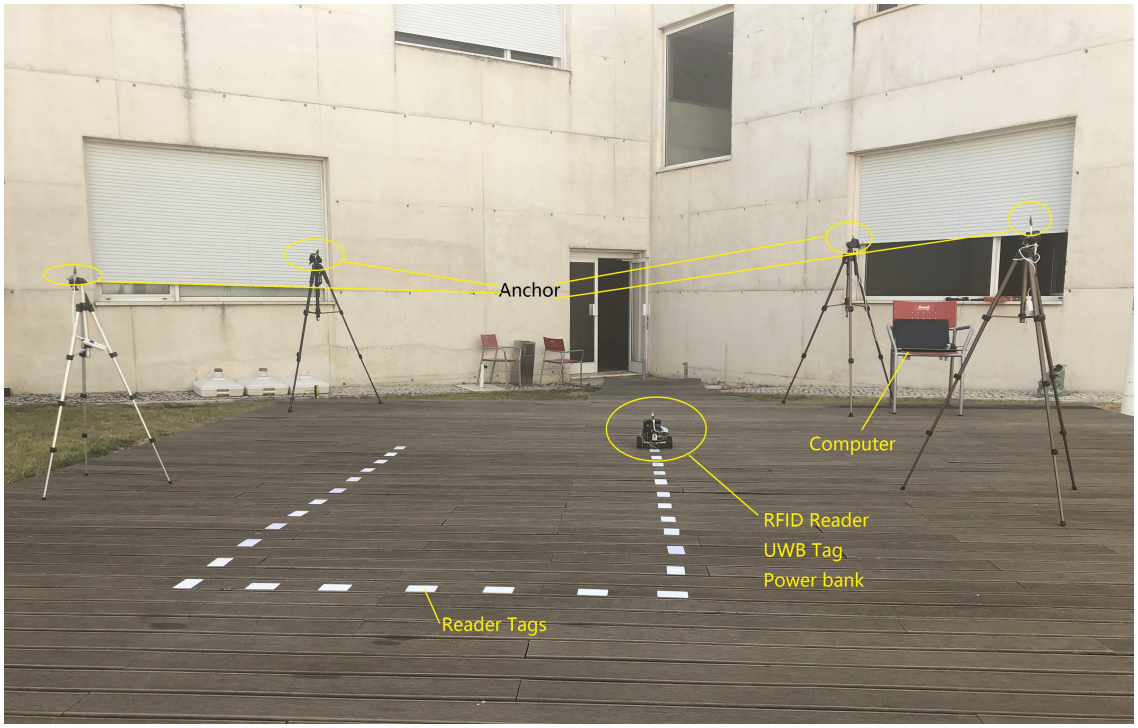

Figure 6.6 - Experimental setup

The experimental equipment includes 4 UWB anchors, one UWB tag, one

computer, four tripods, four mobile power supplies, several RFID readers and several RFID tags. The anchor is connected to the computer through the data line as shown in the figure above, which is used to measure the tag distance and locate the system. The anchors are powered by the mobile power source. The entire device needs to be reset before start experimental. After the device is properly connected, the tag, anchors and real-time data location software is opened. We click the “monitor” button in the real-time the data locating software to detect the connection status of the ranging and the positioning devices, and start data measurement when the connection is normal.

6.2.3 Experimental procedure

(1) The experiment is divided into two parts. The first part verifies the effect of improved UWB localization algorithm. The second part verifies the experimental effect of the composite system.

(2) According to the area and route shown above, the path points and coordinates are measured accurately. Then install tripods, fix the tag, connect the anchors and the connection test is completed. Along the preset route, the measurement is carried out around the distance measuring tag at a constant speed, starting from a starting point and going all the way, and returning to the starting point to complete the measurement of the closed area.

(3) It obtains UWB and RFID positioning data separately and compare with the actual path to analyze the positioning accuracy.

(4) The UWB data is optimized by KF and RFID reader transmits the collected tag information to the database, obtains the positioning data. Then it compares the positioning accuracy between two groups of data.

6.2.4 Experimental Results

To verify the performance of UWB/RFID composite positioning based on joint Kalman filter and Particle filter, MATLAB experimental positioning simulation is performed on the target of a uniform motion in a room. In a two-dimensional plane, the moving target moves at a constant speed from the initial coordinates (x, y) = (1, 0.5) at a speed of v = 0.02 m/s.

The experiment is divided into three parts, and the results are:

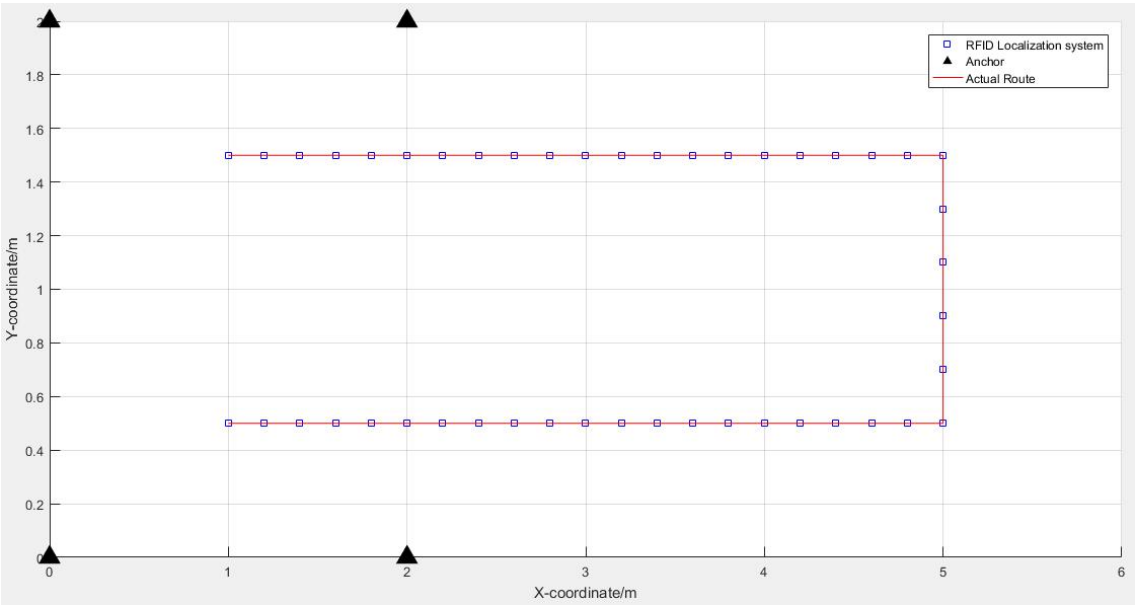

Figure 6.7 - Comparison of RFID positioning results with actual routes

As shown in the Figure 6.8 above, the results of RFID system positioning are shown. The result of RFID positioning is quite consistent with the actual route, and the positioning accuracy is high, but the disadvantage is that RFID can only perform point coordinate positioning and cannot perform continuous positioning. And the density of laying RFID tags is also very large and the cost is high.

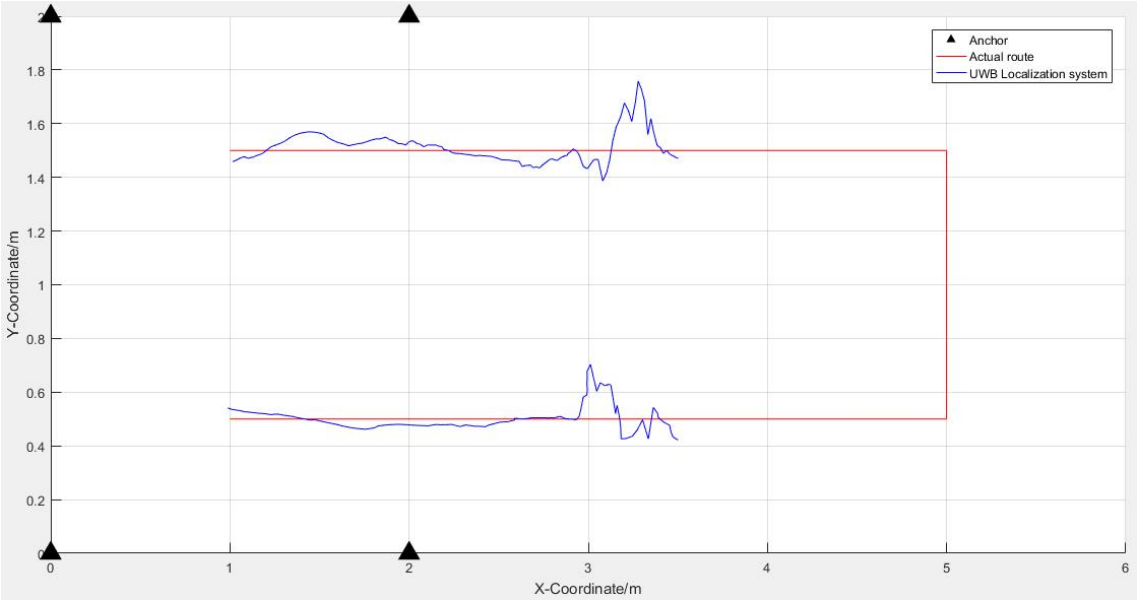

Figure 6.8 - Comparison of UWB positioning results with actual routes

In the above Figure 6.9 , the results of UWB system positioning are shown. In the antenna array, the positioning of UWB is relatively stable, and the error is about 7~13cm. However, when moving target is gradually far away from antenna array, the UWB signal becomes weak and the received signal is unstable. The positioning accuracy is large, and the error is about 20-30cm. Finally, the UWB signal was lost and could not be located.

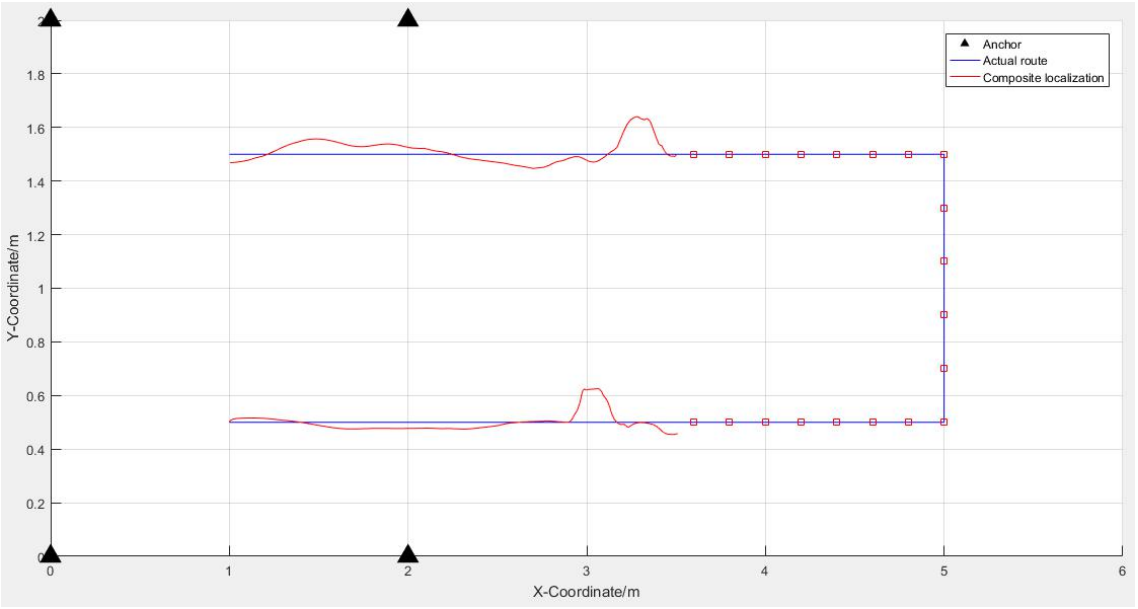

Figure 6.9 - Comparison of UWB/RFID composite positioning results with actual routes

As shown in the Figure 6.10, the results of UWB/RFID composite positioning are shown. When the system starts running and the target is in the antenna array, UWB positioning is better, and the composite system is switched to UWB positioning system. However, when moving target is gradually far away from the antenna array, the UWB signal becomes weak and the positioning becomes unstable. Then, Particle filtering combines UWB positioning data and RFID positioning data to obtain data with high positioning accuracy. When the target does not receive the UWB signal, the composite system switches to the RFID system. It can be verified that the positioning accuracy of this method is improved by 20% compared to UWB positioning or RFID positioning, with a positioning accuracy of about 12 cm, which can be seen in Table 6.2.

Table 6.2 Error analysis among RFID、UWB and composite localization

	UWB/RFID composite localization	**UWB localization**	**RFID localization**
Maximum error/m	0.2045	0.3068	0.1
Average error/m	0.1286	0.2285	0.06
Minimum error/m	0.0891	0.1259	0

Chapter 7 Conclusions and Future Work

7.1 Conclusion

The composite system based on UWB and RFID for localization in port including the performance evaluation was designed and implemented that satisfy the main objective of my thesis.

At present, the location of AGV in the port is mainly based on RFID technology due to the high accuracy of RFID positioning. However, in the port environment, in order to achieve high-precision positioning, the density of magnetic nails to be laid is larger, and the laying and maintenance cost are high, which is not conducive to port remodeling and upgrading. Thus, it is necessary to choose another positioning technology which not only does not affect positioning accuracy, but also can reduce the cost in the open area of port. The UWB technology has the advantages of high positioning accuracy and low cost. Therefore, the research of UWB and RFID compound positioning is carried out.

The system capabilities were tested in the experiments and the obtained data allows to compare the results coming from different experiments, that may be used to extract differences between the experimental sessions. With the analyzed data it is possible to have feedback, based on following values: Motion trail, UWB Localization data, RFID Localization data and Fluctuation of positioning error. Thus, we may know to use different positioning systems to achieve better positioning results.

Another objective was to improve the UWB positioning algorithm, which was also achieved. The modified UWB positioning algorithm is very important for the positioning performance of UWB. It improves the positioning accuracy of UWB and further reduces the positioning error.

It was proven the accuracy of the composite system, by the analysis of the collected UWB positioning information and RFID positioning information. The

positioning system used by the compound positioning system on the route track was obtained.

To summarize, this system can acquire location information from UWB and RFID sensors and send them to PC. Then, through data analysis by Matlab software, we can know the positioning system used by the compound system in each position of the route track.

7.2 Contributions

This dissertation's main contributions are:

- A new idea for composite positioning in ports.;
- Improved UWB localization algorithm.
- Verify the rationality of compound positioning.
- Designed KF and PF that has been applied to composite localization

The developed work and the initial results were included in the article and the poster in Appendix A, which were accepted and presented at the IEEE ATEE 2019 the 11th International Symposium, March 28-30, Bucharest, Romania. The article has been published in IEEE Xplorer.

Dongchen NI. and Octavian Adrian POSTOLACHE.et al, "UWB Indoor Positioning Application based on Kalman filter and 3D TOA Localization Algorithm", ATEE 2019, Bucharest Romania. The 11th International Symposium on Advanced Topics in Electrical Engineering

7.3 Future work

The research in this work is mainly aimed at the composite positioning of UWB positioning and RFID positioning technology. Due to the limitation of hardware resources, the signal degree that can be collected by the reader and passive tags used in

this work has already been calibrated. The RFID reader based on the Raspberry Pi 3B is used, which in itself brings a certain measurement error to the positioning. If the higher-level reader is used to collect data, it can improve the localization accuracy of RFID system. Improved algorithm will be better used for measurement.

For the RFID positioning technology, this paper uses the RFID reader to collect the tag data and brings the real data into the database algorithm. The obtained positioning result does not have a real-time positioning system. Next work can be carried out by using a single chip read/write program embedded in a computer for data processing design real-time positioning system to obtain positioning results.

At the same time, outside the UWB antenna array, there is a weak UWB signal in a relatively close position. How to better combine the UWB signal and RFID position information in this area to obtain more accurate positioning accuracy is also an important direction for future research.

References

[1] Jianxin Li, Jinhang Shi and Guojun Li et al. AGV technology application analysis[J]. Automotive Practical Technology,2018,(8):104-106.

[2] Lianyi Zhu, Guoli An and Xiliang Dong et al. Development Status and Enlightenment of World Automated Container Terminals[J]. Containerization,2015(1):7-10.

[3] Chenbeixi Zhang and Zhiqiu Huang et al. Summary of AGV Development[J]. China's manufacturing informationization,2010,39(1):P118-120.

[4] http://cn.chinadaily.com.cn/lhxzc/2017-12/10/content_35270144.htm?bsh_bid=1894374671

[5] Tong Feng,Xu tian Zeng. An ultrasonic navigation automatic guided vehicle system used in CIMS[J]. Intelligent Control and Automation,2002,(4):2645-2649.

[6] Abilio Azenha,Adriano Carvalho. Instrumentation and Iocalization in quasi-structed environment for AGV positioning[J]. IFAC Proceeding Volumes,2003,(7):65-72.

[7] Y. Yang, M. Zhong, H. Yao, F. Yu, X. Fu and O. Postolache, "Internet of things for smart ports: Technologies and challenges," in *IEEE Instrumentation & Measurement Magazine*, vol. 21, no. 1, pp. 34-43, February 2018.

[8] Y. Yang, M. Zhong, H. Yao, F. Yu, X. Fu and O. Postolache, "Internet of things for smart ports: Technologies and challenges," in *IEEE Instrumentation & Measurement Magazine*, vol. 21, no. 1, pp. 34-43, February 2018.

[9] Location Based Services(www.wirelesstoday.com/wtm/llcommerce.htm)

[10] Xin Zhao. Application of Fractal Theory in Channel Estimation of UWB Communication System[D]. BeiJing: Beijing University of Posts and Telecommunications,2006:9-11.

[11] Bennett C L, Ross G F. Time-domain Electromagnetics and its Applications[J]. Proceedings of the IEEE,1978,66(3):299-318.

[12] Oppermann I, Hamalainen M, Linatti J. UWB Theory and Applications[M]. New York: John Wiley&Sons,2004.

[13] Porcino D, Hirt W. Ultra-Wideband Radio Technology: Potential and Challenge Ahead[J]. IEEE Communication Magazine, 2003, 41(7):66-74.

[14] Fontana R, Gunderson S. UWB Precision Asset Location System[C]//IEEE Conference on Ultra Wide-band Systems and Technologies(UWBST'02), Baltimore, 2002:147-150.

[15] Shibing Zhang, Lijun Zhang. UWB Wireless Communication and its Key Technologies[J]. Telecommunications Technology, 2004,44(1):1-6.

[16] Gang Zhu. Ultra-wideband Principle and Interference[M]. Beijing: Tsinghua University Press, Beijing Jiaotong University Press, 2009.

[17] XU Y. The argument of standards of UWB[J]. Telecommunication Science,2004,(3):33-35.

[18] ROBERTO A. Discrete time PHY proposal for TG3a[EB/OL]. http://ieee802.org/15pub/Download.html,2003.

[19] BATRA A,et al. Multi-band OFDM physical layer proposal for IEEE802.15 task group 3a[EB/OL]. http://ieee802.org/15pub/Download.html,2003.

[20] Rui Xue. Comprehensive Comparative Study of DS-CDMA-UWB System and MB-OFDM-UWB System[D]. Harbin:Harbin Engineering University,2006.

[21] Huoping Jiang. Research on Channel Estimation Technology of UWB Wireless Communication System Based on MB-OFDM[D], Xidian: Xidian University of Electronic Technology, 2010.

[22] Guangguo Bi. Review and Prospect of China's High-speed UWB Communication System. State Key Laboratory of Mobile Communications, School of Information Science and Engineering, Southeast University, 2006.10.

[23] National Communications and Information Administration(NTIA) Special Publication 01-383. Assessment of compatibility between ultra wideband devices and selected federal systems. Jan. 2001.

[24] National Communications and Information Administration(NTIA) Special Publication 01-45. Assessment of compatibility between ultra wideband devices and selected federal systems. Jan. 2001.

[25] Lijia Ge, Fanxin Zeng and Yulin Liu et al. UWB Wireless Communication[M]. Beijing : National Defense Industry Press, 2005.

[26] Stockman H. Communication by Means of Reflected Power[J]. Proceedings of the Ire, 1948,36(10):1196-1204.

[27] Costin A, Pradhananga N, Teizer J. Leveraging passive RFID technology for construction resource field mobility and status monitoring in a high-rise renovation project[J]. Automation in Construction, 2012, 24(24):1-15.

[28] Schapranow M P. Real-time Security Extensions for EPC global Networks[M]. Springer Berlin Heidelberg, 2014.

[29] Highttower J, Borriello G, Want R. SpotON: an indoor 3D location sensing technology based on RF signal strength. UW CSE Technical Report[J]. UW CSE, 2000.

[30] Ni L M, Liu Y, Lau Y C,et al. LANDMARC: Indoor Location Sensing Using Active RFID[J]. Wireless Networks, 2004, 10(6):701-710.

[31] Baskakov S. Landmarks Selection Algorithm for Virtual Coordinates Routing[C]//: International Conference on Wireless Algorithm, Systems, and Application, 2008.

[32] Choi J S, Lee H, Elmasri R,et al. Localization Systems Using Passive UHF RFID[C]//: Fifth International Joint Conference on Inc, Ims and IDC, 2009.

[33] https://www.wendangwang.com/doc/c4e800ff6148da207fb2d508/6

[34] Long V H, Nguyen-Manh H,Phan-Duy C, et al. A new technique to enhance accuracy of WLAN fingerprinting based indoor positioning system[C]//:IEEE Fifth International Conference on Communications and Electronics, 2014.

[35] http://www.sohu.com/a/216978081_810044

[36] Pittet S, Renaudin V, Merminod B. UWB and MEMS based indoor navigation[J]. Journal of Navigation,2008,61(3):369-384.

[37] Huang C C, Manh H N. RSS-Based Indoor positioning Based on Multi-Dimensional Kernel Modeling and Weighted Average Tracking[J]. IEEE Sensors Journal, 2016,16(9):3231-3245.

[38] N. Y. Ko, S. J. Lee, S. Jeong and Y. S. Moon, "Attitude estimation of an unmanned surface vehicle using MEMS-AHRS and GNSS," *2017 17th International Conference on Control, Automation and Systems (ICCAS)*, Jeju, 2017, pp. 723-725.

[39] Pittet S, Renaudin V, Merminod B. UWB and MEMS based indoor navigation[J]. Journal of navigation, 2008,61(3):369-384.

[40] S. Bartoletti, M. Guerra, A. Conti, "UWB passive navigation in indoor environments", *Proc. Int. Symp. Appl. Sci. Biomed. Commun. Technol.*, 2011.

[41] A. Conti, M. Guerra, D. Dardari, N. Decarli, "Network experimentation for cooperative localization", *IEEE J. Sel. Areas Commun.*, vol. 30, no. 2, pp. 467-475, Feb. 2012.

[42] Y. Zhou, C. L. Law, Y. L. Guan, F. Chin, "Indoor elliptical localization based on asynchronous UWB range measurement", *IEEE Trans. Instrum. Meas.*, vol. 60, no. 1, pp. 248-257, Jan. 2011.

[43] G. D. Angelis, A. Moschitta, P. Carbone, "Positioning techniques in indoor environments based on stochastic modeling of UWB round-trip-time measurements", *IEEE Trans. Intell. Transp. Syst.*, vol. 17, no. 8, pp. 2272-2281, Aug. 2016.

[44] W. Liu, H. Ding, X. Huang, Z. Liu, "Toa estimation in ir UWB ranging with energy detection receiver using received signal characteristics", *IEEE Commun. Lett.*, vol. 16, no. 5, pp. 738-741, May 2012.

[45] J. Wang, X. Zhang, Q. Gao, H. Yue, H. Wang, "Device-free wireless localization and activity recognition: A deep learning approach", *IEEE Trans. Veh. Technol.*, vol. 66, no. 7, pp. 6258-6267, Jul. 2017.

[46] M. Yasir, S. W. Ho, B. N. Vellambi, "Indoor position tracking using multiple optical receivers", *J. Lightw. Technol.*, vol. 34, no. 4, pp. 1166-1176, 2016.

[47] J. H. Seong, E. C. Choi, J. S. Lee, D. H. Seo, "High-speed positioning and automatic updating technique using wi-fi and UWB in a ship" in Wireless Personal Communications, Berlin, Germany:Springer-Verlag, pp. 1-17, 2016.

[48] F. Despaux, K. Jaffres-Runser, A. V. D. Bossche, T. Val, "Accurate and platform-agnostic time-of-flight estimation in ultra-wide band", *Proc. IEEE Annu. Int. Symp. Personal Indoor Mobile Radio Commun.*, pp. 1-7, 2016.

[49] J. Wang, X. Zhang, Q. Gao, X. Ma, "Device-free simultaneous wireless localization and activity recognition with wavelet feature", *IEEE Trans. Veh. Technol.*, vol. 66, no. 2, pp. 1659-1669, Feb. 2017.

[50] M.S. Grewal, A.P. Andrews. Kalman filitering: theory and practice using MATLAB. John Wiley&Sons, 2011.

[51] S.M. Kay. Fundamentals of statistical signal processing. Volume i:Estimation theory(v.1), 1993.

[52] C.D. Wann, C.S. Hsueh. Non-line of sight error mitigation in ultra-wideband ranging systems using biased Kalman filitering. Journal of Signal Processing Systems, 2011, 64(3), pp.1058-1062.

[53] Metropolis N, Ulam S. The Monte Carlo Method[J]. Journal of the American Statistical Association, 1949, 44(247):335-341.

[54] Gordon N J, Salmond D J, Smith A F M. Novel approach to nonlinear/non-Gaussian Bayesian state estimation[J]. IEEE Proceedings F(Radar and Signal Proceeding), 1993, 140(2):107-113.

[55] Fasheng Wang, Mingyu Lu, Qingjie Zhao et al. Particle Filter Algorithm[J]. Journal of Computer, 2014, 37(8):1679-1694.

[56] Xiaoping Huang, Yan Wang Pengcheng Liao et al. Particle Filter Principle and Application Matlab Simulation[M]. Beijing: Electronic Industry Press, 2017.

[57] Peng Peng, Weili Han, Yiming Zhao. Research on Security Requirements of Internet of Things Based on RFID[J]. Chinese Journal of Inertial Technology, 2011,(1):75-79.

[58] Lianjun Zhang, Chunli He. Development of radio frequency identification technology[J]. Mechanical management development,2009,(112):89-90.

[59] Xuejun Shi. Research on Indoor Wireless Positioning Control Method Based on RFID[D]. Jiangnan University, 2015.

[60] https://www.basemu.com/rc522-rfid-tag-reading-with-the-raspberry-pi-1.html

[61] Shaorong Liu, Lijuan Zhang, Yeli Du. Comparison of high frequency and ultra high frequency RFID in libraries[J]. Chinese modern educational equipment, 2011,(3):148-150.

[62] Jwo-Shiun Sun, Chia-Hao Wu. A broadband circularly polarized antenna of squarening patch UHF RFID reader applications[J].AEU-International Journal of Electronics and Communications, 2018,2(85):84-90.

[63] Xiaohui Wang, Yunjia Wang, Wei Zhang. Review of RFID-based indoor positioning technology[J]. Sensors and microsystems, 2016,(2):1-5.

[64] Shijun Guo, Huafeng Wu, Xia Liu. Mobile node location based on adaptive and trajectory[J]. Chinese navigation, 2016,(2):1-5.

[65] Haoquan Wu, Zhefu Wu, Rongliang Yuan. Research on Indoor Wireless Location Technology Based on RFID[J]. Electroacoustic technology, 2013,(3):76-78.

[66] Zhongliang Zhang. Indoor and outdoor wireless positioning and navigation[M].Beijing University of Posts and Telecommunications, 2013.

[67] Xiaoting He, High Speed Pulse Technology[M]. Zhejiang University, 2007.

[68] Qiang Zhang. Positioning Research and System Realization of UWB Technology in Indoor Environment[D]. Harbin Institute of Technology, 2015.

[69] Zhen Shi, Xiuping Yu,, Pengtian Ma et al. Gyroscope-free strapless inertial navigation system[M]. Harbin: Harbin Engineering University Press, 2005.

[70] Si Tao. Research on UWB Indoor SDS-TWR Ranging Optimization and Location Algorithm Fusion[D]. East China Normal University, 2016.

[71] https://www.semiconductorstore.com/cart/pc/viewPrd.asp?idproduct=50013

[72] http://www.elecfans.com/tongxin/rf/20180608691701.html

[73] http://push.hibor.com.cn/ios/newscenter/2019/10/2019100606580266_1.asp

[74] L. Taponecco, A. A. D'Amico and U. Mengali, "Joint TOA and AOA Estimation for UWB Localization Applications," in *IEEE Transactions on Wireless Communications*, vol. 10, no. 7, pp. 2207-2217, July 2011.

[75] A. Jafari *et al*., "UWB Interferometry TDOA Estimation for 60-GHz OFDM Communication Systems," in *IEEE Antennas and Wireless Propagation Letters*, vol. 15, pp. 1438-1441, 2016.

[76] S. Wang *et al*., "System implementation study on RSSI based positioning in UWB networks," *2010 7th International Symposium on Wireless Communication Systems*, York, 2010, pp. 36-40.

[77] D. Ni, O. A. Postolache, C. Mi, M. Zhong and Y. Wang, "UWB Indoor Positioning Application Based on Kalman Filter and 3-D TOA Localization Algorithm," *2019 11th International Symposium on Advanced Topics in Electrical Engineering (ATEE)*, Bucharest, Romania, 2019, pp. 1-6.

Appendix A - Scientific Articles

Article: **UWB Indoor Positioning Application based on Kalman filter and 3D TOA Localization Algorithm.**

The link of article is: https://ieeexplore.ieee.org/document/8724907.

This article has been accepted and presented at the IEEE ATEE 2019 the 11th International Symposium, March 28-30, Bucharest, Romania. The article has been published in IEEE Xplorer.

ATEE is the forum that stimulates active and effective exchange of information between researchers in various areas of theoretical and applied electrical engineering. Key leaders from private and state owned companies involved in will also be in attendance.

THE 11th INTERNATIONAL SYMPOSIUM ON ADVANCED TOPICS IN ELECTRICAL ENGINEERING
March 28-30, 2019
Bucharest, Romania

UWB Indoor Positioning Application Based on Kalman Filter and 3-D TOA Localization Algorithm

Dongchen Ni[1,2*], Octavian Adrian Postolache[1], Chao Mi[2], Meisu Zhong[2] and Yongshuang Wang[1,2]
1. ISCTE-University Institute of Lisbon, Lisbon, Instituto de Telecomunicacoes, Portugal
2. Shanghai Maritime University, Shanghai,Logistics Engineering College, China
dongchen_ni@iscte-iul.pt, opostolache@lx.it.pt

***Abstract*- In recent years, with the continuous development of short-range wireless communication and mobile technology, location-based services in indoor environments have paid more and more attention several solutions being reported in the literature. Ultra-Wide Band positioning technology has become one of frequently selected solution due to its low power consumption, anti-multipath capabilities, high security, low system complexity, and high precision. In this paper, 3D positioning algorithms were discussed, and a new one 3D time of arrival (TOA) positioning algorithm was proposed. The main idea of the proposed algorithm is to replace the quadratic term in the positioning estimation with a new variable and the usage of the weighted least squares linear estimation followed by the combination with Kalman filter to reduce the interference error in the transmission process.**

***Keywords*: UWB, indoor positioning, 3D, TOA, Kalman filter**

I. INTRODUCTION

The continuous development of wireless sensor networks (WSN) the indoor positioning technology has been also developed. It has a wide range of applications in smart buildings, shopping malls, smart healthcare and other. Some of the common used indoor localization technologies are based on communication protocols such as Wi-Fi, Bluetooth, ZigBee as so as RFID positioning technology, infrared positioning technology, and Ultra-Wide Band (UWB) positioning technology [1]. However, existing indoor positioning technology cannot meet the needs of people, especially for: high-precision positioning, strong adaptability in complex environments, low power consumption and low cost. As one of indoor positioning technologies the UWB one however is still necessary new studies for complex environments and multiple dynamic targets.

UWB signals have a large bandwidth and good temporal resolution, so they are widely used in high-rate and short-range wireless communication [2]. UWB positioning technology can be roughly divided into three categories: Time of Arrival (TOA), Angle of Arrival (AOA), and Received Signal strength (RSS)[3]. The AOA and RSSI methods cannot effectively guarantee the positioning accuracy in a complex indoor environment when used alone. Generally, they are used as an auxiliary method for TOA and TDOA [4][5][6], and the TOA/TDOA technology can make full use of the good temporal resolution of the UWB signal. It has been widely used in the localization of traditional 2D scene, but the localization in the 3D scene has not been popularized. Xue et. al proposed a minimum error algorithm based on TOA measurement, which achieved good 3D positioning accuracy [7]. Additional optimization algorithm is described in [8] that focuses on TOA optimization model algorithm that permits to get location information for indoor 3D positioning of wireless communication stations. The paper [9] the iterative time-of-arrival and multivariate model are used to eliminate time synchronization providing accurate indoor localization.

Hence, this paper aims to improve the traditional TOA positioning algorithm to 3D space for higher precision requirements combining TOA with Kalman filtering algorithm.

II. UWB LOCALIZATION ALGORITHM

A. TOA Ranging Principle

Using two ways-time of flight (TW-TOF) technique can be achieving good accuracy on estimating the point-to-point distance between two wireless transceivers. In the UWB case TOF ranging method is a two-way ranging technology, which mainly use the time of flight of a signal between two asynchronous transceivers to measure the distance between transceivers. The two-way ranging principle is presented in Fig 1. The Device A transmits the signal at time T_{a1}, and the Device B receives the signal at time T_{a2}. After waiting for the TW time, Device B forwards the signal to Device A at time T_{b1} and Device A receives the signal at time T_{b2}. Thus, the time of flight of the signal between Device A and B can be calculated to determine the flight distance [10], where c – is the light velocity.

$$S = c * \left[\left(T_{a2} - T_{a1} \right) - \left(T_{b2} - T_{b1} \right) \right] \quad (1)$$

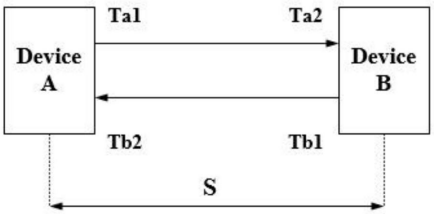

Fig 1.Two-way ranging principle

B. 3D TOA Localization Principle

If the coordinates of the nodes to be positioned are (xi, yi, zi) in a 2D space, only three anchor nodes are needed for positioning comparing with 3D space, where at least four anchor nodes are required for positioning. Considering the work objective the coordinates of four anchor nodes are assumed to be $A(x_1,y_1,z_1)$, $B(x_2,y_2,z_2)$, $C(x_3,y_3,z_3)$, $D(x_4,y_4,z_4)$ respectively. d is the distance between the tag (with unknown position) and each base station, as shown in Fig 2[11][12].

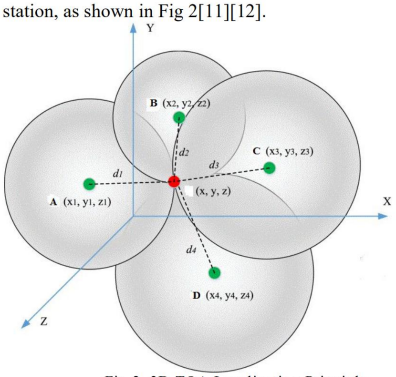

Fig 2. 3D TOA Localization Principle

The distances d_i from nodes to the target X are given by:

$$\begin{cases} d_1^2=(x_1-x)^2+(y_1-y)^2+(z_1-z)^2 \\ d_2^2=(x_2-x)^2+(y_2-y)^2+(z_2-z)^2 \\ d_3^2=(x_3-x)^2+(y_3-y)^2+(z_3-z)^2 \\ d_4^2=(x_4-x)^2+(y_4-y)^2+(z_4-z)^2 \end{cases} \tag{2}$$

By calculation, the node location can be determined using the following equation:

$$X=(A^TA)^{-1}A^Tb \tag{3}$$

Where:

$$A=\begin{bmatrix} 2(x_1-x_4) & 2(y_1-y_4) & 2(z_1-z_4) \\ 2(x_2-x_4) & 2(y_2-y_4) & 2(z_2-z_4) \\ 2(x_3-x_4) & 2(y_3-y_4) & 2(z_3-z_4) \end{bmatrix}$$

$$b=\begin{bmatrix} (x_1^2+y_1^2+z_1^2)-(x_4^2+y_4^2+z_4^2)-(d_1^2-d_4^2) \\ (x_2^2+y_2^2+z_2^2)-(x_4^2+y_4^2+z_4^2)-(d_2^2-d_4^2) \\ (x_3^2+y_3^2+z_3^2)-(x_4^2+y_4^2+z_4^2)-(d_3^2-d_4^2) \end{bmatrix}$$

C. The modified 3D TOA localization

When TOA technology is used to locate our tag using UWB positioning system the TOA value can be measured to get the distance between tag and four base stations. Multiple TOA measurements can form a set of circular equations about the position of the tag in 3D coordinates. We assumed that the tag coordinate are (x, y, z) in 3D space, the known positions of the base stations are (X_i,Y_i,Z_i) , and the distances between base stations and the tag are R_i where Ri is given by :

$$\begin{aligned} R_i^2&=(X_i-x)^2+(Y_i-y)^2+(Z_i-z)^2 \\ &=K_i-2X_ix-2Y_iy-2Z_iz+R=(c\tau)^2 \end{aligned} \tag{4}$$

where τ_i is the time of arrival and:

$$K_i=X_i^2+Y_i^2+Z_i^2, i=1,2,3\cdots, R=x^2+y^2+z^2,$$

Assuming $z_a=[z_p^T,R]^T$ as an unknown vector, and $z_p=[x,y,z]^T$, so linear equations with z_a as the variable are established from formula(4):

$$h=G_az_a \tag{5}$$

Then the error vector corresponding to the estimated position of the tag is given by:

$$\psi=h-G_az_a^0 \tag{6}$$

Where: z_a^0 is the value of z_a corresponding to the actual position of tag.

$$h=\begin{bmatrix} R_1^2-K_1 \\ R_2^2-K_2 \\ \vdots \\ R_M^2-K_M \end{bmatrix}, G_a=\begin{bmatrix} -2X_1 & -2Y_1 & -2Z_1 & 1 \\ -2X_2 & -2Y_2 & -2Z_2 & 1 \\ \vdots & \vdots & \vdots & \vdots \\ -2X_M & -2Y_M & -2Y_M & 1 \end{bmatrix}$$

Weighted least squares (WLS) is used to replace the covariance matrix of error ψ approximately by the covariance matrix Q of the measured value of TOA:

$$z_a=(G_a^TQ^{-1}G_a)^{-1}(G_a^TQ^{-1}h) \tag{7}$$

Considering:(x,y,z) as the estimated position of the tag, Q as TOA covariance matrix and each TOA measurement is independent, the Q matrix is a diagonal matrix:

$$Q=diag\{\sigma_1^2,\sigma_2^2,\cdots,\sigma_M^2\} \tag{8}$$

In formula (6), replacing the covariance matrix of the error vector ψ by the Q matrix approximation will also bring some errors. Therefore, when the TOA error is small, the

error vectors corresponding to the TOA measurements of M are:

$$\psi = 2Bn + n \odot n \approx 2Bn \quad (9)$$
$$B = diag\left\{R_1^0, R_2^0, \cdots, R_M^0\right\}$$

Set: R_i^0 is the actual distance between tag and base station of i,n is TOA measurement error in distance(approximate normal distribution).

The covariance matrix of the error vector ψ constructed from TOA measurements in formula (6):

$$\Psi = E\left[\psi\psi^T\right] = 4BQB \quad (10)$$

In order to get the matrix B, the measured R_i can be substituted for R_i^0, then the first WLS estimate of z_a is:

$$z_a = \left(G_a^T\Psi^{-1}G_a\right)^{-1}\left(G_a^T\Psi^{-1}h\right) \quad (11)$$

New matrix B can be obtained by using the value of z_a. Using the above process to perform another WLS calculation can result in a modified estimated position. The above calculation assumes that the elements of z_a are independent of each other, but R is related to the position of the tag(x, y, z), which we can use to get a more accurate position estimate. We first calculate the covariance matrix of the estimated position in the presence of noise:

$$R_i = R_i^0 + cn_i, G_a = G_a^0 + \Delta G_a, h = h^0 + \Delta h \quad (12)$$

Where $G_a^0 z_a^0 = h^0$, formula (5) indicates:

$$\psi = \Delta h - \Delta G_a z_a^0 \quad (13)$$

We set $z_a = z_a^0 + \Delta z_a$,reusing formula (9) and (13), Δz_a and its covariance matrix are:

$$\Delta z_a = c\left(G_a^T\Psi^{-1}G_a\right)^{-1}G_a^T\Psi^{-1}Bn$$
$$\mathrm{cov}\left(z_a\right) = E\left[\Delta z_a \Delta z_z^T\right] = \left(G_a^T\Psi^{-1}G_a\right)^{-1} \quad (14)$$

The vector z_a is the actual value, the covariance matrix is determined by the random variable of formula (14), so the elements of z_a can be expressed as:

$$z_{a,1} = x^0 + e_1, z_{a,2} = x^0 + e_2$$
$$z_{a,3} = x^0 + e_3, z_{a,4} = x^0 + e_4 \quad (15)$$

Of which: e_1, e_2, e_3, e_4 is estimation error of z_a. According to the correlation between (x, y, z) and R, a new error vector can be constructed as follows:

$$\psi' = h' - G_a' z_a' \quad (16)$$

Of which: $h' = \begin{bmatrix} z_{a,1}^2 \\ z_{a,2}^2 \\ z_{a,3}^2 \\ z_{a,4}^2 \end{bmatrix}, G_a' = \begin{bmatrix} 1 & 0 & 0 \\ 0 & 1 & 0 \\ 0 & 0 & 1 \\ 1 & 1 & 1 \end{bmatrix}, z_a' = \begin{bmatrix} x^2 \\ y^2 \\ z^2 \end{bmatrix}$

ψ' is defined as the estimated error of z_a, and the formula 15 is substituted into the formula 6 to get:

$$\psi_1' = 2x^0 e_1 + e_1^2 \approx 2x^0 e_1; \psi_2' = 2y^0 e_2 + e_2 \approx 2y^0 e_2 \quad (17)$$
$$\psi_1' = 2x^0 e_1 + e_1^2 \approx 2x^0 e_1; \psi_2' = 2y^0 e_2 + e_2 \approx 2y^0 e_2$$

The covariance matrix of the error is:

$$\Psi' = E[\psi'\psi'] = 4B'\,\mathrm{cov}\left(z_a\right)B'$$
$$B' = diag\left\{x^0, y^0, z^0, \frac{1}{2}\right\} \quad (18)$$

In the matrix B', $\left(x^0, y^0, z^0\right)$ can be approximately replaced by the value of the formula z_a, and WLS of z_a' is estimated as:

$$z_a' = \left(G_a'\Psi'^{-1}G_a'\right)^{-1}\left(G_a'^T\Psi'^{-1}h\right) \quad (19)$$

The final positioning calculation result of tag is:

$$z_p = \pm\sqrt{z_a'} \quad (20)$$

In the matrix z_p, (x, y, z) selection of plus-minus sign should be consistent with corresponding elements in z_a of formula 11, so as to eliminate the ambiguity of positioning results.

D. *Kalman Filtering*

In the complex indoor environment, it is inevitable to encounter non-line-of-sight obstacles in the process of signal transmission. For this problem, the Kalman filter error detection algorithm is used to eliminate the transmission error as was presented in [13]. The calculation of Kalman filtering is based on the following assumption: all the measured results are based on real signals and additive Gaussian noise. If the above hypotheses are true, Kalman filtering can effectively obtain signal information from noise-containing measurement results.

Suppose the state equation of a discrete control process system is:

$$x_{k+1} = Ax_k + Bu_{k+1} + \omega_{k+1} \quad (21)$$

Of where: x_{k+1} is the system state at time k+1; ω_{k+1} is Gaussian random variable of process noise; u_{k+1} is the amount of control of the system at time k+1;A and B are system parameters, they are matrices for this system.

The corresponding observation matrix is:

$$Z_{k+1} = \left[\theta_{s,k+1} \quad \gamma_{s,k+1}\right]^T = H_{k+1}x_{k+1} + \nu_{k+1} \quad (22)$$

Of where: Z_{k+1} is a measurement at time k+1; H_{k+1} is unit matrix; ν_{k+1} is Gaussian random variable that measures noise.

The model of the process system is used to predict the next state. The iterative process of the Kalman filter principle described in [14] [15] includes:

Estimate the current state based on the previous state of the system:

$$\hat{x}_{k+1|k} = Ax_{k|k} + Bu_{k+1} \tag{23}$$

Of where: $\hat{x}_{k+1|k}$ is predicted result of previous state; $x_{k|k}$ is optimal result of previous state; u_{k+1} is control of current state.

The minimum mean square error matrix is:

$$P_{k+1|k} = AP_{k|k}A^T + Q \tag{24}$$

where: $P_{k|k}$ is minimum mean square error matrix for estimated value $x_{k|k}$; $P_{k+1|k}$ is covariance of $\hat{x}_{k+1|k}$; Q is covariance of the system process.

Kalman gain is:

$$K_{k+1} = P_{k+1|k}H_{k+1}^T\left(R_{k+1} + H_{k+1}P_{k+1|k}H_{k+1}^T\right)^{-1} \tag{25}$$

Of where: R_{k+1} is covariance matrix of observed noise v_{k+1} .

The optimization estimates for K+1 state is:

$$\hat{x}_{k+1|k+1} = \hat{x}_{k+1|k} + K_{k+1}\left(Z_{k+1} - H_{k+1}\hat{x}_{k+1|k}\right) \tag{26}$$

Keep the continuity of the system until the end, update the $x_{k+1|k+1}$ covariance of k+1 state.

$$P_{k+1|k+1} = (I - K_{k+1})HP_{k+1|k} \tag{27}$$

Through the above-mentioned process, the interference caused by the transmission can be eliminated.

III. EXPERIMENTAL TESTING AND VERIFICATION

A. *Experimental Setup*

This experiment was carried out in an indoor environment with a size of 4m * 2m. It was used for 4 UWB positioning base stations, which are placed in 4 positions, and their position coordinates are $(0,0,2)$ 、 $(4,0,2)$ 、 $(4,2,2)$ 、 $(0,2,0.8)$, the unit is meter. The experimental arrangement is presented in Fig 3. In this experiment, the modified positioning algorithm combined with this paper will be compared with the standard 3D TOA positioning method.

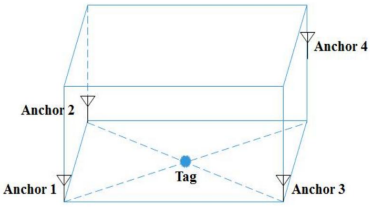

Fig 3.3D Positioning Arrangement of anchors and tag

The positioning server in this article uses a 4-core 4-thread Intel i5-4770 processor with 8GB of RAM. The positioning program is developed on the platform of CoIDE. It is used to program windows form control and C++ language. The GUI is shown in Fig 4. Before the positioning starting, the coordinates of the base stations are applied on the algorithm inputs. The 3D coordinate information (X, Y, Z) of the tag is displayed directly above, the distance between tag and each base station is displayed at the top right, and the movement track of the tag can be displayed at the bottom left, which can be displayed the geographic location of the tag visually.

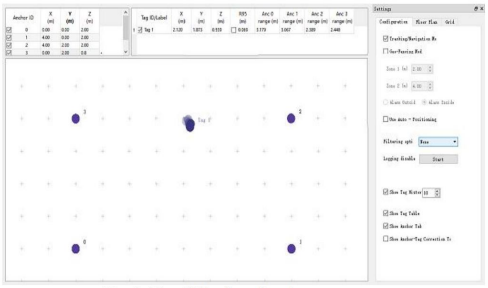

Fig 4. The GUI of application system

B. *The comparison of RMSE*

This paper compared the standard 3D TOA positioning algorithm with the modified 3D TOA positioning algorithm. The RMSE is selected as the measurement index of the positioning accuracy, and then the difference of the RMSE value between two methods under different mean square errors is explored.

$$MSE = E\left[(x-\hat{x})^2 + (y-\hat{y})^2 + (z-\hat{z})^2\right] \tag{28}$$

Of which: (x, y, z) is the actual position of tag; $(\hat{x}, \hat{y}, \hat{z})$ is the measured position of the tag. RMSE is often used to estimate the positioning accuracy and its calculation formula:

$$RMSE = \sqrt{E\left[(x-\hat{x})^2 + (y-\hat{y})^2 + (z-\hat{z})^2\right]} \tag{29}$$

RMSE comparison of standard and modified 3D TOA positioning algorithms is shown in Fig 5.

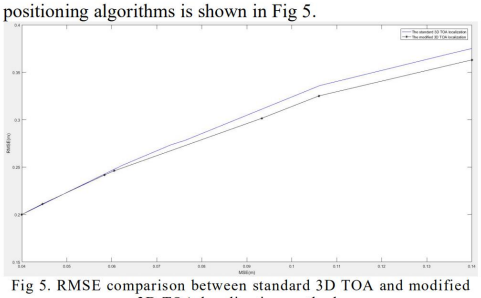

Fig 5. RMSE comparison between standard 3D TOA and modified 3D TOA localization methods

It can be judged from Figure 4 that the performance of the standard 3D TOA and modified 3D TOA positioning method is very close when the mean square error is 0.06 /m or less. When the mean square error gradually increasing, RMSE of the two localization methods also increases gradually. We can see that RMSE values of the standard and modified TOA algorithm are basically the same. However, compared with the standard TOA algorithm, the modified TOA algorithm has higher positioning accuracy.

C. Simulation of joint location algorithm

Through the simulation by MATLAB, the performance of the standard and modified 3D TOA positioning in X, Y, and Z coordinates are analyzed and compared. The abscissa represents the number of measurement point, and the ordinate represents each simulated object coordinate. As can be seen from the figure6, 7, 8, the estimated values of X coordinate errors is relatively stable, while Y and Z estimation are less stable. Y and Z coordinate maximum error are about 15/cm and positioning accuracy are within the allowable range.

In the ideal conditions, the accuracy of standard 3D TOA positioning combined with the Kalman filtering algorithm can reach about 15~25/cm. As shown in the figure, compared with the standard 3D TOA joint Kalman filter algorithm, simulation results show that the modified 3D TOA positioning combined with the Kalman filter algorithm is stable at 5~10/cm. This result proves that the modified 3D TOA positioning algorithm combined with Kalman filtering is effective.

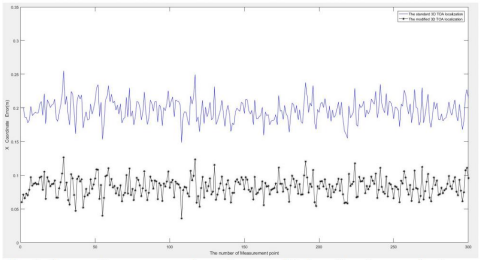

Fig 6. X coordinate comparison for two 3D localization methods

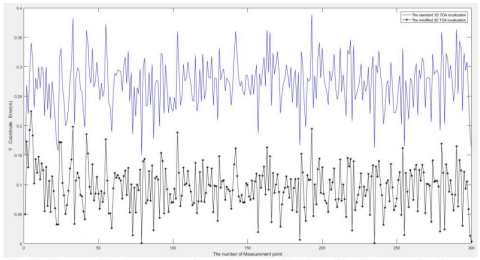

Fig 7. Y coordinate comparison for two 3D localization methods

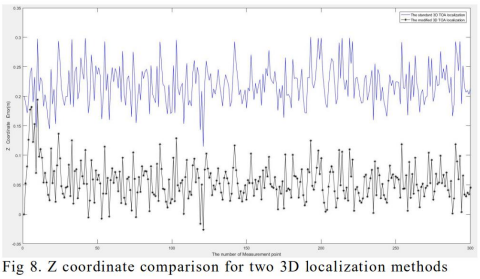

Fig 8. Z coordinate comparison for two 3D localization methods

D. Experimental Results

The experiment measures positioning information of the tags at six locations in the field. The information of tag localization was obtained by application of the standard and modified 3D TOA methods. Several results are presented in the table. The modified 3D TOA positioning algorithm results compared with the standard 3D TOA positioning method results are more accurate taking into account the real position of the tag.

Table 1. Experimental data of tag localization

Actual Coordinates(m)	Measured Coordinates (standard 3D TOA)	Measured Coordinates (modified 3D TOA)
(1,0,2)	(0.8645,0.1517,1.8506)	(0.9785,0.0895,2.0531)
(1,1,1.2)	(0.8486,1.2141,1.4075)	(0.9513,1.1246,1.2845)
(1,2,0.6)	(0.8522,1.7811,0.7523)	(1.0675,2.0494,0.5387)
(2,0,2)	(1.8548,0.1629,1.8711)	(2.1027,0.0786,1.9397)
(2,1,1.2)	(2.1465,0.8611,1.3789)	(2.0682,0.9548,1.1376)
(2,2,0.6)	(2.1850,2.2083,0.8144)	(1.9365,1.9546,0.7114)
(3,0,2)	(3.2047,0.1202,2.1816)	(2.9486,0.0593,2.0872)
(3,1,1.2)	(3.1800,1.2543,1.0475)	(3.1148,1.0763,1.2794)
(3,2,0.6)	(3.1599,2.1848,0.7865)	(3.0596,1.9372,0.5289)

IV. CONCLUSION

The proposed 3D TOA positioning algorithm in this paper breaks through the limitations of considering the two-dimensional in the previous positioning algorithm. The modify 3D TOA positioning algorithm improves the positioning accuracy, and joint Kalman filtering to further eliminates the error interference in the transmission process. The simulation results show that the positioning accuracy can reach about 5~10/cm, which verifying the feasibility of the joint the modified 3D TOA positioning algorithm and Kalman filtering algorithm. Based on the results of this paper, future research will focus on visualization tag trajectories.

REFERENCES

[1] C. Fretzagias and M. Papadopouli, "Cooperative location-sensing for wireless networks," 2004 *Second IEEE Annual Conference on Pervasive Computing and Communications*, Orlando, FL, USA, 2004, pp. 121-131.

[2] J. Hightower and G. Borriello, "Location systems for ubiquitous computing," in *Computer*, vol. 34, no. 8, pp. 57-66, Aug. 2001.

[3] Farahani S ， Helle B. Zig Bee wireless networks and transceivers.MUSA: Newnes Publications，2008.

[4] F. Shang, B. Champagne, and I. Psaromiligkos, "Joint TOA/AOA estimation of IR-UWB signals in the presence of multiuser interference," *2014 IEEE 15th International Workshop on Signal Processing Advances in Wireless Communications (SPAWC)*, Toronto, ON, 2014, pp. 504-508.

[5] F. Shang, B. Champagne and I. N. Psaromiligkos, "An ML-Based Framework for Joint TOA/AOA Estimation of UWB Pulses in Dense Multipath Environments," in *IEEE Transactions on Wireless Communications*, vol. 13, no. 10, pp. 5305-5318, Oct. 2014.

[6] B. Hanssens *et al*., "An indoor localization technique based on ultra-wideband AoD/AoA/ToA estimation," *2016 IEEE International Symposium on Antennas and Propagation (APSURSI)*, Fajardo, 2016, pp. 1445-1446.

[7] Q. Xue and J. Li, "The minimum error algorithm based on TOA measurement for achieving approximate optimal 3D positioning accuracy," *2017 14th International Computer Conference on Wavelet Active Media Technology and Information Processing (ICCWAMTIP)*, Chengdu, 2017, pp. 319-322.

[8] N. Yang, M. Xiong and L. Chen, "A three-dimensional indoor positioning algorithm based on the optimization model," *2017 13th International Conference on Natural Computation, Fuzzy Systems and Knowledge Discovery (ICNC-FSKD)*, Guilin, 2017, pp. 348-352.

[9] Y. Kang, Q. Wang, J. Wang and R. Chen, "A High-Accuracy TOA-Based Localization Method Without Time Synchronization in a Three-Dimensional Space," in *IEEE Transactions on Industrial Informatics*, vol. 15, no. 1, pp. 173-182, Jan. 2019.

[10] Jiaxing, Zhu Rong, Chen Xuan. UWB positioning system based on an improved TWR-TDOA location algorithm. *Journal of Computer Applications*,2017.

[11] Q. Du, X. Sun, R. Ding, Z. Qian and S. Wang, "TOA-Based Location Estimation Accuracy for 3D Wireless Sensor Networks," *2009 5th International Conference on Wireless Communications, Networking and Mobile Computing*, Beijing, 2009, pp. 1-4.

[12] X. Li and S. Yang, "The indoor real-time 3D localization algorithm using UWB," *2015 International Conference on Advanced Mechatronic Systems (ICAMechS)*, Beijing, 2015, pp. 337-342.

[13] Y. Xu, Y. S. Shmaliy, Y. Li and X. Chen, "UWB-Based Indoor Human Localization With Time-Delayed Data Using EFIR Filtering," in *IEEE Access*, vol. 5, pp. 16676-16683, 2017.

[14] P. J. Hargrave, "A tutorial introduction to Kalman filtering," *IEE Colloquium on Kalman Filters: Introduction, Applications, and Future Developments*, London, UK, 1989, pp. 1/1-1/6.

[15] Reza Zekavat; R. Michael Buehrer, "An Introduction to Kalman Filtering Implementation for Localization and Tracking Applications," in *Handbook of Position Location: Theory, Practice, and Advances*, IEEE, 2019, pp.143-195

Appendix B - Technical manual

Department of Information Science and Technology

Technical Manual

Research on Port AGV Composite Positioning Based on UWB/RFID

Dongchen Ni

A Dissertation presented in partial fulfillment of the Requirements for the Degree of

Master in Telecommunications and Computer Engineering

Supervisor:

Dr. Octavian Adrian Postolache, Associate Professor with Habilitation

ISCTE-IUL

Co-supervisor:

Dr. Chao Mi, Associate Professor

Shanghai

September, 2019

Content

List of Figures

List of Tables

Technical Manual

This manual aims to describe the technical features of the composite localization system. Chapter 1 intends to explain how the anchors communicate with the tag and how the anchor communicates with the PC. Chapter 2 explains how to make RFID reader and use it to locate. Chapter 3 explains the main functions of the Kalman Filtering. Chapter 4 is intended to explain how to fuse UWB positioning data and RFID positioning data with Particle Filtering.

4

Chapter 1 UWB localization system

This chapter intends to explain how the anchors communicate with the tag and how the anchor communicates with the PC. Also, how to use UWB system to locate object.

1.1 Communications

All the communications between the anchors and the tag are made through wireless ranging based on the IEEE 802.15.4a.

1.1.1 UWB Mini Configuration

UWB Mini(Figure 1.1) module adopts STM32F105 microcontroller as the main control chip. Peripheral circuit includes: DWM1000 module, power module, LED indicator module, dial-code switch, reset circuit, etc. The module can be used as an anchor or as a tag, which can be switched by a code switch.

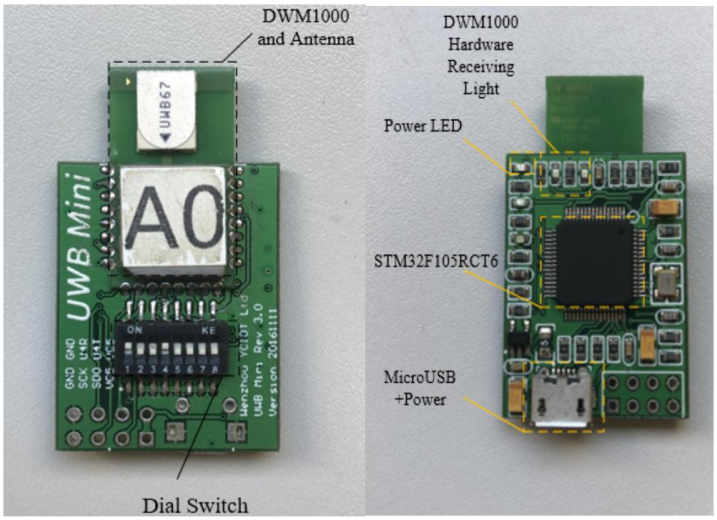

Figure 1.1 - UWB Mini module

5

1.1.2 UWB Mini Hardware parameters

Table 1.1 - UWB Mini Hardware parameters

Essential parameter		Wireless parameters	
PCB	Four layers - epoxy	BAUD	110kbit/s,850kbit/s
Power	Micro-USB(5.0V)	Work Frequency	3.5GHz~6.5GHz
SWD	have	Work channel	5
Serial port	1	Transmitted power	-35dbm/MHZ~ -62dbm/MHZ
Controller	STM32F105RCT6		
External crystals	12Mhz	Distance	Indoor:30m
PCB size	35mm*35mm	Data error	10cm/30cm

1.1.3 Sending data to the anchor

The method in Figure 1.2 shows the PC communicate with the anchor.

6

```
*/
#pragma GCC optimize ("O3")
int readfromspi_serial
(
    uint16       headerLength,
    const uint8 *headerBuffer,
    uint32       readlength,
    uint8       *readBuffer
)
{

    int i=0;

    decaIrqStatus_t  stat ;

    stat = decamutexon() ;

    /* Wait for SPIx Tx buffer empty */
    //while (port_SPIx_busy_sending());

    SPIx_CS_GPIO->BRR = SPIx_CS;

    for(i=0; i<headerLength; i++)
    {
        SPIx->DR = headerBuffer[i];

        while((SPIx->SR & SPI_I2S_FLAG_RXNE) == (uint16_t)RESET);

        readBuffer[0] = SPIx->DR ; // Dummy read as we write the header
    }

    for(i=0; i<readlength; i++)
    {
        SPIx->DR = 0;  // Dummy write as we read the message body

        while((SPIx->SR & SPI_I2S_FLAG_RXNE) == (uint16_t)RESET);

        readBuffer[i] = SPIx->DR ;//port_SPIx_receive_data(); //this clears RXNE bit
    }

    SPIx_CS_GPIO->BSRR = SPIx_CS;

    decamutexoff(stat) ;

    return 0;
} // end readfromspi()
```

Figure 2- send data to the anchor

In the code part(Figure 1.2), it is possible to see that the values began to be read after the micro-controller is turned on and that the values are sent every minute.

1.1.4 Receiving data between anchor and tag

Figure 1.3 shows the part of the code where the anchor receives a package coming from the UWB tag.

```
166 void writetoLCD
167 (
168     uint32       bodylength,
169     uint8        rs_enable,
170     const uint8 *bodyBuffer
171 )
172 {
173     int i = 0;
174     int sleep = 0;
175     //int j = 10000;
176
177     if(rs_enable)
178     {
179         port_LCD_RS_set();
180     }
181     else
182     {
183         if(bodylength == 1)
184         {
185             if(bodyBuffer[0] & 0x3) //if this is command = 1 or 2 - exsecution time is > 1ms
186                 sleep = 1 ;
187         }
188         port_LCD_RS_clear();
189     }
190
191     port_SPIy_clear_chip_select();  //CS low
192
193
194     //while(j--); //delay
195
196     for(i=0; i<bodylength; i++)
197     {
198         port_SPIy_send_data(bodyBuffer[i]); //send data on the SPI
199         while (port_SPIy_no_data()); //wait for rx buffer to fill
200         port_SPIy_receive_data(); //this clears RXNE bit
201     }
202
203     //j = 10000;
204
205     port_LCD_RS_clear();
206
207     //while(j--); //delay
208
209     port_SPIy_set_chip_select();  //CS high
210
211     if(sleep)
212         Sleep(2);
213 } // end writetoLCD()
214 #endif
```

Figure 3 - Receiving data between anchor and tag

After the anchor receives the package, the data contained in it is read and processed according to its information. All the anchors send a flag in the message that identifies the tag where it comes from.

8

Chapter 2 RFID localization system

The RFID is connected to the Raspberry Pi 3 Model B through the SPI protocol, as shown in Figure 2.1. This module is used to identify the reader to start collecting data and sent it to the database. The sensor used in this project is the MFRC522 with the MFRC522 library.

2.1 RFID Reader

The reader of this work is an RFID reader made by connecting Raspberry Pi3, feeder and RC522(Figure 2.2), as shown in Figure 2.3. The RFID reader is a low-cost RFID reader based on MFRC522 microcontroller. The microcontroller provides data via the SPI protocol and works by creating a 13.56 MHz electromagnetic field that is used to communicate with the RFID tag. The interface correspondence is shown in Table 2.1.

Figure 4 - Raspberry Pi 3 Model B

9

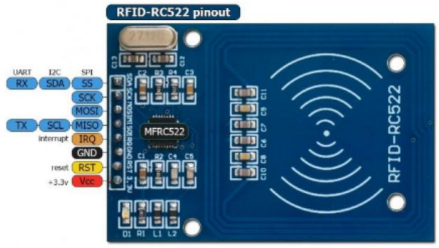

Figure 5 - Definition of RC522 RFID Module

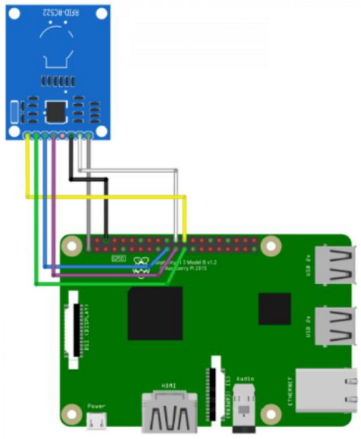

Figure 6 - RC522 RFID Module and Raspberry Pi Circuit Connection

Table 2.1 - Interface Correspondence

RC522 Header	Diagram Colour	Pi Header	Notes
3.3V	Grey	1	3.3V
RST	White	22	GPIO25
GND	Black	6	Ground
IRQ	-	-	Not connected
MISO	Purple	21	GPIO9
MOSI	Blue	19	GPIO10
SCK	Green	23	GPIO11
SDA	Yellow	24	GPIO8

10

2.2 Sending data between Raspberry Pi and RC522

The method in Figure 2.4 and 2.5 shows Raspberry Pi communicate with RC522.

```
import RPi.GPIO as GPIO
import MFRC522
import signal

continue_reading = True

# Capture SIGINT for cleanup when the script is aborted
def end_read(signal,frame):
    global continue_reading
    print "Ctrl+C captured, ending read."
    continue_reading = False
    GPIO.cleanup()

# Hook the SIGINT
signal.signal(signal.SIGINT, end_read)

# Create an object of the class MFRC522
MIFAREReader = MFRC522.MFRC522()

# Welcome message
print "Welcome to the MFRC522 data read example"
print "Press Ctrl-C to stop."

# This loop keeps checking for chips. If one is near it will get the UID and authenticate
while continue_reading:

    # Scan for cards
    (status,TagType) = MIFAREReader.MFRC522_Request(MIFAREReader.PICC_REQIDL)

    # If a card is found
    if status == MIFAREReader.MI_OK:
        print "Card detected"

    # Get the UID of the card
    (status,uid) = MIFAREReader.MFRC522_Anticoll()

    # If we have the UID, continue
    if status == MIFAREReader.MI_OK:

        # Print UID
        print "Card read UID: %s,%s,%s,%s" % (uid[0], uid[1], uid[2], uid[3])

        # This is the default key for authentication
        key = [0xFF,0xFF,0xFF,0xFF,0xFF,0xFF]

        # Select the scanned tag
        MIFAREReader.MFRC522_SelectTag(uid)

        # Authenticate
        status = MIFAREReader.MFRC522_Auth(MIFAREReader.PICC_AUTHENT1A, 8, key, uid)

        # Check if authenticated
        if status == MIFAREReader.MI_OK:
            MIFAREReader.MFRC522_Read(8)
            MIFAREReader.MFRC522_StopCrypto1()
        else:
            print "Authentication error"

```

Figure 7 - RFID read.py code

```
import RPi.GPIO as GPIO
import MFRC522
import signal

continue_reading = True

# Capture SIGINT for cleanup when the script is aborted
def end_read(signal,frame):
    global continue_reading
    print "Ctrl+C captured, ending read."
    continue_reading = False
    GPIO.cleanup()

# Hook the SIGINT
signal.signal(signal.SIGINT, end_read)

# Create an object of the class MFRC522
MIFAREReader = MFRC522.MFRC522()

# This loop keeps checking for chips. If one is near it will get the
while continue_reading:

    # Scan for cards
    (status,TagType) = MIFAREReader.MFRC522_Request(MIFAREReader.PICC

    # If a card is found
    if status == MIFAREReader.MI_OK:
        print "Card detected"

    # Get the UID of the card
    (status,uid) = MIFAREReader.MFRC522_Anticoll()

    # If we have the UID, continue
    if status == MIFAREReader.MI_OK:

        # Print UID
        print "Card read UID: %s,%s,%s,%s" % (uid[0], uid[1], uid[2],

        # This is the default key for authentication
        key = [0xFF,0xFF,0xFF,0xFF,0xFF,0xFF]

        # Select the scanned tag
        MIFAREReader.MFRC522_SelectTag(uid)

        # Authenticate
        status = MIFAREReader.MFRC522_Auth(MIFAREReader.PICC_AUTHENT1
        print "\n"

        # Check if authenticated
        if status == MIFAREReader.MI_OK:

            # Variable for the data to write
            data = []

            # Fill the data with 0xFF
            for x in range(0,16):
                data.append(0xFF)

            print "Sector 8 looked like this:"
            # Read block 8
            MIFAREReader.MFRC522_Read(8)
            print "\n"

            print "Sector 8 will now be filled with 0xFF:"
            # Write the data
            MIFAREReader.MFRC522_Write(8, data)
            print "\n"

            print "It now looks like this:"
            # Check to see if it was written
            MIFAREReader.MFRC522_Read(8)
            print "\n"

            data = []
            # Fill the data with 0x00
            for x in range(0,16):
                data.append(0x00)

            print "Now we fill it with 0x00:"
            MIFAREReader.MFRC522_Write(8, data)
            print "\n"

            print "It is now empty:"
            # Check to see if it was written
            MIFAREReader.MFRC522_Read(8)
            print "\n"

            # Stop
            MIFAREReader.MFRC522_StopCrypto1()

            # Make sure to stop reading for cards
            continue_reading = False
        else:
            print "Authentication error"
```

Figure 8 - RFID write.py code

12

2.3 Sending data to Firebase

In Figure 2.6 is part of the RFID code, this is function that sends the values of the RFID tags to the Firebase.

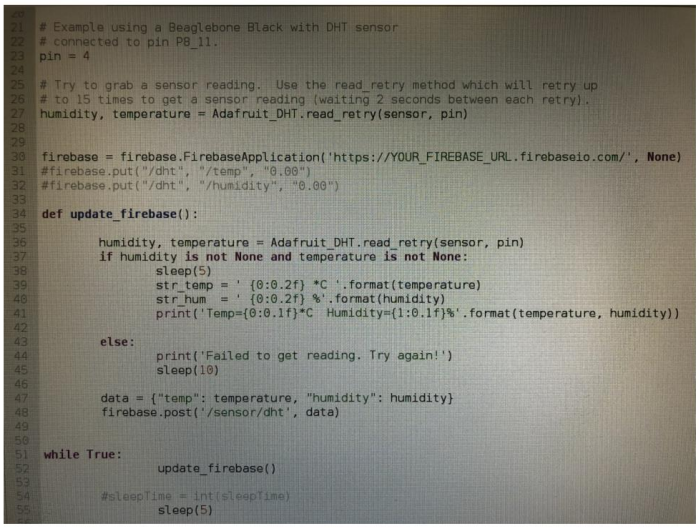

```
# Example using a Beaglebone Black with DHT sensor
# connected to pin P8_11.
pin = 4

# Try to grab a sensor reading.  Use the read_retry method which will retry up
# to 15 times to get a sensor reading (waiting 2 seconds between each retry).
humidity, temperature = Adafruit_DHT.read_retry(sensor, pin)


firebase = firebase.FirebaseApplication('https://YOUR_FIREBASE_URL.firebaseio.com/', None)
#firebase.put("/dht", "/temp", "0.00")
#firebase.put("/dht", "/humidity", "0.00")

def update_firebase():

        humidity, temperature = Adafruit_DHT.read_retry(sensor, pin)
        if humidity is not None and temperature is not None:
                sleep(5)
                str_temp = ' {0:0.2f} *C '.format(temperature)
                str_hum  = ' {0:0.2f} %'.format(humidity)
                print('Temp={0:0.1f}*C  Humidity={1:0.1f}%'.format(temperature, humidity))

        else:
                print('Failed to get reading. Try again!')
                sleep(10)

        data = {"temp": temperature, "humidity": humidity}
        firebase.post('/sensor/dht', data)


while True:
                update_firebase()

        #sleepTime = int(sleepTime)
                sleep(5)
```

Figure 9 - send data() Function

2.4 RFID interface

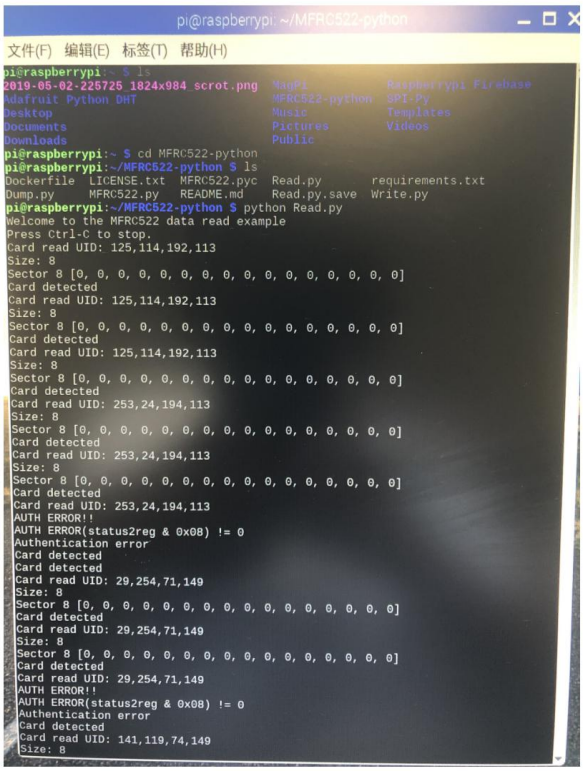

Figure 10 - RFID interface

Chapter 3 Kalman Filtering

This chapter introduces the functions of Kalman filtering and its model algorithm, and finally shows how to implement Kalman filtering.

3.1 Kalman filtering model

KF consists of two phases: prediction and update. In the prediction phase, the filter estimates the current state by using an estimate of the previous state. During the update phase, the filter uses the observations of the current state to optimize the predictions obtained during the prediction phase to obtain a more accurate new estimate. In this way, KF becomes a problem for solving unknown state equations and measuring equations. The equation of state and measurement equation of the KF are as follows:

$$s(k+1) = A \bullet s(k) + \Gamma \bullet w(k) \tag{3.1}$$

$$z(k) = G(k) \bullet s(k) + v(k) \tag{3.2}$$

Where, $s(k)$ is the state vector, $z(k)$ is the measurement vector, A is the state transition matrix of the sampling interval Δ, Γ is the noise coupling matrix, $G(k)$ is the measurement matrix, $w(k)$ and $v(k)$ are the noise components.

The iteration of the KF has two steps. The first step is the prediction of the state, as follows:

$$\hat{s}(k/k-1) = As(k-1) \tag{3.3}$$

$$P(k/k-1) = AP(k-1)A^T + \Gamma Q(k)\Gamma^T \tag{3.4}$$

$$K(k) = P(k/k-1)G(k)^T \left[G(k)P(k/k-1)G(k)^T + R(k)\right]^{-1} \tag{3.5}$$

The second step is the correction of the measured values as follows:

$$\hat{s}(k) = \hat{s}(k/k-1) + K(k)\left[z(k) - G(k)\hat{s}(k/k-1)\right] \tag{3.6}$$

$$P(k) = \left[I - K(k)G(k)\right]P(k/k-1) \tag{3.7}$$

Where, $\hat{s}(k/k)$ and $\hat{s}(k+1/k)$ are state estimation vectors and state prediction vectors, $P(k/k)$ and $P(k+1/k)$ represent the covariance matrix of the estimation error and the prediction error, respectively, and $K(k)$ represents the Kalman gain.

1.2 Extended Kalman filtering

Using KF to achieve positioning, we first need to design the matrix and vector in the KF equation to accurately model the positioning process.

Set the coordinates of the mobile station at time k be (x_k, y_k), the coordinates of the base station be x_i , y_i , and the time of arrival(TOA) of the N base stations multiplied by the speed of light to obtain $r_1, r_2, \cdots r_N$. Taking the estimated state $s(k)$ as $s(k) = [x_k, y_k]^T$ at time k, the system state equation is

$$s(k) = As(k-1) + w(k-1) \tag{3.8}$$

A is a one-step transfer matrix, $A = \begin{bmatrix} 1 & 0 \\ 0 & 1 \end{bmatrix}$

The system measurement equation is:

$$z(k) = f(s(k)) + v(k) \tag{3.9}$$

Where: $z(k) = [r_1, r_2, \cdots r_N]^T / c$, $f(s(k)) = \begin{bmatrix} f_1(s(k)) \\ \vdots \\ f_N(s(k)) \end{bmatrix} / c$.

$$f_i(s(k)) = \sqrt{(x_n - x_i)^2 + (y_n - y_i)^2} \tag{3.10}$$

$f(s(k))$ is a nonlinear transformation that uses Taylor series expansion to simplify expressions. When converting at time k-1, $F(k)$ is the Jacobian matrix of $f(s(k))$:

$$F(k)=\begin{bmatrix} \frac{\partial f_1}{\partial x} & \frac{\partial f_1}{\partial y} \\ \vdots & \vdots \\ \frac{\partial f_N}{\partial x} & \frac{\partial f_N}{\partial y} \end{bmatrix}/c \tag{3.11}$$

$$F(k)=\begin{bmatrix} (x_{k/k-1}-x_1)/D_1 & (y_{k/k-1}-y_1)/D_1 \\ \vdots & \vdots \\ (x_{k/k-1}-x_N)/D_N & (y_{k/k-1}-y_N)/D_N \end{bmatrix}/c \tag{3.12}$$

Of which, $D_1=\sqrt{(x_{k/k-1}-x_1)^2+(y_{k/k-1}-y_1)^2}$.

Set $w(k)$, and v have a covariance matrix of Q and R, respectively, which are diagonal arrays with the number of columns being 2 and the number of TOAs. The iterative equation is as follows:

$$\hat{s}(k/k-1)=As(k-1) \tag{3.13}$$

$$P(k/k-1)=AP(k-1)A^T+Q \tag{3.14}$$

$$K(k)=P(k/k-1)F(k)^T[F(k)P(k/k-1)F(k)^T+R(k)]^{-1} \tag{3.15}$$

$$\hat{s}(k/k)=\hat{s}(k/k-1)+K(k)[z(k)-f(s(k/k-1))] \tag{3.16}$$

$$P(k/k)=[I-K(k)F(k)P(k/k-1)] \tag{3.17}$$

The implemented Kalman Filter code in Matlab is shown in Figure 3.1:

```matlab
%%%%%%%%%%%%%%%%%%%%%%%%%%%%%%%%%%%%%%%%%%
N=312;                              %Samplings
x=[1,5,5,1];                        %real route
y=[0.5,0.5,1.5,1.5];
Xkf=zeros(1,N);                     %Kalman filter estimated value
P=zeros(1,N);                       %covariance
%-------------Initialization-----------------
P(1)=0.01;                          %The covariance of the initial value
Xkf(1)=Z(1);                        %The initial estimated state of the filter
%-------------noise error--------------------
Q=0.01;                             %process variance
R=0.25;                             %mearsuremnt variance
W=sqrt(Q)*randn(1,N);               %state-transition matrix
V=sqrt(R)*randn(1,N);               %Measurement noise matrix
%-------------system matrix-------------------
F=1;
G=1;
H=1;
I=eye(2);
%%%%%%%%%%%%%%%%%%%%%%%%%%%%%%%%%%%%%%%%%%%%%%%%%
%-------------Kalman filter-------------------
for k=2:N
    X_pre=F*Xkf(k-1);               %state prediction
    P_pre=F*P(k-1)*F'+Q;            %Covariance prediction
    Kg=P_pre*inv(H*P_pre*H'+R);     %Calculate the Kalman gain
    e=x(k)-H*X_pre;
    Xkf(k)=X_pre+Kg*e;              %update the state
    P(k)=(I-Kg*H)*P_pre;            %Covariance update
end
%-------------calculation error---------------
Err_Messure=zeros(1,N);             %The deviation between the measured value and the true value
Err_Kalman=zeros(1,N);              %The deviation between the kalman filter estimate and the measured value
for k=1:N
    Err_Messure(k)=abs(x(k)-Xexpect);
    Err_Kalman(k)=abs(Xkf(k)-x(k));
end
```

Figure 11 - Kalman Filter code in Matlab

18

Chapter 4 Particle Filtering

This chapter introduces the functions of particle filtering and its model algorithm, and finally shows how particle filtering is implemented.

4.1 Particle filter model

The PF algorithm is a filtering algorithm based on Bayesian estimation and Monte Carlo method.

4.1.1 Bayesian estimation theory

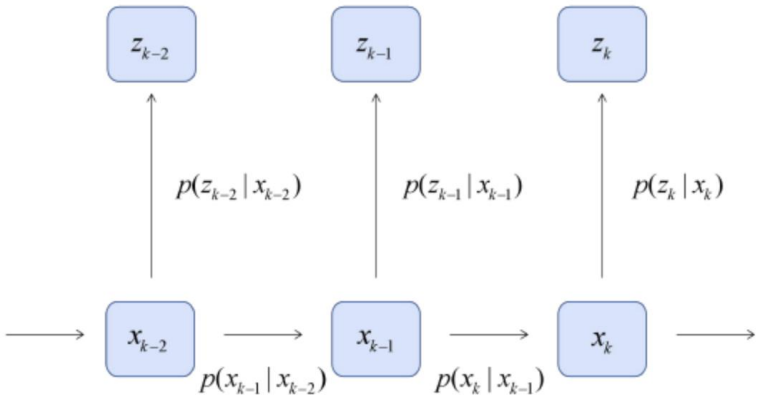

Figure 12 -Bayesian estimation method model diagram

The Bayesian estimate consists of two phases: forecast phase and update phase. The model of Bayesian estimation is shown in Figure 4.1.

In the implementation process, it is assumed that the posterior probability $p(x_{k-1}|z_{1:k-1})$ at the time of system k-1 is known. The Bayesian estimation process is as follows:

(1) forecast phase: It is known that the posterior probability $p(x_{k-1} \mid z_{1:k-1})$ at time k −1 obtains the prior probability density $p(x_k \mid z_{1:k-1})$ of the current moment of the system, as shown in equation (4.1):

$$p(x_k \mid z_{k-1}) = \int p(x_k \mid x_{k-1}) p(x_{k-1} \mid z_{1:k-1}) dx_{k-1} \tag{4.1}$$

Where, $p(x_k \mid x_{k-1})$ is the state transition probability of the first-order Markov chain, that is, the current time position information is only related to the previous time position information.

(2) update phase: The posterior probability is obtained by the equation (4.2) by the prior probability $p(x_k \mid z_{1:k-1})$ obtained in the prediction stage.

$$p(x_k \mid z_{1:k}) = \frac{p(z_k \mid x_k) p(x_k \mid z_{1:k-1})}{p(z_k \mid z_{1:k-1})} \tag{4.2}$$

After obtaining the observed value z_k at time k, the posterior probability is obtained according to equation (4.2), where the denominator is $p(x_z \mid z_{1:k-1})$ is the normalization constant, and the calculation formula is as shown in equation (2.3):

$$p(z_k \mid z_{1:k-1}) = \int p(z_k \mid x_k) p(x_k \mid z_{1:k-1}) dx_k \tag{4.3}$$

After obtaining the posterior probability of each particle, the maximum posterior probability is obtained according to the Maximum aposterior estimation (MAP), and the particle position of the maximum posterior probability is used as the optimal position estimation of the system. Among them, the maximum posterior probability criterion is as shown in equation (4.4):

$$x_k = \arg\max p(x_k \mid z_{1:k}) \tag{4.4}$$

20

4.1.2 Monte Carlo approximation

The Monte Carlo approximation method randomly collects N samples $\{x_{0:k}^{i}\}_{i=1}^{N}$ in the posterior probability density $p(x_k \mid z_{1:k})$, and each sample point is independent of each other. The posterior probability of the system is calculated as shown in equation (4.5):

$$p(x_k \mid z_{1:k}) \approx \frac{1}{N}\sum_{i=1}^{N}\delta(x_{0:k} - x_{0:k}^{i}) \tag{4.5}$$

Of which, $\delta(\cdot)$ is dirac function.

4.1.3 Sequential importance sampling(SIS)

The important sampling method adopted by the PF algorithm is the Sequential Important Sampling (SIS) method, which introduces the sequential idea, and decomposes the importance density function to obtain a recursive calculation method. As shown in equation (4.6):

$$q(x_{0:k}^{(i)} \mid z_{1:k}) = q(x_k \mid x_{0:k}^{(i)}, z_{1:k})q(x_{0:k-1}^{(i)} \mid z_{1:k-1}) \tag{4.6}$$

The posterior probability is calculated as shown in equation (4.7):

$$\begin{aligned} p(x_k \mid z_{1:k}) &= \frac{p(z_k \mid x_{0:k}, z_{1:k-1})p(x_{0:k} \mid z_{1:k-1})}{p(z_k \mid z_{1:k-1})} \\ &= \frac{p(z_k \mid x_{0:k}, z_{1:k-1})p(x_k \mid x_{0:k-1}, z_{1:k-1})p(x_{0:k-1} \mid z_{1:k-1})}{p(z_k \mid z_{1:k-1})} \\ &= \frac{p(z_k \mid x_k)p(x_k \mid x_{k-1})p(x_{0:k-1} \mid z_{1:k-1})}{p(z_k \mid z_{1:k-1})} \\ &\propto p(z_k \mid x_k)p(x_k \mid x_{k-1})p(x_{0:k-1} \mid z_{1:k-1}) \end{aligned} \tag{4.7}$$

The particle weight can be calculated by recursion, as shown in equation (4.8):

$$\omega_k^{(i)} \propto \frac{p(z_k \mid x_k)p(x_k \mid x_{k-1})p(x_{0:k-1} \mid z_{1:k-1})}{q(x_{0:k-1}^{(i)} \mid z_{1:k-1})q(x_k^{(i)} \mid x_{0:k-1}^{(i)}, z_{1:k})} \tag{4.8}$$

$$= \omega_{k-1}^{(i)} \frac{p\left(z_k \mid x_k^{(i)}\right) p\left(x_k^{(i)} \mid x_{k-1}^{(i)}\right)}{q\left(x_k^{(i)} \mid x_{0:k-1}^{(i)}, z_{1:k}\right)}$$

Finally, the weight w needs to be normalized, as shown in equation (4.9):

$$\tilde{\omega}_k^{(i)} = \frac{\omega_k^{(i)}}{\sum_{i=1}^{N} \omega_k^{(i)}} \tag{4.9}$$

The implemented Particle Filter code in Matlab is shown in Figure 4.2:

```
%--------------initialize the variables----------------
x = 0;                                  % initial actual state
x_N = 1;                                % The covariance of system process noise
x_R = 1;                                % Measure the covariance of noise in the process
T = 75;
N = 100;                                % The particle number. The larger the effect, the better
                                           %and the larger the computation
%--------------initilize our initial, prior particle distribution as a gaussian around
%--------------the true initial value--------------------
V = 2;                                  %The variance of the initial distribution
z_out = [x^2 / 20 + sqrt(x_R) * randn]; %Observation of the particle
x_out = [x];                            %the actual output vector for measurement values.
x_est = [x];                            % time by time output of the particle filters estimate
x_est_out = [x_est];                    % the vector of particle filter estimates.
for t = 1:T
    x = 0.5*x + 25*x/(1 + x^2) + 8*cos(1.2*(t-1)) +  sqrt(x_N)*randn;
    z = x^2/20 + sqrt(x_R)*randn;
    for i = 1:N
%--------------Sampling from prior probabilities--------------
        x_P_update(i) = 0.5*x_P(i) + 25*x_P(i)/(1 + x_P(i)^2) + 8*cos(1.2*(t-1)) + sqrt(x_N)*randn;
%--------------Calculate the value of the sample particle-----
        z_update(i) = x_P_update(i)^2/20;
%--------------Calculate the weight for each particle---------
        P_w(i) = (1/sqrt(2*pi*x_R)) * exp(-(z - z_update(i))^2/(2*x_R));
    end
%--------------The normalized.--------------------------------
    P_w = P_w./sum(P_w);
%--------------Resampling-------------------------------------
    for i = 1 : N
        x_P(i) = x_P_update(find(rand <= cumsum(P_w),1));% Particle weight will be more important to get offspring
    end
%--------------state estimation-------------------------------
    x_est = mean(x_P);
%--------------Save data in arrays for later plotting---------
    x_out = [x_out x];
    z_out = [z_out z];
    x_est_out = [x_est_out x_est];
end
```

Figure 13 - Particle filter code in Matlab